MODELING, SIMULATION AND EXPERIMENTAL VERIFICATION OF A HYDRAULIC FAN DRIVE SYSTEM

A THESIS SUBMITTED TO
THE GRADUATE SCHOOL OF NATURAL AND APPLIED SCIENCES
OF
MIDDLE EAST TECHNICAL UNIVERSITY

BY

ERSEN TORAMAN

IN PARTIAL FULLFILLMENT OF THE REQUIREMENTS FOR
THE DEGREE OF MASTER OF SCIENCE
IN
MECHANICAL ENGINEERING

SEPTEMBER 2013

Approval of the thesis:

MODELING, SIMULATION AND EXPERIMENTAL VERIFICATION OF HYDRAULIC FAN DRIVE SYSTEM

submitted by **ERSEN TORAMAN** in partial fulfillment of the requirements for the degree of **Master of Science in Mechanical Engineering Department, Middle East Technical University** by,

Prof. Dr. Canan Özgen
Dean, Graduate School of **Natural and Applied Sciences** _____

Prof. Dr. Süha Oral
Head of Department, **Mechanical Engineering** _____

Prof. Dr. Tuna Balkan
Supervisor, **Mechanical Engineering Dept., METU** _____

Examining Committee Members:

Prof. Dr. Y. Samim Ünlüsoy
Mechanical Engineering Dept., METU _____

Prof. Dr. Tuna Balkan
Mechanical Engineering Dept., METU _____

Assist. Prof. Dr. Yiğit Yazıcıoğlu
Mechanical Engineering Dept., METU _____

Assist. Prof. Dr. Kıvanç Azgın
Mechanical Engineering Dept., METU _____

Serhat Başaran, M.Sc.
R&D, FNSS Defense Systems Co. _____

Date: 10/09/2013

I hereby declare that all information in this document has been obtained and presented in accordance with academic rules and ethical conduct. I also declare that, as required by these rules and conduct, I have fully cited and referenced all material and results that are not original to this work.

Name, Last name: Ersen Toraman

Signature:

ABSTRACT

MODELING, SIMULATION AND EXPERIMENTAL VERIFICATION OF A HYDRAULIC FAN DRIVE SYSTEM

Toraman, Ersen
M. Sc., Department of Mechanical Engineering
Supervisor: Prof. Dr. Tuna Balkan

September 2013, 83 pages

Environmental factors, global legislations and economic reasons force vehicle industry to produce more efficient systems. Displacement controlled hydraulic fan drive system is one of the energy efficient alternatives for stationary highway vehicles, construction machines and military vehicles that have moderate engine size and less benefit from ram air cooling.

In this thesis study, hydraulic fan drive system of a military vehicle is investigated and a dynamic model of the system is developed. MATLAB/Simulink® software, a block diagram environment, is used for model based design and multidomain simulation of mechanical and hydraulic components. Beside the predefined blocks under Simulink® library, custom models are developed, i.e. variable displacement axial piston pump with swash plate dynamics, fan, compensator.

In order to verify the developed model, simulation results are compared with experimental data (pressure, flow rate, engine and fan speeds). Then, by the help of the model, effect of orifice sizes on the system performance is investigated.

Developed model can be used for deeper understanding behind the hydraulic fan drive system of the vehicle. In addition, if a modification in an existing system is to be made, effect of the alteration can be examined over the model in advance.

Keywords: Hydraulic Fan Drive System, Variable Displacement Pump, Swash Plate Mechanism, SimHydraulics® Modeling

ÖZ

HİDROLİK TAHRİKLİ FAN SİSTEMİNİN MODELLENMESİ, SİMÜLASYONU VE DENEYSEL YÖNTEMLE DOĞRULANMASI

Toraman, Ersen
Yüksek Lisans, Makina Mühendisliği Bölümü
Tez Yöneticisi: Prof. Dr. Tuna Balkan

Eylül 2013, 83 sayfa

Çevresel faktörler, küresel mevzuatlar ve ekonomik sebepler araç endüstrisini daha verimli sistemler üretimi konusunda zorlamaktadır. Orta dereceli motor hacmine sahip ve çarpan hava soğutmasından yeterince beslenemeyen durağan karayolu araçları, inşaat makineleri ve askeri araçlar için deplasman kontrollü hidrolik tahrikli fan sistemleri enerji verimli bir alternatiftir.

Bu tez çalışmasında, askeri bir aracın hidrolik tahrikli fan sistemi incelenmiş ve dinamik modeli geliştirilmiştir. Mekanik ve hidrolik elemanlar, MATLAB/Simulink® yazılımı kullanılarak modellenmiş ve çoklu ortam simülasyonu gerçekleştirilmiştir. Simulink® kütüphanesi içinde bulunan hazır blokların dışında özel modeller de geliştirilmiştir, ör. deplasman plakası dinamik modelini içeren değişken deplasmanlı pompa, fan, kompansatör.

Geliştirilen modelin doğrulaması için simülasyon ve test verileri (basınç, debi, motor ve fan devri) karşılaştırılmıştır. Sonrasında, orifis çaplarının sistem performansı üzerindeki etkisi model yardımıyla araştırılmıştır.

Geliştirilen model, hidrolik sistemin daha detaylı incelenmesi için kullanılabilir. Ayrıca, eğer mevcut sistem üzerinde bir değişiklik yapılacaksa, bu değişikliğin etkileri model üzerinden önceden incelenebilir.

Anahtar kelimeler: Hidrolik Tahrikli Fan Sistemi, Değişken Deplasmanlı Pompa, Deplasman Plakası Mekanizması, SimHydraulics® Modelleme

To My Family

ACKNOWLEDGEMENTS

First of all, I would like to express my sincere appreciation to Prof. Dr. Tuna BALKAN, for his supervision and helpful critics throughout the progress of my thesis study.

I would like to thank my colleagues Semih ATABEY, Gökhan YAŞAR, Necip CAYAN, and Ahmet TAŞ for their support and friendship.

I would like to express my special thanks to my family for their endless support not only during my thesis preparation, but also throughout my life.

Also thanks to Scientific and Technological Research Council of Turkey (TÜBİTAK) for their financial support.

On a personal note, I am grateful to my fiancée Nihan for supporting me during this lengthy endeavor. And thanks to the rest of you who I didn't acknowledge by name. I appreciate your help, too.

TABLE OF CONTENTS

LIST OF FIGURES

FIGURES

LIST OF TABLES

TABLES

LIST OF SYMBOLS AND ABBREVIATIONS

SYMBOLS

c : Damping Coefficient

c_{bp} : Damping Coefficient of Bias Piston

c_{cp} : Damping Coefficient of Control Piston

d_p : Displacement of the Pump

d_m : Displacement of the Hydromotor

k : Spring Constant of Bias Spring

k_{leak} : Leakage Coefficient

l : Instantaneous Length of Bias Spring

l_0 : Natural Length of Bias Spring

m : Mass

m_{bp} : Mass of Bias Piston

m_{cp} : Mass of Control Piston

m_p : Mass of the Piston

r : Moment Arm of Individual Piston

x : Position

A_{bp} : Cross Sectional Area of the Bias Piston

A_{cp} : Cross Sectional Area of the Control Piston

A_{leak} : Leakage Area

A_p : Cross Sectional Area of the Piston

C_d : Flow Discharge Coefficient

C_{dl} : Flow Discharge Coefficient

D_{fan} : Constant for Simplified Fan-Torque Equation

D_h : Instantaneous Orifice Hydraulic Diameter

F_{bp} : Bias Piston Force

F_{bs} : Bias Spring Force

F_{cp} : Control Piston Force

I : Mass Moment of Inertia of Swash Plate

I_{fan} : Mass Moment of Inertia of Fan

K_{sp} : Swash Plate Control Gain

L : Length

N : Number of Pistons

P : Pressure

P_{bp} : Bias Piston Pressure

P_{cp} : Control Piston Pressure

P_d : Discharge Pressure

P_i : Intake Pressure

P_{nom} : Nominal Pressure

Re : Reynolds Number

Q : Flow Rate

Q_{leak} : Leakage Flow Rate

Q_P : Flow Supplied by the Pump

T : Torque

T_{fan} : Torque Driven by the Fan

T_s : Swivel Torque

α : Swash Plate Angle

ρ : Density

γ : Pressure Carry-Over Angle

ξ_{sp} : Swash Plate Damping Ratio

μ : Dynamic Viscosity

$\eta_{m,m}$: Mechanical Efficiency of the Hydromotor

$\eta_{m,v}$: Volumetric Efficiency of the Hydromotor

$\eta_{p,v}$: Volumetric Efficiency of the Pump

η_{mec} : Mechanical Efficiency

υ : Kinematic Viscosity

υ_{nom} : Nominal Kinematic Viscosity

ω : Rotational Speed

ω_e : Rotational Speed of the Engine

ω_f : Rotational Speed of the Fan

ω_f : Nominal Rotational Speed

ω_{sp} : Swash Plate Natural Frequency

ΔP : Pressure Differential

ABBREVIATIONS

bp : Bias Piston

cp : Control Piston

lpm : Liter per Minute

ppm : Parts per million

rpm : Revolution per Minute

ECU : Electronic Control Unit

EPRV : Electro-Proportional Relief Valve

FDM : Fixed Displacement Hydromotor

FDP : Fixed Displacement Pump

HFDS : Hydraulic Fan Drive System

ORF : Orifice

PTO : Power Take Off

RV : Relief Valve

VDM : Variable Displacement Hydromotor

VDP : Variable Displacement Pump

CHAPTER 1

INTRODUCTION

1.1 Motivation of the Study

Day by day, system efficiency, power consumption and fuel saving subjects are becoming more and more important for motor vehicle manufacturers. Not only the initial cost of the system is important; ongoing cost, maintenance cost and life cycle cost are also taken into account. Thus, designing more efficient and less power consuming products is one of the most important goals for companies.

Beside efficiency and power consumption issues, there are global legislations for noise levels [1]. Companies should guarantee these low noise levels on their products. Last but not least, the other important subject is engine emission rate. Euro V and VI standards force and obligate companies to run engines at higher and more efficient temperatures [2].

Efficiency, power consumption, noise level, emission rate and etc. All these subjects are related to nearly all of the systems in the vehicle such as power generation, drive train, cooling system, aerodynamic and even the wheels. So it will be rational to spare systems and dwell on a single system. In this work, cooling system of a vehicle will be investigated.

In commercial vehicles, for gasoline engines, approximately one third of the energy in the fuel converted into useful power. For diesel engines, efficiency is better but not more than 45% [3]. Approximately 30% of energy goes out from the exhaust pipe unused. The remaining energy is converted into heat energy and it is the cooling system's duty to remove this excess heat. In order to decrease emission rate and provide fuel economy, engine should be run at constant and ideal temperature. Engine temperature must be maintained constant by cooling system whatever the outside temperature and heat generated by the engine are.

Basically, there are two types of cooling systems on motor vehicles; these are liquid and air cooled systems. Liquid cooling system is used on modern vehicles. A few older cars and modern motorcycles still use air cooling.

Water pump, thermostat, radiator, radiator cap, hoses, heater core, fan, coolant, passages inside the engine and tank are the components of a liquid cooling system. Coolant is circulated by the water pump. Duty of the thermostat is to control the temperature of the coolant. Pressure in the system is controlled by the radiator cap and finally coolant is cooled by the radiator. In order to warm up the vehicle on cold days, a heater system is also integrated into the system. System components can be seen in the Figure 1-1.

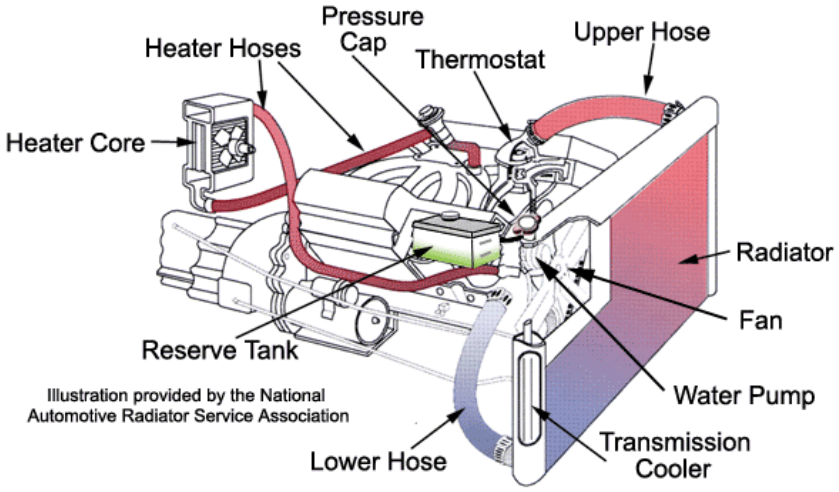

Figure 1-1 Automotive Cooling System [4]

Liquid coolant, passing through engine passages, absorbs heat. Heated coolant passes through the hoses and enters to the radiator. As the coolant passes inside the thin tubes in the radiator, it is cooled by the air entering the engine compartment from the grill which is called as "Ram Air". Cooled coolant exits the radiator and re-pass the passages inside the engine block to pick up more heat [5].

If the coolant temperature decreases below a certain temperature, thermostat blocks the coolant flow to the radiator. Blocked coolant circulates inside the engine and when its temperature increase above a certain temperature, thermostat opens. In summary, thermostat prevents coolant temperature to decrease under a certain temperature. In contrast to thermostat, radiator cap prevents coolant temperature to increase above its boiling temperature.

When the air flow from the grill (ram air) is not sufficient for decreasing the coolant temperature inside the radiator, fans provide the necessary air flow. There are electric fans in modern commercial vehicles which are controlled by the vehicle's electronic control unit (ECU) according to temperature sensor which monitors the engine temperature. According to data sent by the sensor, it is decided whether fan will be turned off or on. In addition fan speed is also adjusted. For example, while a vehicle is travelling down a highway, ram air is generally sufficient for cooling so fan can be turned off.

However, when the vehicle is driven slowly or stopped while the engine is running, there is no air flow from the grill. Then, fan must be turned on and appropriate fan speed must be adjusted.
As can be understood, cooling system is composed of many different components with different purposes. Although every component has important duty in the system, the cooling

capacity of the system directly depends on heat exchanger (radiator) capacity and the flow provided through the radiator which depends on ram air and/or the fan.

When the radiator is taken into consideration, there are many parameters that determine cooling capacity of the radiator. Some of them are geometry of construction (tubular heat exchangers, plate type heat exchangers, extended surface heat exchangers), arrangement of flow path (parallel flow, counter flow, cross flow), material (steel, aluminum) and heat transfer mechanism [6].

In this study, fan drive part of the cooling system will be investigated. There are basically 3 different fan drive systems, these are;

- Direct Driven
- Electric Driven
- Hydraulic Driven

Direct driven fan system is an old technology. Fan is whether directly connected to the engine crank or driven by a belt mechanism as shown in Figure 1-2.

The speed of the fan and the speed of the engine are proportional. Excessive fan noise can be heard during the car acceleration through the gears. In addition, due to continuous fan rotation there is always energy consumption independent from air flow requirement by cooling system.

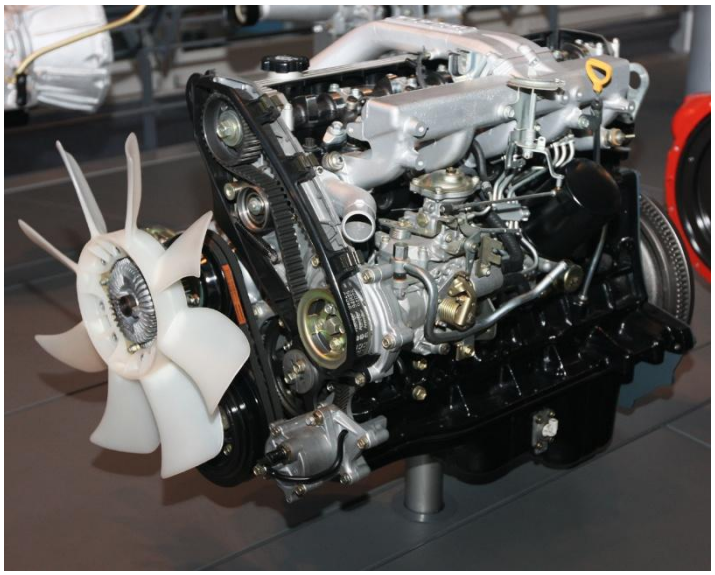

Figure 1-2 Direct Driven Fan [7]

In order to control fan speed, viscous fan drive systems were developed. However, it is not completely possible to control fan speed independent from the engine speed. Beside control deficiency for direct driven fans, fan and radiator locations are limited. They must be in an order.

Finally, for belt driven direct drive systems, belt must be changed regularly, which increases down time, in addition, breakdown risk always exists.

Electric driven fan systems become very common in modern day. Main air stream source for radiator is the ram air. Electric fan is an auxiliary equipment. If the air flow becomes insufficient, then electric fans step in and provide additional air flow to the radiator.

The electric fans are controlled by the vehicle's electronic control unit. Temperature sensors monitor the engine and if it is beginning to run too hot, fan is turned on to draw air through the radiator. Since the fan is not driven from the engine directly, there will be no extra load on the engine, when the ram air is sufficient for cooling.

Electric fans provide better installation with respect to direct driven fans. They are generally designed to mount directly on the radiator and provide better installation. Figure 1-3 shows an electric driven fan.

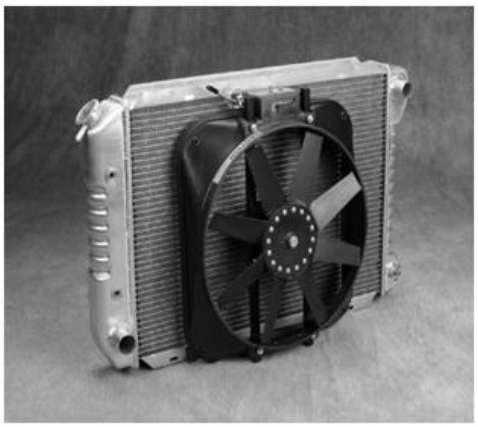

Figure 1-3 Electric Driven Fan

The third and the final fan driven system that will be investigated is hydraulic fan drive system (HFDS). Hydraulic fan drive system is completely different from the previous two concepts. For direct driven fan systems, fan is either directly connected to engine crank or driven by belt mechanism. For electric driven fan systems, only additional component is an electric motor integrated to the fan. However, HFDS requires additional components such as pump, hydromotor, filter, control valve, proper oil, connection hoses and tubes, and a proper

hydraulic tank. Hydraulic system components can be seen in Figure 1-4. Direct or belt driven pump provides necessary oil flow to the hydromotor which is directly connected to fan. A proportional pressure control valve, controlled electrically, adjusts the fan speed depending on engine temperature. Optimum design temperature of the coolant is maintained by the electronic control system.

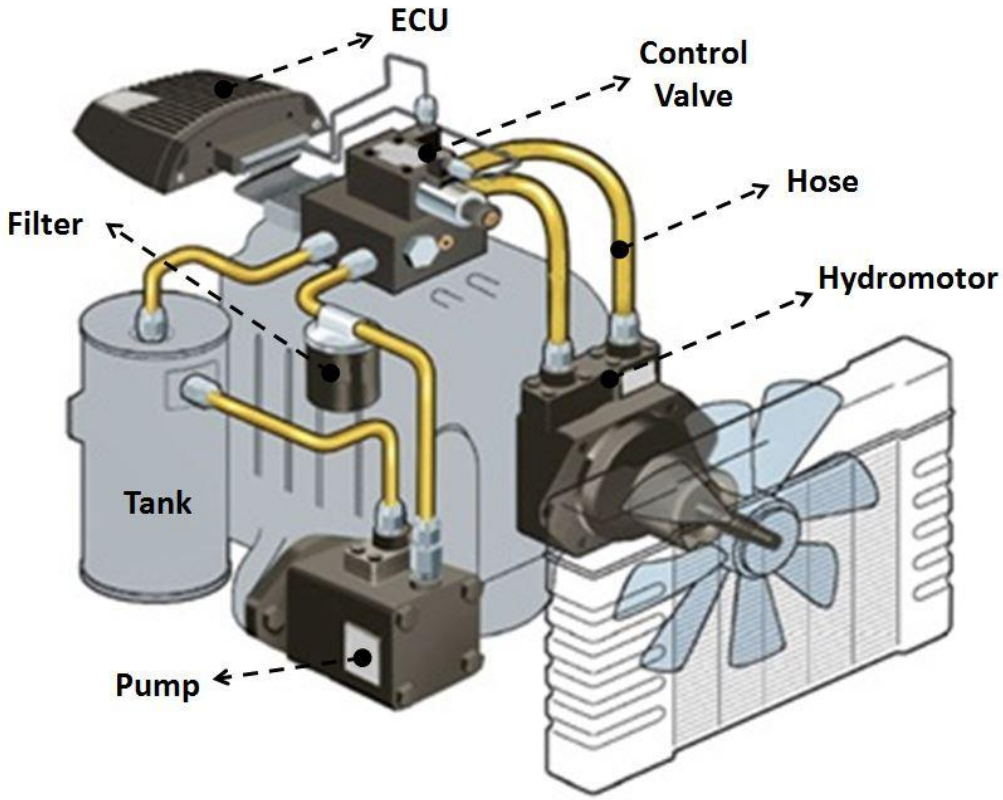

Figure 1-4 Hydraulic Fan Drive System [8]

One of the most important advantages of the hydraulic system is the installation flexibility. Only the hydromotor location is limited. Hydromotor must be coupled with the fan similar to electric motor in electric driven fan systems. Other components can be regularly placed and their connections can be done by flexible hoses.

Hydraulic components have high power density and high efficiency when compared to electric driven fan systems. Thus, system efficiencies are also moderately high. Thereby, high fan speeds and cooling rates can be achieved. In addition, properly designed and assembled hydraulic systems are highly reliable and durable.

Another important property of the HFDS is sensitive fan speed control. Flow delivered to the hydromotor by the pump can be controlled by changing the displacement (flow delivered by the pump per rotation) of the pump. Displacement of the pump can be decreased to achieve low fan speeds in a cold environment. Similarly pump displacement can be adjusted to maximum and high fan speed will be achieved in a hot environment. In this way, coolant temperature can be precisely controlled.

When three different fan drive systems are compared, direct driven fan systems are the cheapest but the least efficient one. On the other hand, electric and hydraulic driven fan systems have quite high efficiencies. In terms of installation, hydraulic and electric fan drive systems are more flexible for placement of components. Control capability, reliability and cooling capacity are the strong points of HFDS. However commercial vehicles are still using electric fans. The reason is that, in commercial vehicles, air entering from the grill in front of the car generally be sufficient for cooling. If it is insufficient, electric fan steps in. In addition, it will be unnecessary to use hydraulic components which will require additional space which is generally not available in commercial vehicles. However, for stationary highway and construction machines, situation is different. They require high cooling rates and they generally do not benefit from the ram air cooling. Thus, their main and primary air flow supplier is fan. As mentioned before, direct driven fans are the least effective ones. On the other hand, to make use of electric fans for primary cooling, it is required to use huge electric motors since cooling demand of such vehicles are quite high. In addition, adequate alternator capacity is required to provide necessary power to electric motor. Therefore, hydraulic driven fans are suitable for the vehicles that require high cooling rates and also do not benefit from ram air cooling. Excavators, back hoes, diggers, graders, road and landscape preparation vehicles, tunneling and boring machines, mining machines, and military vehicles are the basic examples for vehicles that have moderate engine size and also not benefiting sufficiently from ram air cooling.

In this work, a hydraulic fan drive system of a military vehicle is investigated. Military vehicle industry has been in a rapid growth in the last 25 years and companies are in a competitive race in order to produce more powerful and durable vehicles. The more power means the more heat rejection demand from the cooling system. Due to armored plated hull and allocation of power pack and cooling system, ram air cannot be used for primary cooling. Thus, hydraulic fan drive system seems to be the best option for military vehicles.

In order to design and manufacture hydraulic fan drive system for a military vehicle, designer must be well aware of the properties of each component and interaction between them. In addition, the pressure and flow levels in system play an important role for component selection. Apart from these, designer's life will be easier, if it is available to determine achievable minimum and maximum fan speeds, system response to control signal and external effects and possible problem sources before production of the system.

At this point modeling and simulation come to designer's rescue. Situations in which simulation, modeling and analysis used are explained by A. Maria [9];

- Observation of certain processes in the real world is impossible or extremely expensive.
- Mathematical model can be formulated however obtained analytical solutions are too complicated.
- Validation of mathematical model of the system is impossible or extremely expensive.

In addition, simulation modeling is beneficial if a change in an existing system is to be made. Before implementation of the change into the system, the effects of the alteration can be tested. By the way, it is sometimes impossible to try out the changes in the real system, because, real system may not exist, there are too many changed variables to be tested, it would take too much time to test and finally costs can be too high.

Developing a mathematical model of a system of interest is an invaluable design step in order to obtain a better understanding of the system. However, hydraulic fan drive system is composed of many complex components thus it is nearly impossible to derive simplified formulas for system performance prediction. Thus, in order to obtain a better understanding of the system, hydraulic fan drive system will be modeled and simulated using software packages in computer environment in this work.

Simulink® which is a toolbox of MATLAB® will be used in this work. Numerical computation, visualization and programming can be done by using high level language and interactive environment of MATLAB®. MATLAB® which is a commercially available software program is used for signal processing and communications, image and video processing, control systems, test and measurement, computational finance and a wide range of applications by more than a million engineers and scientists in industry and academia.

Simulink®, which is a block diagram environment for multi-domain simulation and model-based design, is integrated with MATLAB® and enables incorporation with MATLAB® algorithms into models and export simulation results to MATLAB® for further analysis. By deriving the differential equations of system components, every component of the system can be modeled and complete model of the system can be prepared in Simulink® environment.

Simulink® presents different modeling and simulating environments. One of them is Simscape™ in which mechanical, electrical, hydraulic and other physical domains can be simulated. Simscape™ provides prepared models for fundamental components of these domains such as diesel engine, electric motor, pump and some common mechanisms. Under the Simscape™ environment, SimHydraulics® and SimMechanics™ are found which are the specialized toolboxes for modeling and simulation of hydraulic and mechanical components, respectively.

1.2 Basic Concepts about Hydraulic Systems

In this part, initially, basic concepts about hydraulic fan drive system will be explained. Afterwards, subcomponents and swash plate mechanism of variable displacement pump is clarified.

1.2.1 Hydraulic Fan Drive Systems

In hydraulic fan drive systems, vehicle's cooling fan is driven by a hydraulic motor which is driven by a hydraulic pump. Hydraulic pump is driven by PTO (Power Take Off) of the engine or a belt drive. A simple hydraulic fan drive system is shown in Figure 1-5.

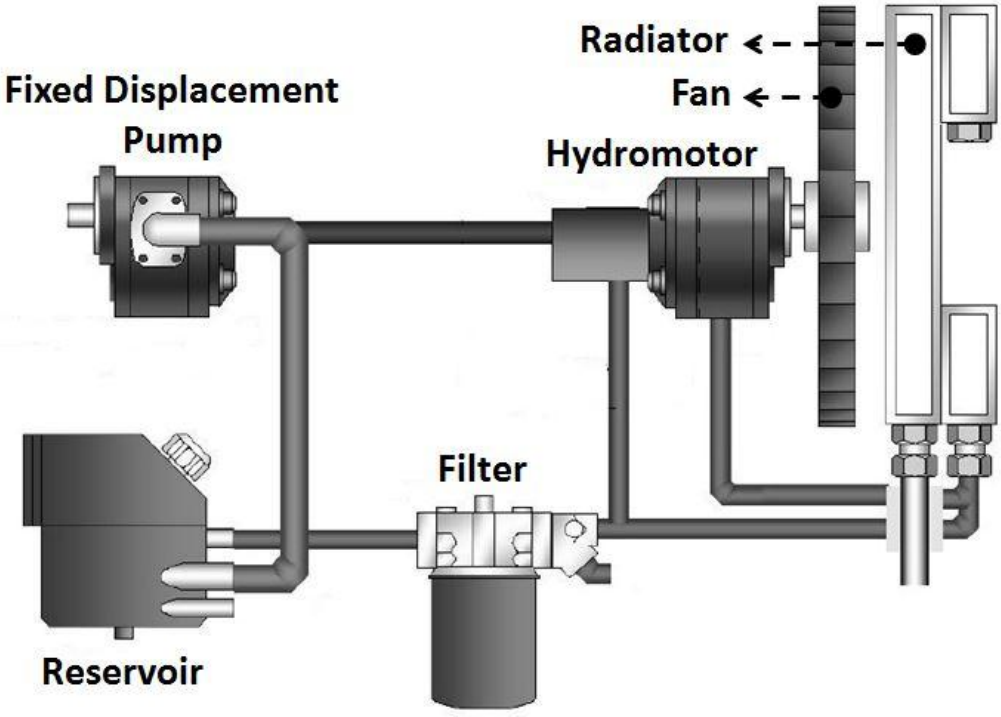

Figure 1-5 HFDS with Fixed Displacement Pump and Motor [10]

In the system shown in Figure 1-5, fixed displacement pump (FDP) and fixed displacement hydromotor (FDM) are used. Flow provided by the pump, Q_P, depends on the engine rotational speed, ω_e, displacement of the pump, d_p, and the volumetric efficiency of the pump, $\eta_{p,v}$. For coupled hydraulic motor and the fan, rotational speeds, ω_f, are equal and depend on the flow provided to hydraulic motor by the pump, displacement of hydromotor, d_m, and volumetric efficiency of hydromotor, $\eta_{m,v}$. Note that amount of fluid pumped per revolution of the pump's input shaft is defined as pump displacement.

$$Q_p = \omega_e d_p \eta_{p,v} \tag{1.1}$$

$$\omega_f = \frac{Q_p}{d_m \eta_{m,v}} \tag{1.2}$$

Fan speed directly depends on the pump drive unit which is the engine in the vehicle. There is no control option for HFDS with fixed displacement pump and motor. Such a system is similar to direct driven fan system except hydraulic motor and fan couple can be allocated freely.

In order to control the fan speed independent from engine speed, variable displacement pump (VDP) and/or variable displacement hydromotor (VDM) are used. In Figure 1-6, hydraulic fan drive system with variable displacement pump is shown.

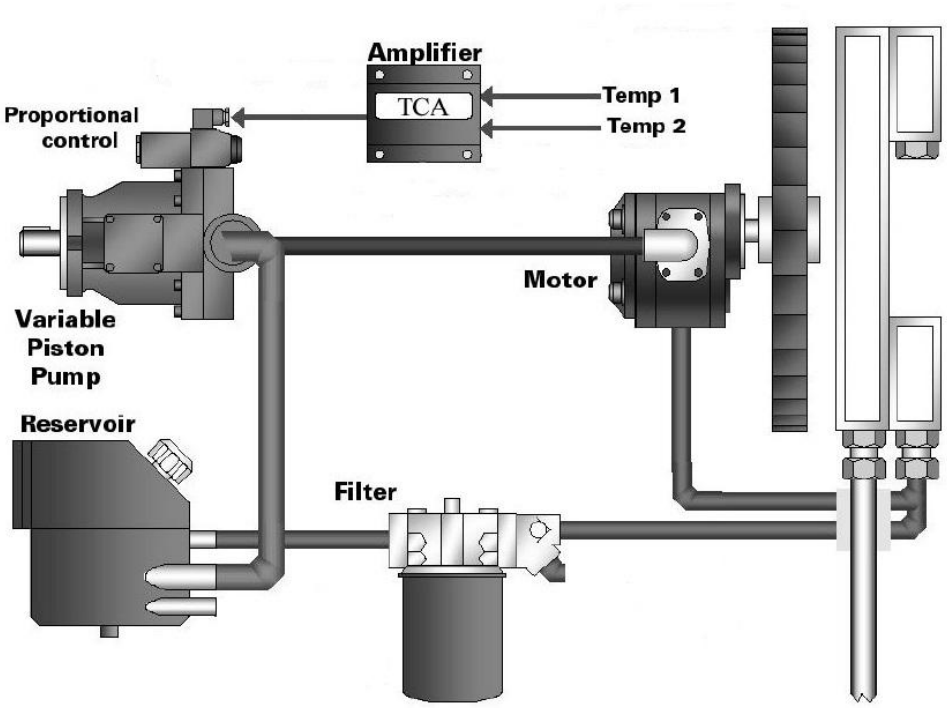

Figure 1-6 HFDS with VDP and FDM [10]

In the system, variable displacement pump is controlled by the control unit according to temperature values in the system and the rotational speed of the engine. By decreasing the displacement of the pump, fan speed can be lowered and vice versa, by increasing the displacement of the pump, higher fan speeds can be achieved. For example, on a cold day, when there is no need for fan rotation, theoretically, by lowering the displacement of the pump to 0, rotation of the hydromotor and fan can be stopped. Similarly, on a hot day, when

maximum fan rotation is needed, theoretically, by adjusting the displacement of the pump, maximum fan speed can be achieved. Maximum fan speed depends on engine speed, maximum displacement of the pump and the motor.

For the hydraulic fan drive systems with fixed displacement motor, fan speed directly depends on the flow provided by the pump. Thus, in order to obtain constant fan speed, independent of engine speed, flow provided by the pump must be fixed. According to Equation (1.1), in order to provide constant pump flow, pump displacement must be adjusted according to engine speed. This control algorithm is provided by different ways. One of them is electronic control. Electronic control unit can adjust pump displacement according to temperature values and engine speed. Although cooling system is controlled by a closed loop algorithm, hydraulic fan drive part of the system is an open loop because the fan speed data are not gathered. If fan speed information is also send to ECU, then closed loop control algorithm can be obtained for hydraulic fan drive system.

The other control method is hydraulic control. For the hydraulic fan drive applications, as the flow through hydromotor increases, torque driven by the fan increases. Consequently pressure in the system increases. There is a relation between flow rate and system pressure and pressure is proportional to square of flow rate. Therefore, fan speed can be adjusted by adjusting the system pressure. For fan drive applications, variable displacement pressure compensated pumps are used. Pressure compensated pumps provide full pump flow (maximum displacement) at pressures below the compensator setting. Once the pump flow is restricted, pressure will build up to the setting of the compensator and then the pump will decrease displacement to the level needed to maintain pressure setting. By electronically adjusting pressure compensator setting, different pressure levels can be regulated. Consequently, different fan speeds can be adjusted. Similar to ECU, since the fan speed data are not gathered, system control algorithm is open loop.

1.2.2 Variable Displacement Pump

Gear pumps and screw pumps are the some of the examples for fixed displacement pumps. Some types of rotary vane pumps, axial piston pumps and radial piston pumps are the examples for variable displacement pumps.

Axial piston pump is the common variable displacement pump used in vehicle technology due to their fast dynamic response and high efficiency compared to other pump designs. Figure 1-7 shows the general components of a variable displacement axial piston pump with inclined swash plate angle. Beside this type of axial piston pump, there is also axial piston pump with bent axis.

Swash plate on a ball bearing is positioned on the shaft which connects pump to mechanical power source. Odd numbered pistons and piston shoes placed in cylinder barrel and rigidly connected to swash plate. Cylinder barrel and pistons rotate with shaft while the valve plate is stationary. There are suction and delivery ports on valve plate over which pistons periodically pass during operation. When the piston starts its suction stroke, piston moves

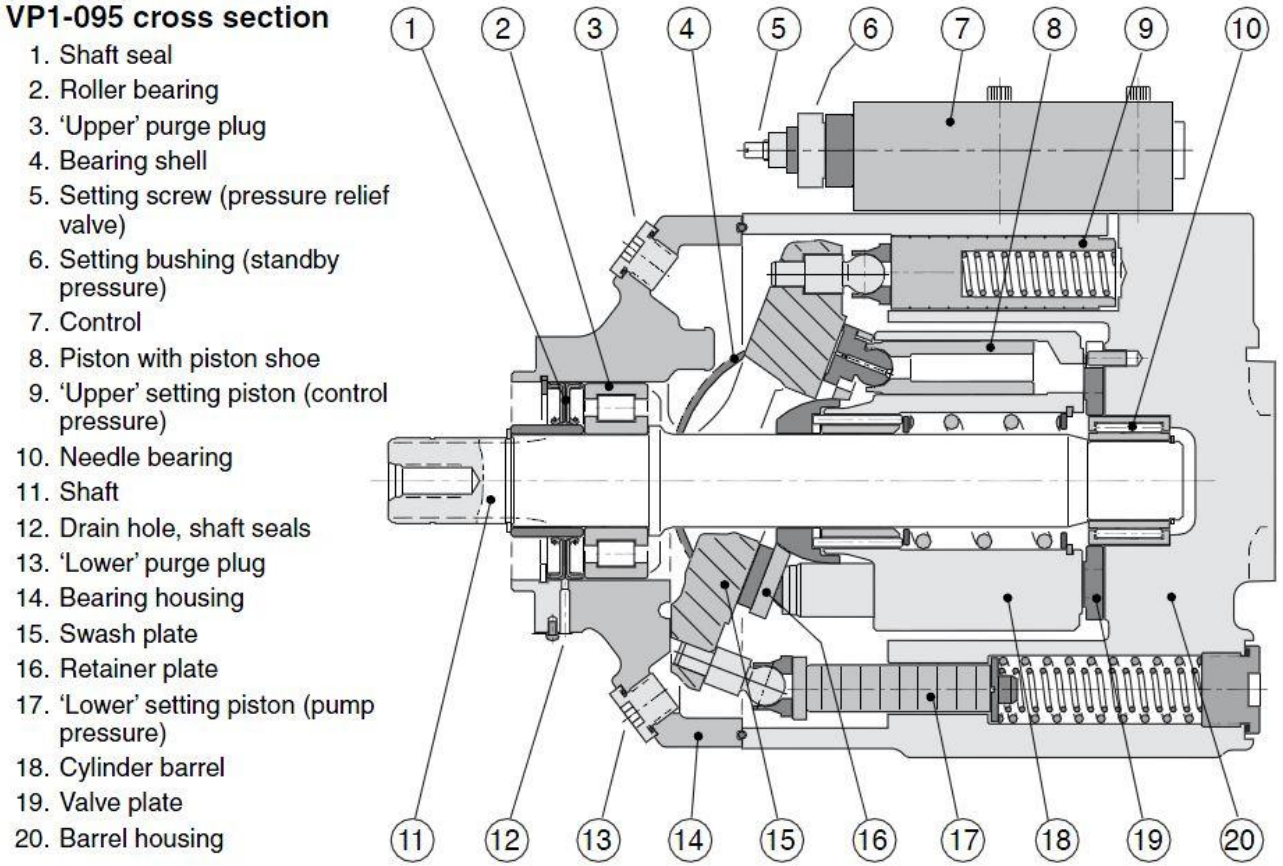

Figure 1-7 Variable Displacement Axial Piston Pump [11]

over suction port of valve plate and sucks the fluid under suction pressure. When the piston comes to end of suction port, it is fully retracted. On the contrary, when the piston comes to delivery port, it starts extending and pushes the fluid out of cylinder.

Displacement of the pump depends on extension rate of pistons inside cylinder barrel. Volume difference of pistons during suction and delivery ports determines the displacement of the pump. When the swash plate angle is maximum (Figure 1-8), extension rate of the piston is maximum, thus maximum flow is delivered to system. When swash plate angle is zero (Figure 1-9), there is no volume difference during the suction and deliver of the pistons. Consequently, displacement of the pump is zero for zero angle of swash plate.

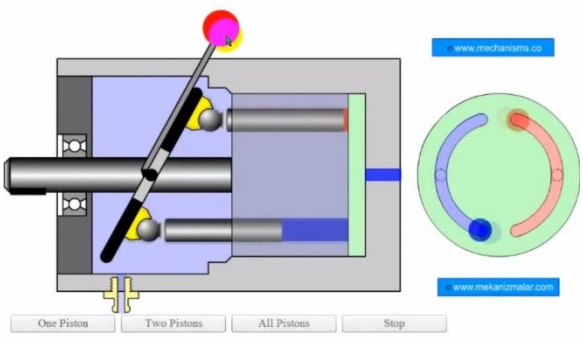

Figure 1-8 Maximum Swash Plate Angle [12]

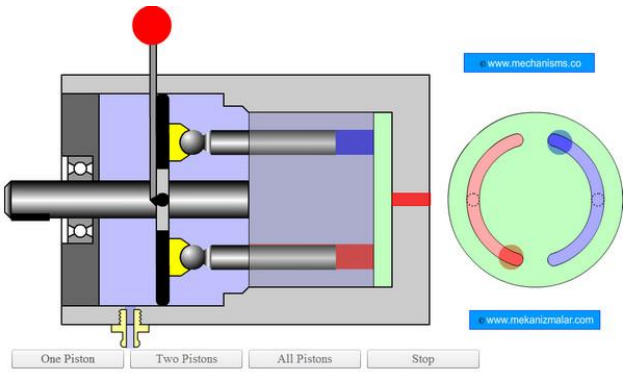

Figure 1-9 Minimum Swash Plate Angle [12]

1.3 Literature Review

In this section, an extensive review is carried out on the variable displacement pump dynamics, and modeling and simulation of hydromechanical systems. This section sets up the background for our study objectives.

1.3.1 Variable Displacement Pump Dynamics

For the displacement controlled hydraulic systems, variable displacement pump is the heart of the system. System efficiency, dynamic performance, response time and many other system parameters depend on the pump. Thus, variable displacement pump dynamics have been studied extensively.

In 1994, by assuming constant shaft rotational speed, P. Kaliafetis and Th. Costopoulos constructed a mathematical model for an axial piston variable displacement pump with pressure control. In addition, after identification of noteworthy parameters of the pump, computer simulation is performed. Good agreement between mathematical model and the manufacturer's dynamic operating curves is obtained [13].

In 1994, N.D. Manring and R.E. Johnson derived an approximate closed-form solution for the moments realized by the swashplate due to individual pistons pressure and piston kinematics and it is called as "Swivel Torque, T_s". In this work, it is mentioned that although the swivel torque is simply ignored in the previous researches; it is too significant to treat. The derived equation is:

$$T_S = \frac{N}{2}\left(\frac{-m_p r^2 \ddot{\alpha}}{\cos^4(\alpha)} - \frac{2m_p r^2 \dot{\alpha}^2 \sin(\alpha)}{\cos^5(\alpha)} - \frac{c_p r^2 \dot{\alpha}}{\cos^4(\alpha)} + \frac{m_p r^2 \omega^2 \tan(\alpha)}{\cos^2(\alpha)} - \frac{A_P r (P_d - P_i)\gamma}{\pi \cos^2(\alpha)}\right) \tag{1.3}$$

where N, m_p, r, c, and A_p are the number, mass, moment arm, damping coefficient and cross sectional area of the pistons, respectively. ω, α, P_d, P_i, and γ are the rotational speed, swash plate angle, discharge pressure, intake pressure, pressure carry-over angle of the pump, respectively.

Derived equation is compared with the experimental data and correlation between them is found good [14]. N.D. Manring and R.E. Johnson continued their studies and in 1996, they developed a closed form equation in order to guide the design of a variable displacement pump. In this work, dynamic equations for swash plate angle and discharge pressure are presented. The result of this study shows that inertial effects due to inertia of the swash plate and masses of the pistons (individual pistons and control pistons) and damping effects of pistons are negligible since they are much less than spring effects [15].

In 1996, G. Zeiger and A. Akers described a mathematical model of an axial piston pump. Swash plate motion is described as a second-order differential equation which contains torque components due to operating states. Authors present a method for computing an average torque at any given operating condition. Theoretical and experimental data are compared and found to be within 10 percent as shown in Figure 1-10 [16].

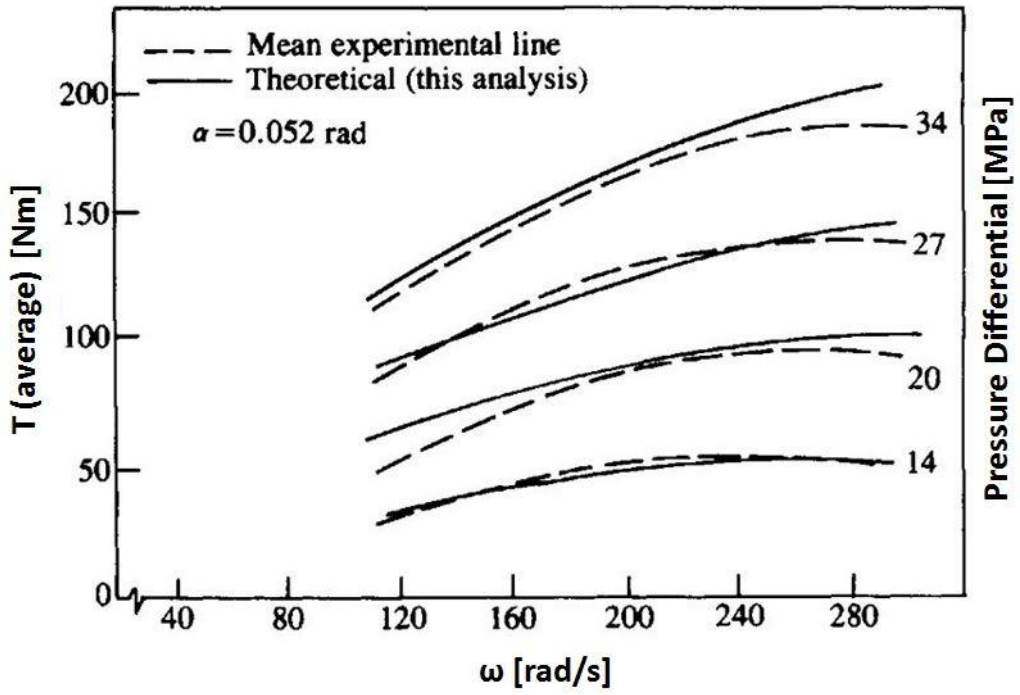

Figure 1-10 Average Swivel Torque vs. Shaft Speed [16]

In 2001, E. A. Prasetiawan developed a dynamic model to describe an earthmoving vehicle powertrain containing a variable displacement pump. Swashplate angle of the pump is regulated via closed-loop controller. Operator specified angle is compared to the actual swashplate angle obtained from angle transducer. According to the deviation between these values, control signal is created and swash plate controlling valve is energized. Author claims that swash plate dynamics is a second order system from an input force to a swashplate angle position. By controlling a servo valve position, the input force is regulated. Since the servo valve is second order system, overall swashplate mechanism is found as fourth-order. However, due to fast dynamics of servo valve with respect to swash plate, servo valve is neglected and transfer function of swash plate angle, α, is expressed as:

$$\frac{\alpha}{\alpha_{ref}} = \frac{K_{sp}}{s^2 + 2\xi_{sp}\omega_{sp}s + \omega_{sp}^2} \tag{1.4}$$

where K_{sp} is the swash plate control gain, ξ_{sp} is the swash plate damping ratio and ω_{sp} is the swash plate natural frequency [17].

In 2009, W. Kemmetmüller, F. Fuchshumer and A. Kugi described the mathematical model of self-supplied variable displacement axial piston pumps subject to fast changing and unknown loads. Schematic diagram of the electro hydraulic system is shown in Figure 1-11. Similar to P. Kaliafetis and Th. Costopoulos [13], researchers assumed almost constant angular velocity for the pump. A nonlinear, two degrees of freedom control strategy is proposed. Stability of the control system is proved by Lyapunov's theory [18].

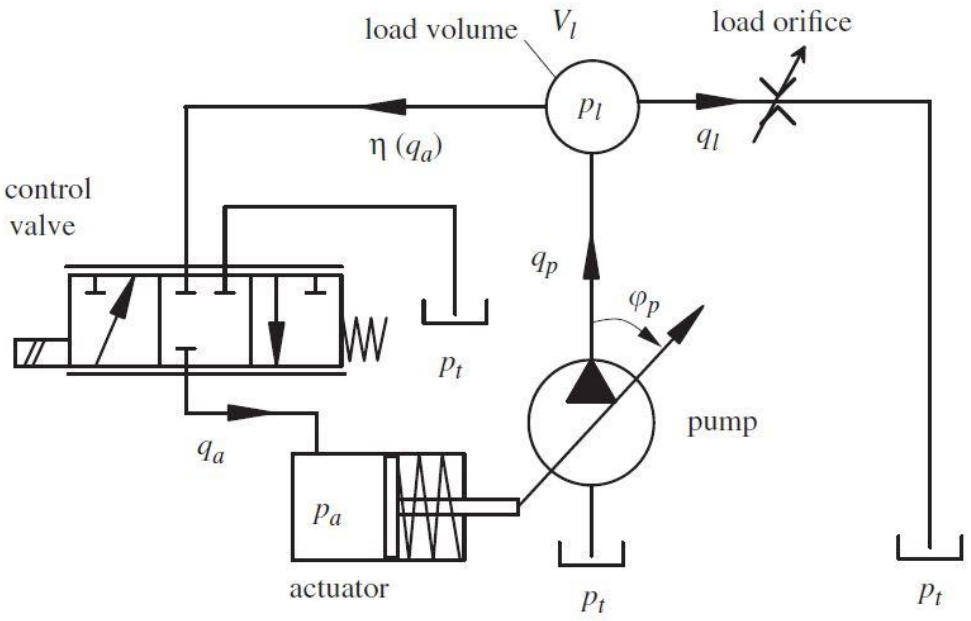

Figure 1-11 Schematic Diagram of Electro Hydraulic System [18]

In 2011, in order to accelerate the control system development time for an excavator, P. Casoli and A. Anthony applied a gray box modeling methodology on hydraulic pump. The flow and pressure compensators have been modeled as white box. On the other hand, flow characteristic of the pump is modeled as a black box. Experimental results showed that there is a linear relationship between control piston pressure and net torque on the swash plate. This relationship is used to develop black box model [19].

1.3.2 Modeling and Simulation of Hydromechanical Systems

Modeling and simulation play an important role during design and development of new systems. By the development of comprehensive and user friendly software packages, designers start to model even simple systems before production and testing.

In 2007, a model based approach for developing off-highway equipment machine systems was presented by M. Prabhu. Author explained the necessity of model based design instead of traditional design process. Verification of dynamic performance of machine systems in the absence of physical hardware, optimization of geometry of the system, rapid design iteration through various system concepts with multiple domains such as hydraulics, mechanics, electronics, traceability of how the machine performance requirements relate to different design decisions were defined as the advantages of model-based design over traditional design process. In order to verify the overall machine behavior, a multi-domain simulation was performed by the help of MATLAB/Simulink®. Pre-modeled system components under SimHydraulics®, SimMechanics™ and SimDriveline™ toolboxes of Simulink® were used to support modeling of the system. Author investigated different wheel holder applications and determined the performance requirements. SimHydraulics® was used to model hydraulic system which consists of cylinders, valves, pumps. In order to model dynamics of Z-Bar linkage of the wheel loader, SimMechanics™ was used. Finally, SimDriveline™ was used to model planetary gear train, the tires, and the longitudinal machine dynamics. All system components were modeled in a common environment [20].

In 2010, P. Marius expressed that fast and efficient computing system and of the algorithm, easy model creating via graphical editor, easy modification of variables and quick simulation make SimHydraulics® proper simulation tool for performing the functional tests of complex hydraulics systems. He modeled and simulated a hydrostatic drive system as shown in Figure 1-12 and Figure 1-13 [21].

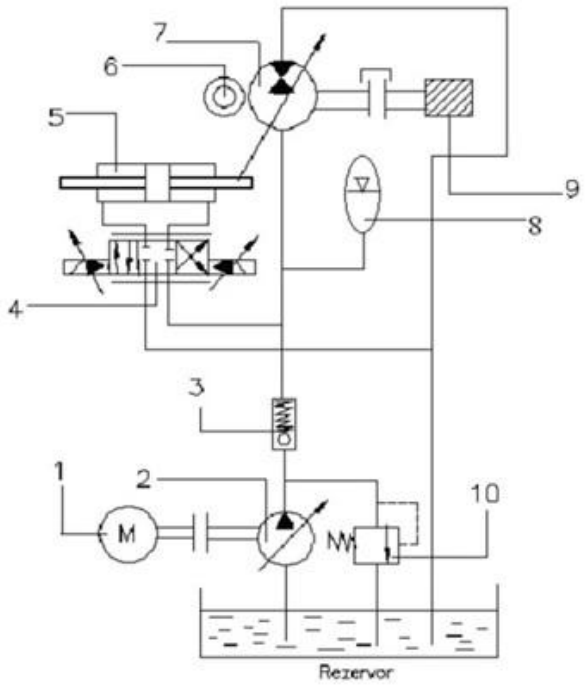

Figure 1-12 Hydrostatic Drive System Schematic [21]

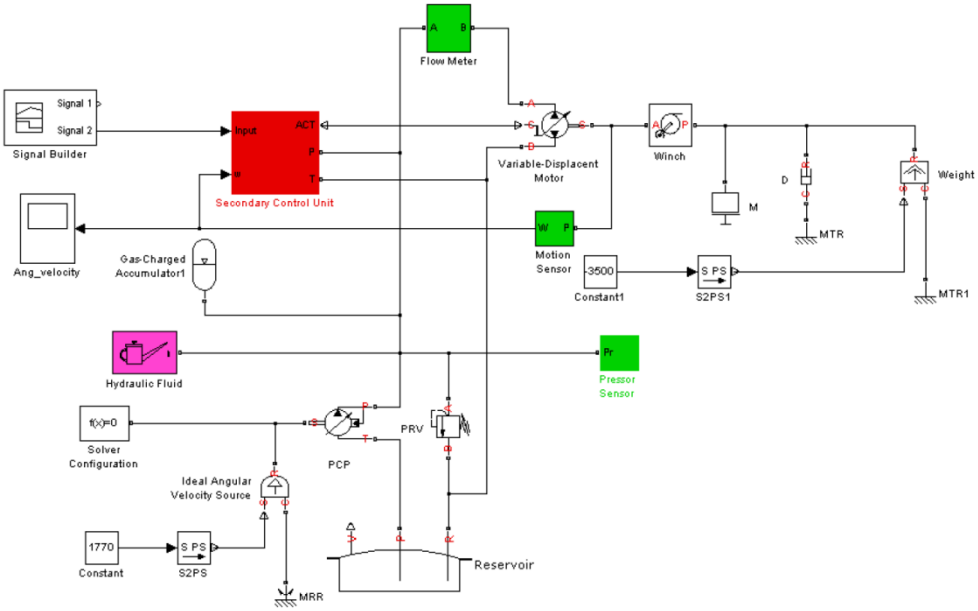

Figure 1-13 Hydrostatic Drive System Model [21]

According to simulation results, author determined the sensivity of the system to system parameters and suggested some improvements for improving the dynamic response of the system and preventing transient pressure oscillations.

In 2010, P. W. Lauvli and B. V. Lund used three different modeling tools to perform modeling and simulation of an existing hydrostatic transmission test bench as shown in Figure 1-14[23].

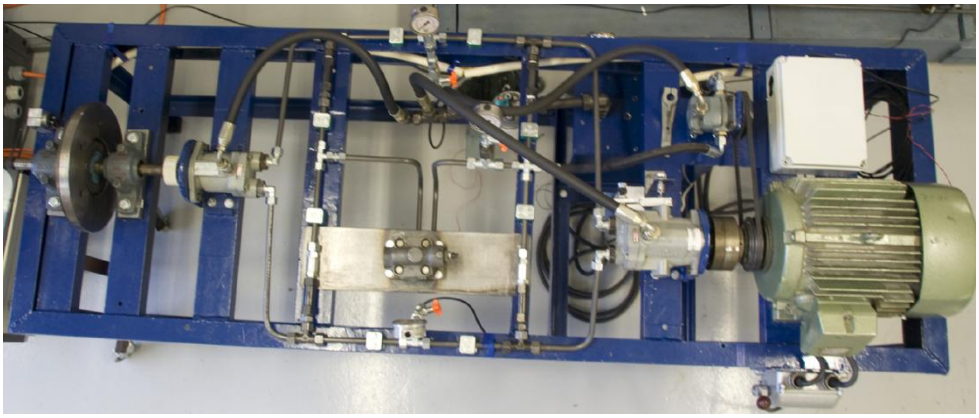

Figure 1-14 Hydrostatic Transmission Test Bench [23]

Prepared models in Simulink®, SimHydraulics® and SimulationX were compared not only with the experimental results in terms of accuracy but also they were compared between each other in terms of effort and time spent during preparation of model and simulating. In Figure 1-15, SimHydraulics model of the system is shown. According to experimental results, the author tried to estimate the frictional losses in the hydraulic motor in order to create a more detailed model.

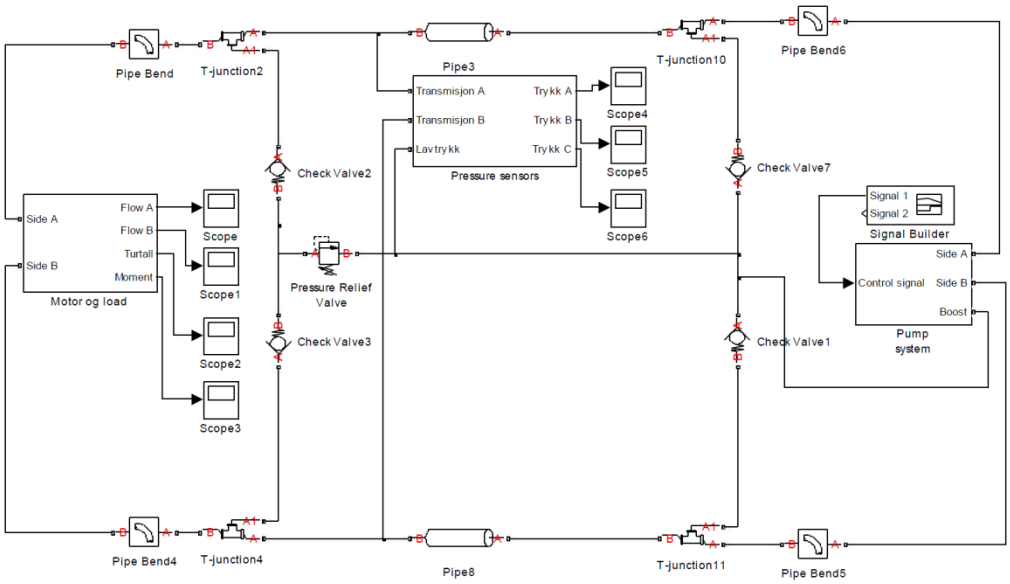

Figure 1-15 Hydrostatic Transmission SimHydraulics® Model [22]

In 2012, S. Hamzehlouia worked on modeling and control of the hydraulic wind energy transfer system. System schematic is shown in Figure 1-16.

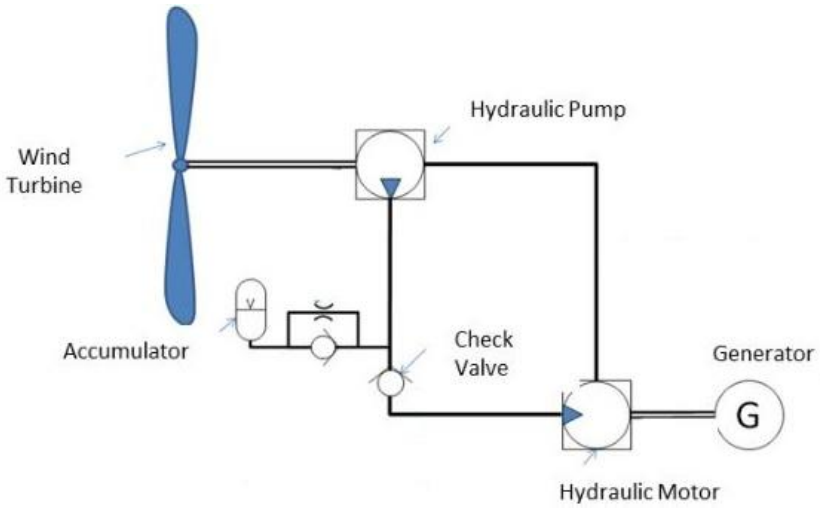

Figure 1-16 Hydraulic Energy Transfer of a Wind Turbine [23]

Complete mathematical model of the system is presented in both ordinary differential equations and state space representation. SimHydraulics® was used to verify the mathematical model in different operating conditions. Results showed that mathematical and SimHydraulics® models are compatible. Results of the system are compared with the experimental results obtained from a prototype. Author designed controllers to address the problems due to fluctuation on wind speeds and tracking of reference angular velocity [23].

1.4 Objective and Scope of the Study

The aim of this study is to model and simulate the hydraulic fan drive system of a military vehicle. Developed model is used for deeper understanding behind the hydraulic system and the components. System response to input signal, bottlenecks of the system are the other research objectives.

The system 'driving' variables - ones that performance measures are most sensitive to – are determined and interrelationships between the variables are analyzed. In addition, effect of each component on the system can be analyzed in a more cost saving and faster manner with the help of this model.

In this study, model is developed by the help of SimHydraulics® and SimMechanics™ software packages. The modeled system is tested experimentally in the vehicle. Vehicle engine rotational speed and fan speed data are collected. In addition, hydraulic system pressures and flow rate data are also gathered. Theoretical and experimental values are compared and accuracy of the model is determined.

1.5 Thesis Outline

This chapter gives a brief introduction on the cooling system in the vehicles and explains different type of fan drive systems. In addition, details about hydraulic fan drive systems and variable displacement pump are clarified. Furthermore, literature survey conducted on variable displacement pump dynamics and modeling & simulation of hydromechanical systems.

Following chapter describe the modeling of hydraulic fan drive system of a military vehicle. Details about system components (diesel engine, variable displacement axial piston pump, hydromotor, compensator, fan, flexible hoses, and hydraulic fluid) are given and prepared models are introduced.

In the third chapter, simulation and experimental results are compared for two selected scenarios. In addition, details about measurement equipments, measurement points, and acquisition system are presented.

In the fourth chapter, effect of orifice sizes (orifices inside the compensator) in the system performance is investigated by the help of the model prepared.

Finally, in the last chapter, brief summary of this work is given. In addition, findings of this study and possible future work on this subject is discussed.

CHAPTER 2

SYSTEM MODELING

2.1 Introduction

Circuit diagram of pre-designed hydraulic fan drive system of a military vehicle is shown in Figure 2-1. In this study, fan drive system of the vehicle is investigated and modeled by using MATLAB/Simulink® software. Main components of the system are diesel engine, variable displacement pump, compensator, hydromotor with an anti-cavitation check valve, fan, and hydraulic tank (reservoir). Diesel engine is the prime mover of the system. Variable displacement pump converts the mechanical energy produced by the engine to hydraulic energy and a fixed displacement hydromotor drives the fan. Finally, compensator is the controller of the system. Swash plate angle or in other words displacement of the pump is controlled by the compensator. Green lines illustrate the flexible hoses.

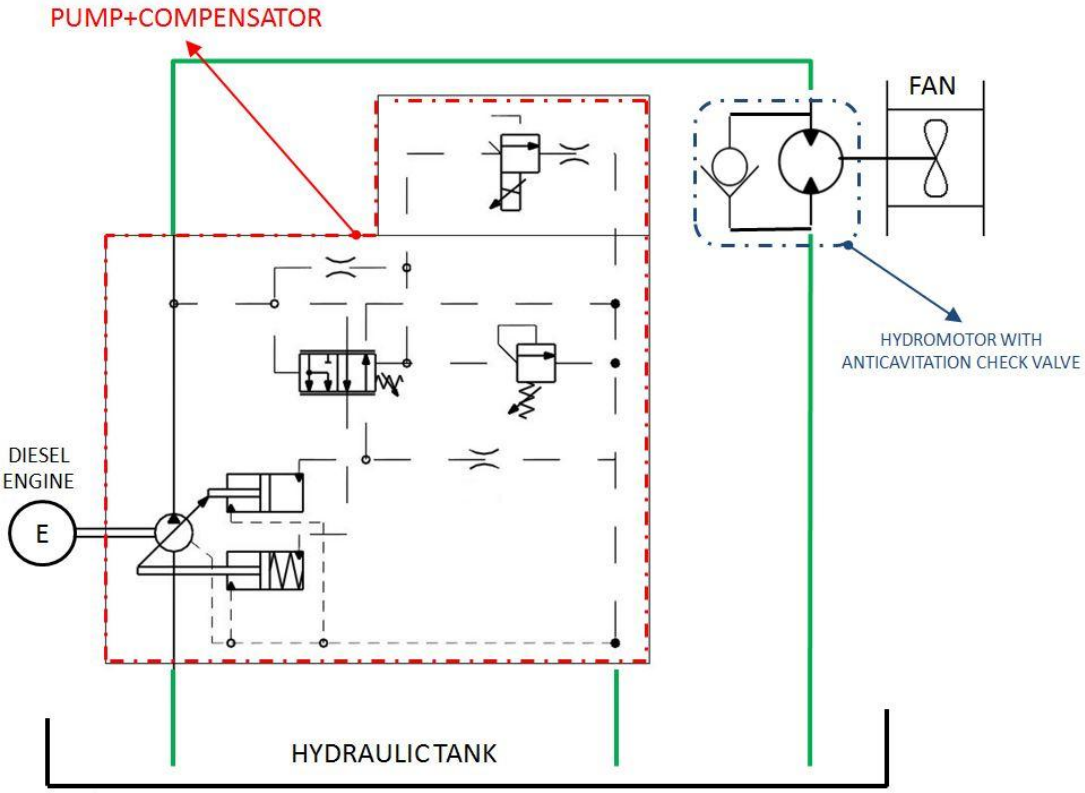

Figure 2-1 Hydraulic Fan Drive System

The engine driven unidirectional pump sucks oil from the hydraulic reservoir and pumps the oil to hydromotor which is coupled with fan. Return line of hydromotor is directly connected to reservoir. The swash plate angle of the variable displacement pump is controlled by the compensator which is integrated over the pump. Flexible hoses are used for connection between tank-pump, pump-hydromotor and hydromotor-tank. Note that although hydromotor is bidirectional, fan is rotated in only one direction since the pump is unidirectional and there is not a proper directional control valve.

Hydromotor, flexible hoses, hydraulic reservoir and hydraulic fluid are modeled by using the standard blocks under the SimHydraulics® library. On the other hand, custom subsystems are modeled for diesel engine, variable displacement pump, compensator, and fan. Models are developed by using the standard blocks under SimHydraulics®, SimMechanics™, SimScape™ and Simulink® libraries.

2.2 Engine Modeling

Deutz V6 engine is used in the vehicle. Engine is the primary source of mechanical energy used in the vehicle. The chemical energy stored in the diesel fuel is converted to mechanical energy after combustion process which takes place inside the cylinders, and resulting high pressure pushes pistons to rotate the crank-shaft.

The main purpose of the engine is to provide sufficient power to overcome the road load (aero drag, roll resistance, internal losses, and grade drag) the vehicle exposed while achieving the targeted acceleration, top speed, gradability and all means of other mobility actions. Secondly, some other subsystems such as alternators, air conditioners and pumps are fed by engine.

The operation range of the engine is between 700 rpm (low idle) and 2200 rpm (high idle) with a rated speed of 2100 rpm with a maximum power output of nearly 400 kW. Maximum torque output is achieved approximately at 1300 rpm with a value of 2130 Nm. Wide open throttle performance curve is given in Figure 2-2.

The variable displacement pump is connected to diesel engine via power take off with a speed ratio of 1. Torque and power consumption of the pump with respect to engine rotational speed is shown in Figure 2-3. Note that torque and power consumption curves are developed according to torque consumption of the fan and by assuming an average hydraulic system efficiency. According to Figure 2-2 and Figure 2-3, at wide open throttle position, maximum power consumption by the pump is less than 20% of engine power capacity.

There is a "Diesel Engine" model under SimDriveline™ toolbox of Simscape™. A diesel-fuel, compression-ignition engine with a speed governor is represented by this model. Maximum power, speed at maximum power and maximum speed are the only three parameters which are taken into account during calculations. However, maximum torque and speed at maximum torque are so important for modeling a diesel engine but the model does not take into account these parameters. Therefore, it is not meaningful to use this model.

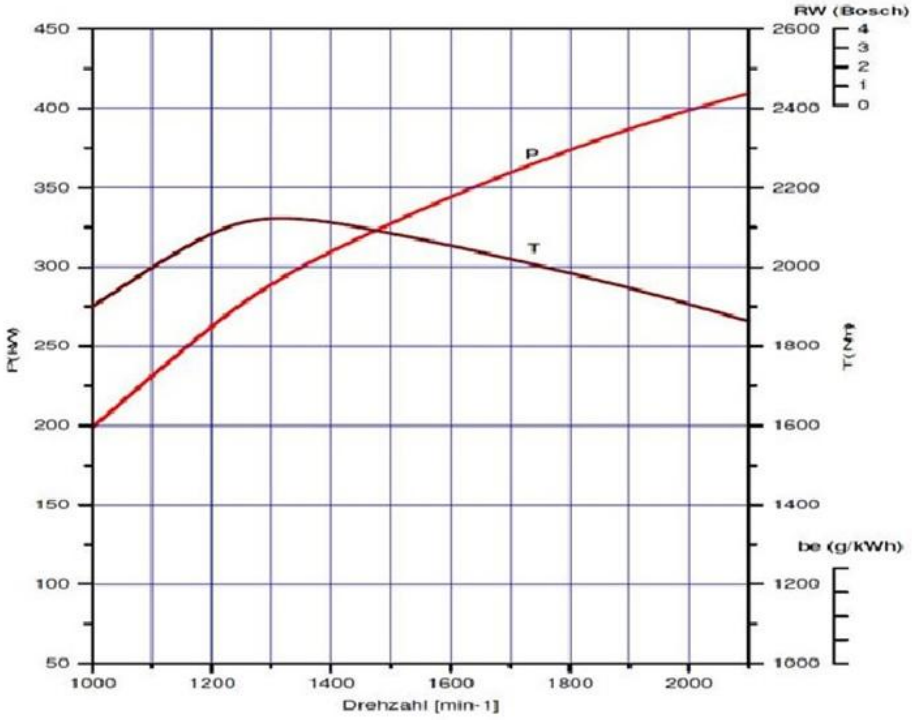

Figure 2-2 Wide Open Throttle Performance Curve

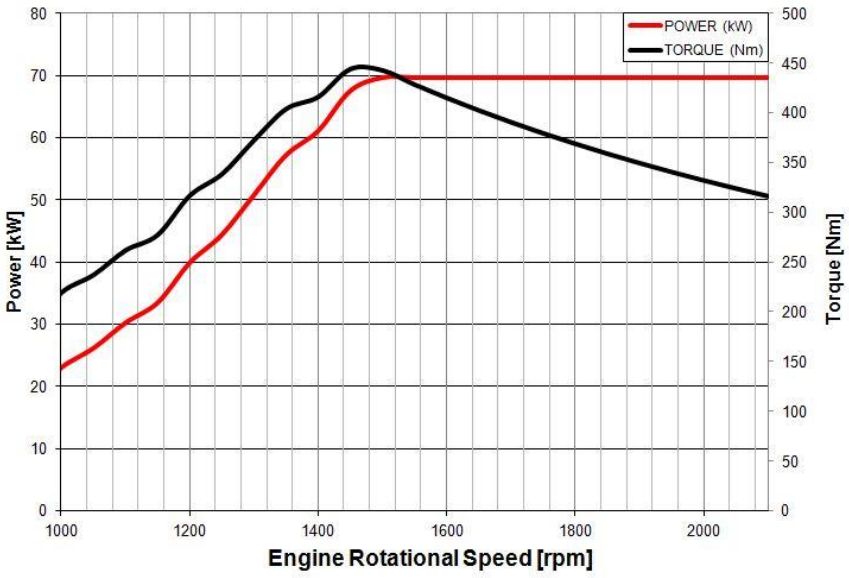

Figure 2-3 Torque and Power Curve vs. Engine Rotational Speed

A comprehensive engine model can be modeled if the required parameters are well defined. However, this model will not be beneficial if other subsystem components are not considered in the model. In other words, if it is required to model and simulate the engine, the other subsystems (driveline, vehicle dynamics, compressors, alternators, air conditioners) should be considered since their effects (80%) are much more than the hydraulic pump (20%). For these reasons, the engine is modeled as an ideal angular velocity source. Simulink® model prepared for the engine shown in Figure 2-4.

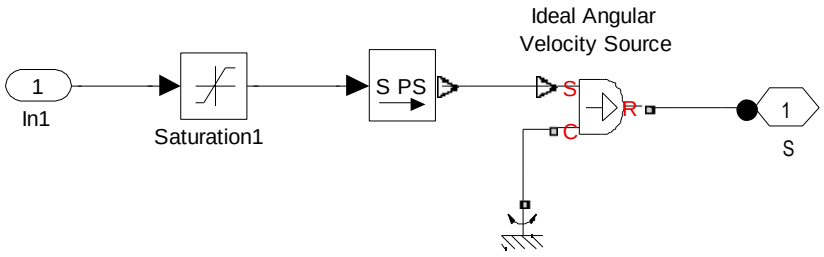

Figure 2-4 Simulink® Engine Model

In1 is the engine angular velocity input and S is the output for pump shaft connection. Saturation block is added in order to limit minimum and maximum angular velocity of the engine.

2.3 Variable Displacement Axial Piston Pump Modeling

Parker P1 Series variable displacement axial piston pump is used in the vehicle. Although SimHydraulics® toolbox offers a couple of variable displacement pump models, they are too simple and do not account swash plate dynamics.

Pump is the heart of a hydraulic system and system performance mainly depend on the pump dynamics. The situation for variable displacement pump is more dramatic. In order to prepare an accurate and comprehensive pump model, sufficient attention should be paid for swash plate dynamics.

Figure 2-5 illustrates the section view of the pump used in the vehicle. Parts with numbered 1, 2, 3, 4 and 6 are swash plate, bias spring, bias piston, cylinder barrel and control piston, respectively. There are 9 individual pistons positioned on the cylinder barrel, part with numbered 5. Swash plate angle is determined by the control and bias pistons, bias spring and the forces due to the reaction between swash plate and individual pistons.

To derive the differential equations for swash plate movement, Figure 2-5 is simplified and free body diagram for swash plate shown in Figure 2-6.

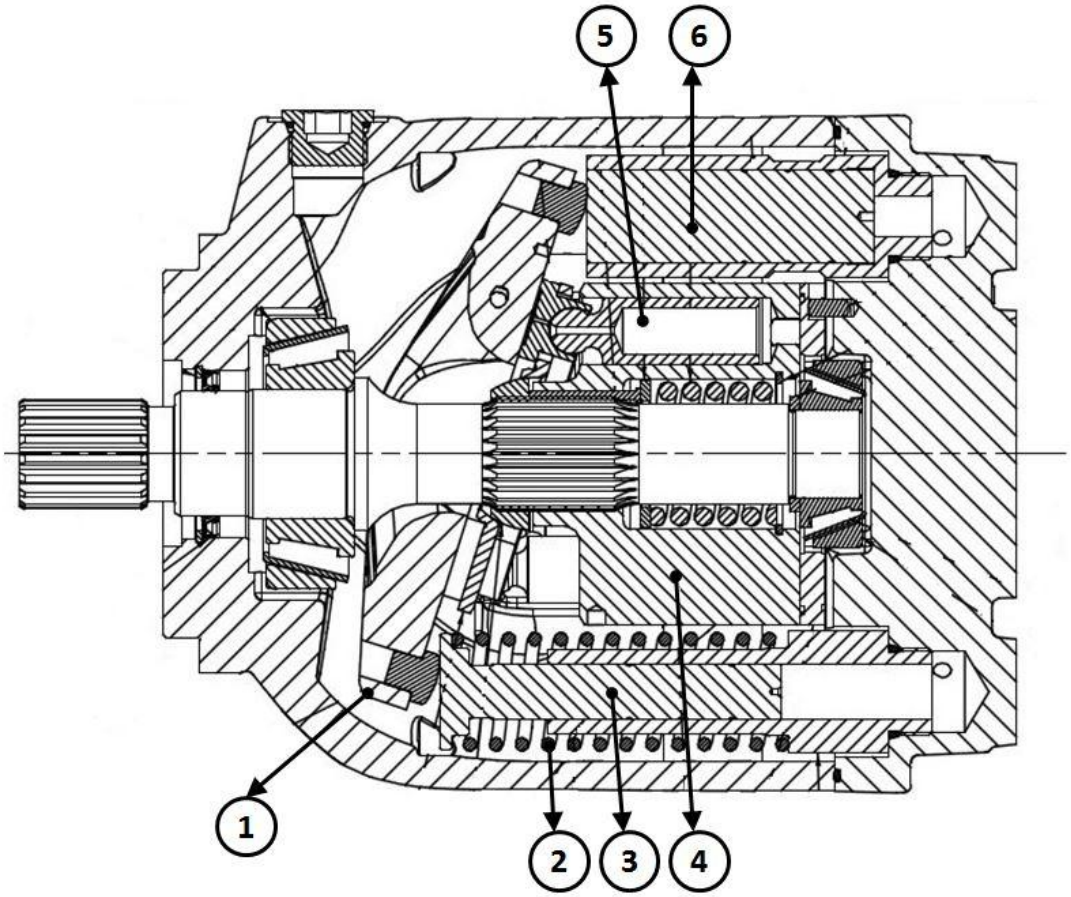

Figure 2-5 Section View of a Variable Displacement Pump

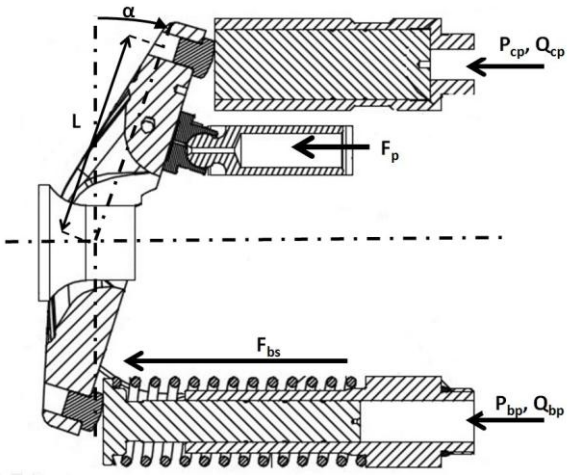

Figure 2-6 Free Body Diagram of Swash Plate

P and Q are the pressure and flow rate through the bias and control pistons, respectively. Subscripts bp and cp refer to bias piston and control piston. Friction between the swash plate and spherical bearing, and gravitational forces on the system are neglected since they are much lower than the other forces acting on the system. In addition, damping effect of oil inside the pump casing is also neglected.

Force exerted by the control piston, Fcp:

$$F_{cp} = m_{cp}\ddot{x} + c_{cp}\dot{x} + P_{cp}A_{cp} \tag{2.1}$$

where m, c and A are the mass, damping coefficient and cross-sectional area of the control piston, respectively and x is the position of piston:

$$\begin{aligned} x &= L\sin(\alpha) \\ \dot{x} &= L\dot{\alpha}\cos(\alpha) \\ \ddot{x} &= L(\ddot{\alpha}\cos(\alpha) - (\dot{\alpha})^2\sin(\alpha)) \end{aligned} \tag{2.2}$$

Similarly, force exerted by bias piston, F_{bp}:

$$F_{bp} = -m_{bp}\ddot{x} - c_{bp}\dot{x} + P_{bp}A_{bp} \tag{2.3}$$

Bias spring force, F_{bs}:

$$F_{bs} = k(l_0 - l) \tag{2.4}$$

where l_0 is the natural length of bias spring.

As mentioned in Literature Review part, in 1994, N.D. Manring and R.E. Johnson investigated the forces acting on an individual piston of a variable displacement axial piston pump [15]. The free-body diagram of a single piston is shown in Figure 2-7. They stated that these forces react against the swashplate. By summing the forces acting on each piston and multiplying with the moment arm, approximate closed form solution for the moments about the swash plate pivot point is found and it is defined as "Swivel Torque, T_s".

$$\begin{aligned} T_s = \frac{N}{2}\Big(&\frac{-m_p r^2\ddot{\alpha}}{\cos^4(\alpha)} - \frac{2m_p r^2\dot{\alpha}^2\sin(\alpha)}{\cos^5(\alpha)} - \frac{c_p r^2\dot{\alpha}}{\cos^4(\alpha)} + \\ &\frac{m_p r^2\omega^2\tan(\alpha)}{\cos^2(\alpha)} - \frac{A_P r(P_d - P_l)\gamma}{\pi\cos^2(\alpha)}\Big) \end{aligned} \tag{2.5}$$

Pressure carry over angle, γ, is defined as the angle between intake and discharge ports of valve plate. Figure 2-8 illustrates the pressure carry over angle.

Intake pressure is negligible when compared to discharge pressure; therefore, following assumption is feasible:

$$P_d - P_i \approx P_d \tag{2.6}$$

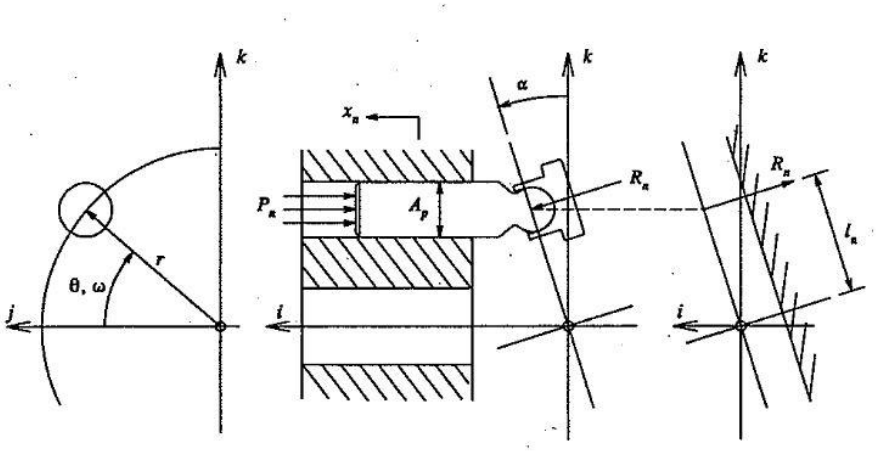

Figure 2-7 Free Body Diagram of a Single Piston [15]

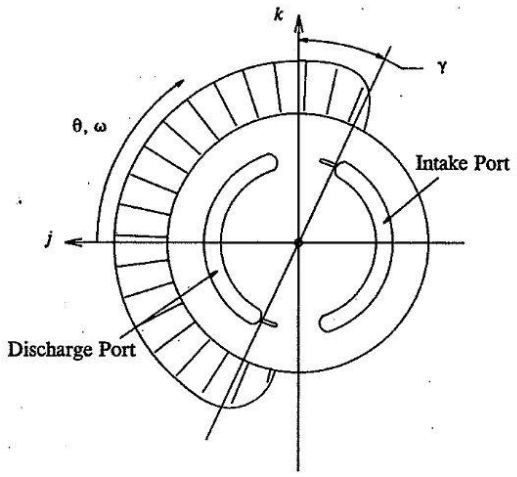

Figure 2-8 Pressure Carry Over Angle [15]

Simplified free body diagram of swash plate with swivel torque is shown in Figure 2-9.

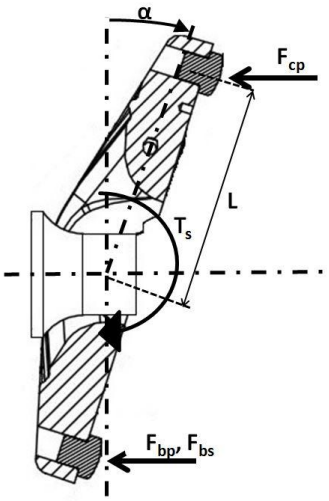

Figure 2-9 Free Body Diagram of Swash Plate with Swivel Torque

By summing the moments about the swash plate rotation axis, equation of motion for the swash plate is:

$$(F_{bp} + F_{bs} - F_{cp})L + T_s = I\,\ddot{\alpha} \tag{2.7}$$

where I is the mass moment of inertia of swash plate. Since maximum swash plate angle does not exceed 15°, equations can be linearized by assuming:

$$\begin{aligned} &\sin(\alpha) \approx \tan(\alpha) \approx \alpha \\ &\cos(\alpha) \approx 1 \end{aligned} \tag{2.8}$$

If equations from (2.1) to (2.6) are inserted into (2.7), a second order differential equation for swash plate angle is obtained:

$$I_{eff}\,\ddot{\alpha} + C_{eff}\,\dot{\alpha} + K_{eff}\,\alpha = T_{eff} \tag{2.9}$$

where

$$I_{eff} = I + (\mathrm{m}_{cp} + m_{bp})L^2 + \frac{N m_p r^2}{2}$$

$$C_{eff} = (\mathrm{c}_{cp} + c_{bp})L^2 + \frac{\mathrm{N c}_p \mathrm{r}^2}{2}$$

$$K_{eff} = \mathrm{kL}^2 - \frac{\mathrm{N}\, m_p\, \mathrm{r}^2\, \omega^2}{2}$$
$$T_{eff} = (\mathrm{A}_{bp}\mathrm{L} - \frac{\mathrm{NA}_p\, \mathrm{r}\, \gamma}{2\pi})\,\mathrm{P}_d + kl_0 L - \mathrm{A}_{cp}\mathrm{LP}_{cp} \qquad (2.10)$$

In 1987, S. Kim, Cho H., and Lee C. showed that pump dynamic behavior is insensitive to viscous friction coefficients [24]. This claim is also supported by Zieger, G. and Akers A. in 1986 [16]. Neglecting c_{cp}, c_{bp} and c_p terms, variable displacement pump model is developed in Simulink® environment, shown in Figure 2-10.

"Double Acting Hydraulic Cylinder" model under SimHydraulics® toolbox is used for modeling control and bias pistons. Block converts hydraulic energy into mechanical energy in the form of translational motion. Fluid compressibility in the cylinder chamber is taken into account. On the other hand, internal and external leakages are neglected. In addition, inertial load (mass of the pistons) are considered on swash plate dynamics model.

In order to model swash plate dynamics, SimMechanics™ toolbox is used. Model is shown in Figure 2-11. Transition between SimHydraulics® and SimMechanics™ models are done via "Prismatic-Translational Interface Element". Position (x), velocity and forces (F_{cp}, F_{bp}) due to pressure inside the cylinders are transferred to SimMechanics™ model from SimHydraulics® part.

Under the Swash Plate Dynamics model, swash plate angle is calculated and sent back to the system. Inertial effects of control and bias pistons (m_{cp}, m_{bp}), and swash plate (I) are modeled by using simple 'Body' model under SimMechanics™. Inertial effect due to 9 individual pistons (m_p) are added to swash plate inertia. "Body Spring&Damper" model is used to model bias spring (F_{bs}). Torque acting on the swash plate due to "Swivel Torque, T_s" is also calculated according to swash plate angle (α), rotational speed of the pump (ω) and system pressure [25].

Finally, "Variable Displacement Pump" model under SimHydraulics® toolbox is used to convert mechanical energy supplied by the diesel engine to hydraulic energy. Swash plate angle and the rotational speed of the engine are fed to block and flow is delivered proportional to these values. Maximum displacement of the pump, volumetric and mechanical efficiencies, nominal pressure, nominal angular velocity and nominal kinematic viscosity are the block parameters used for calculating the output flow. These values are gathered from the graphs and tables on the catalog pages of the product. In APPENDIX A, detailed specifications for the variable displacement pump are given.

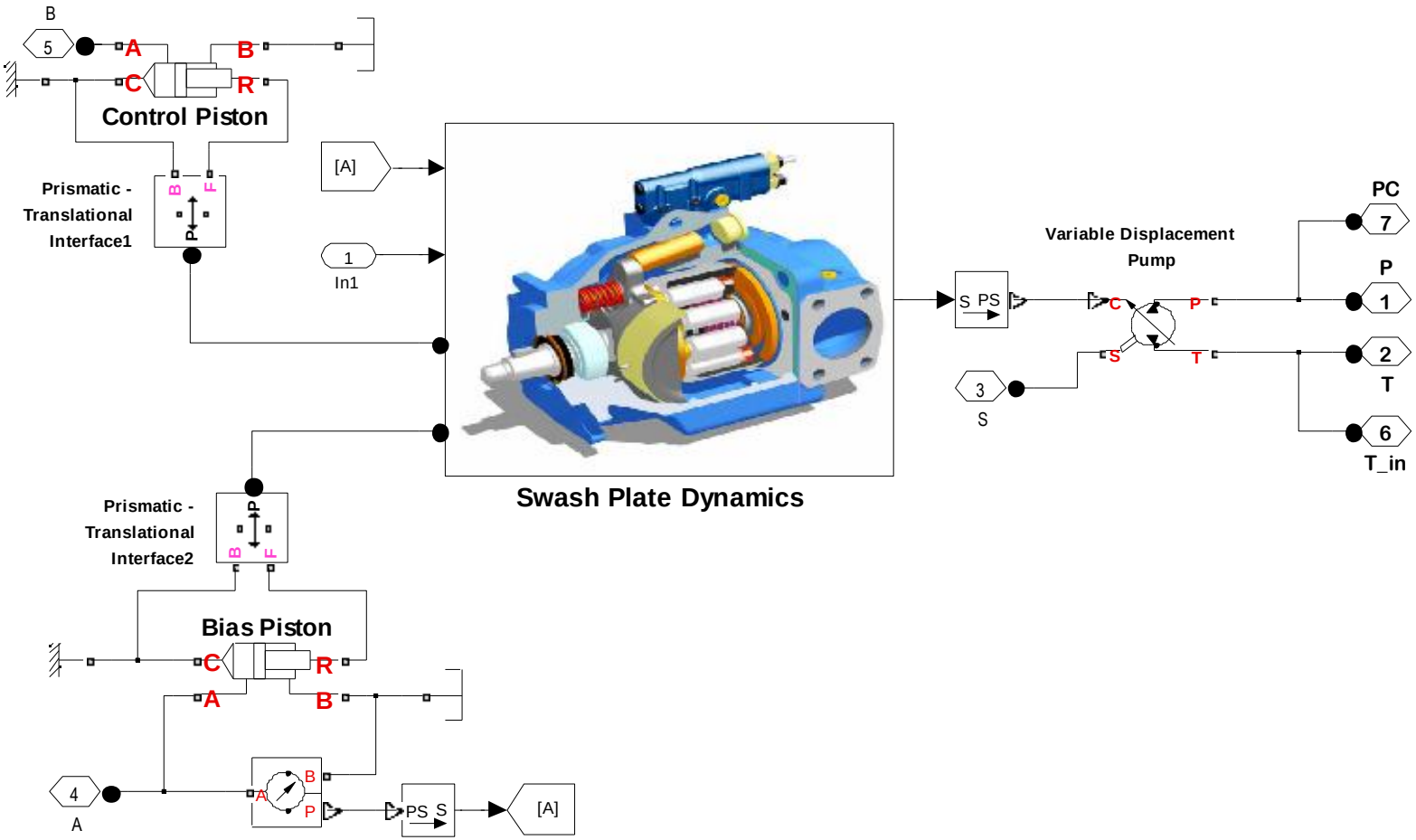

Figure 2-10 Variable Displacement Pump Model

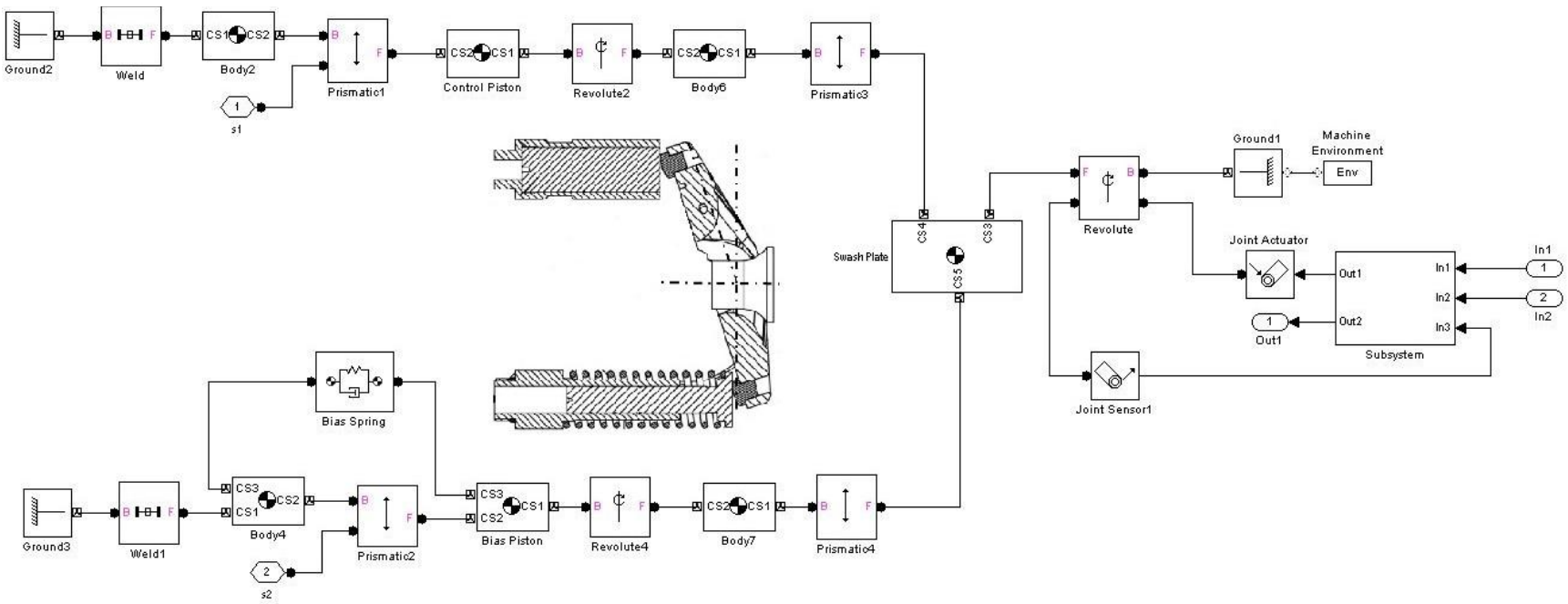

Figure 2-11 Swash Plate Dynamics Model

2.4 Compensator Modeling

Compensator is the controller of the system. Pump displacement or in other words, swash plate angle is controlled by the compensator. Schematic diagram and physical model are shown in Figure 2-12.

Compensator is composed of a spool with a spring, a relief valve, an electro-proportional relief valve, three orifices (ORF1, ORF2, ORF3), and a block with passages. Spool position is controlled via pilot pressures which act on two sides of the spool and the spring acting on the right side of the spool. ORF2 creates pressure drop between the left and right side of the spool and controls the spool movement. ORF1 controls the oil flow to control piston. ORF3 creates a pressure in front of the electro-proportional relief valve in order to damp valve movement. Proportional valve is the only element which is controlled by the ECU. When it is fully energized, it is fully open to tank via ORF3. Thus, pilot pressure on the right side of the spool is low and spool shifts to right side. In this position, compensator supplies oil for both bias and control pistons. Control piston diameter is larger than the bias piston. Consequently, swash plate angle decreases; therefore, flow provided by the pump decreases. On the other hand, when the proportional valve is de-energized, it is fully closed. Thus, pilot pressures acting on both side of the spool become equal, since there is no flow through ORF2. In this situation, spool comes to the position shown in Figure 2-1 and, compensator provides oil only to bias piston. Control piston is open to the tank. Consequently, swash plate angle comes to maximum position, and flow provided by the pump increases. Apart from these, voltage input to valve can be changed proportionally to reach desired output pump flow rate. In summary, pump flow rate is determined by the opening of the inverse proportional valve. Relief valve limits the maximum system pressure. For example, when the system pressure increases above the predetermined relief valve setting, normally closed relief valve opens and pilot pressure acting on the right side of the spool decreases. Then, spool shifts to right side and by the descent of swash plate angle, flow provided by the pump and system pressure decreases.

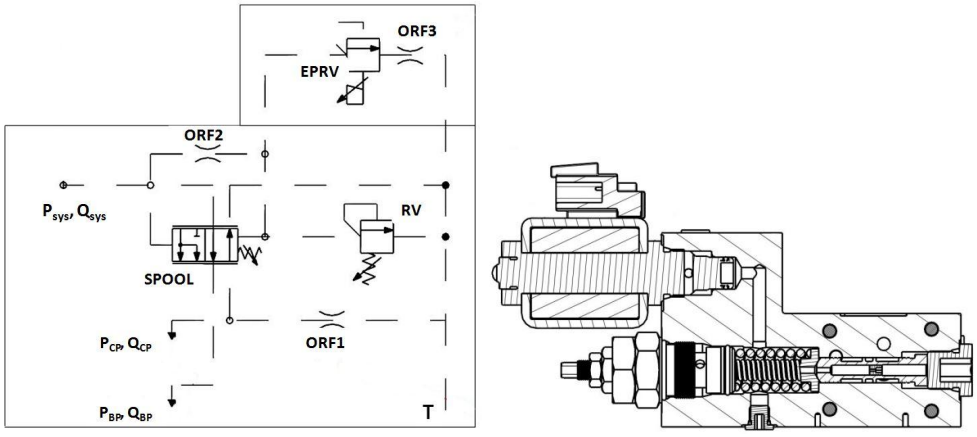

Figure 2-12 Hydraulic Circuit Diagram of Compensator

Prepared compensator model in SimHydraulics® is shown in Figure 2-13. In the next sections, details of the sub-components of the compensator are explained.

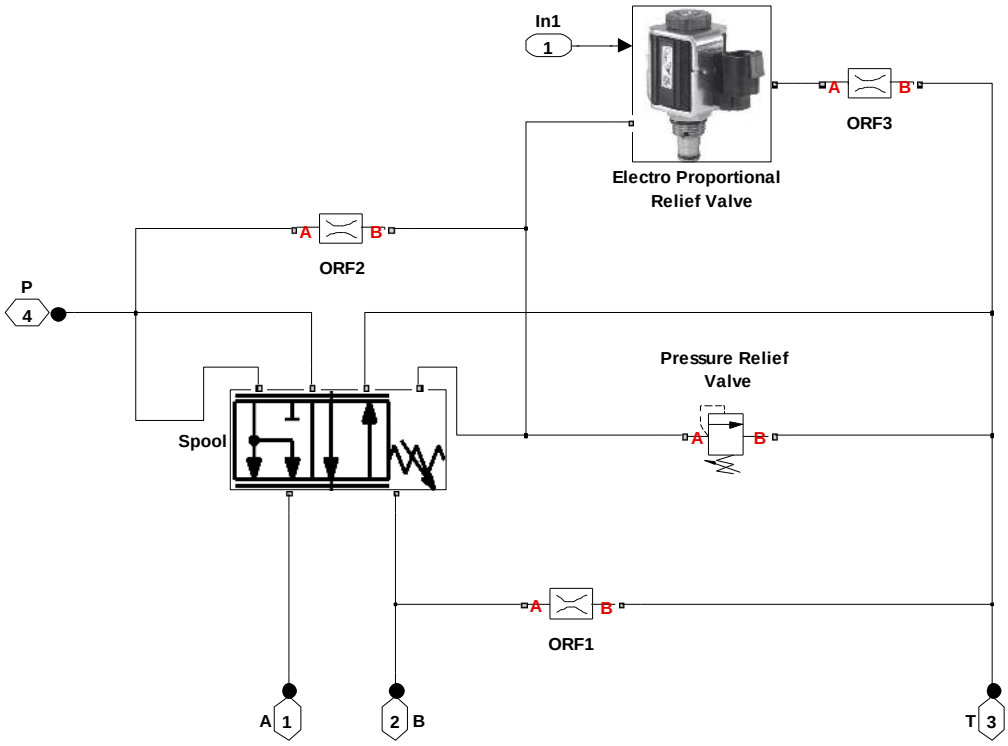

Figure 2-13 SimHydraulics® Compensator Model

2.4.1 Spool Modeling

Spool position determines the opening areas between ports P, A, B and T. Opening areas versus spool position, determined from three dimensional model, is shown in Figure 2-14. Model is developed since there is no proper model under the SimHydraulics® library.

Developed spool model is shown in Figure 2-15. Opening areas between ports are modeled by using "Variable Area Hydraulic Orifice" model under SimHydraulics® toolbox. Pilot pressures, acting on left and right sides of the spool and spring on the right side are modeled via "Hydraulic Double-Acting Valve Actuator" model which is a pilot actuator for directional and flow control valves. The model neglects flow consumption on the left and right side of the spool during the spool movement. In addition, inertial effects of spool and spring, and flow forces on the spool are neglected. Output of this model is the spool position. According to the spool position, valve opening areas determined by the "Lookup Table" prepared according to Figure 2-14.

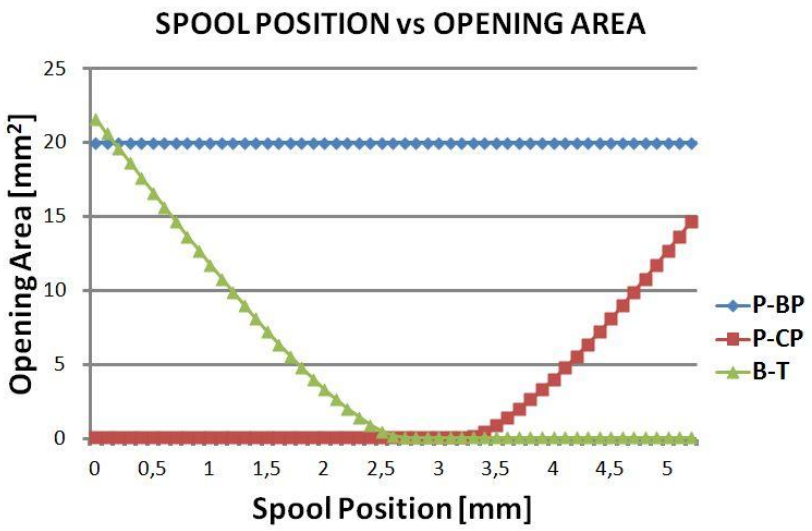

Figure 2-14 Opening Areas vs. Spool Position

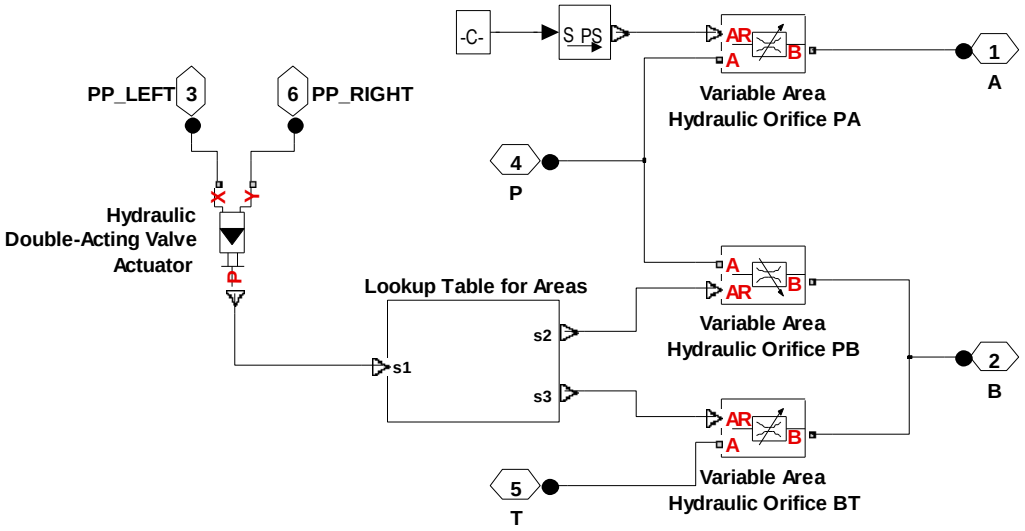

Figure 2-15 Spool Model

2.4.2 Electro-Proportional Relief Valve Modeling

Electro-proportional relief valve (EPRV) is an electro-proportionally controlled, normally closed pressure relief valve. The proportional control allows for infinite adjustability within the pressure range of the valve. When the upstream pressure is sufficient to overcome the set pressure of the valve, normally closed valve opens and allow flow from upstream to downstream. The valve used in the vehicle is inverse proportional relief valve. In other words, as the current increases, relief valve set pressure decreases proportionally. The pressure versus input current graph is shown in Figure 2-16.

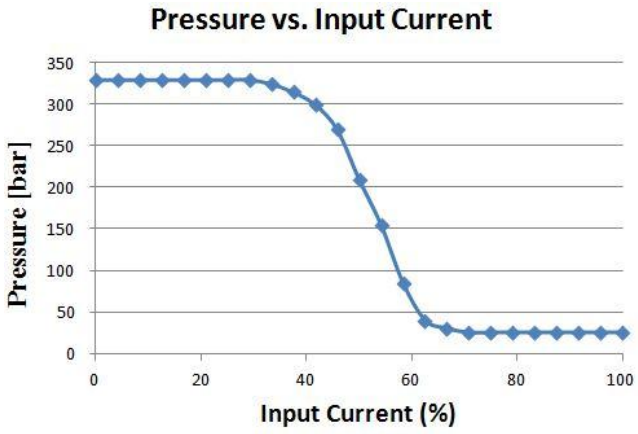

Figure 2-16 Pressure vs. Input Current [26]

Similar to spool, EPRV model is generated since there is no a proper model under SimHydraulics® library. Pressure vs. input characteristic of EPRV is integrated into the model by the Lookup Table. Hydraulic Pressure Source is used to sum the system pressure and the pressure corresponding to input current. Result is compared with the spring rate of the relief valve under the Hydraulic Double-Acting Valve Actuator model. According to output of actuator, opening of the normally closed "2-Way Directional Valve" is determined. "Delay" model is added in order to simulate the response time of the valve.

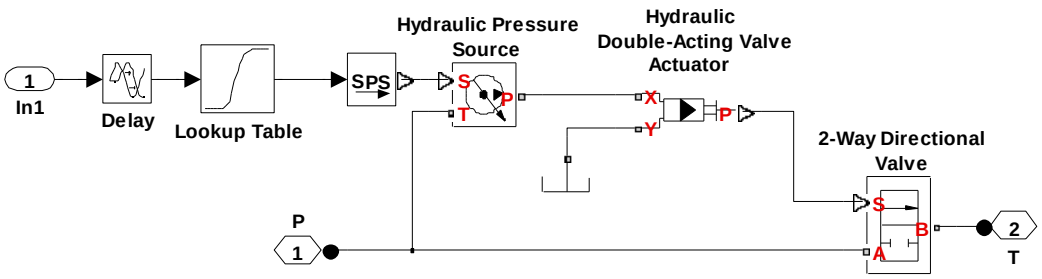

Figure 2-17 Electro-Proportional Relief Valve Model

2.4.3 Pressure Relief Valve Modeling

Standard "Pressure Relief Valve Block" under the SimHydraulics® Library is used for modeling. Valve remains closed while pressure at upstream of the valve is lower than the preset pressure. If pressure reaches the set value, then valve opens and some fluid is drained to tank. If the amount of fluid drained to tank is not enough, pressure continues to rise and opening area of the valve increases up to limit of A_{max}. At this point, if a higher flow rate is passed over the valve, then set pressure increases proportionally. Opening areas vs. upstream pressure of the valve is shown in Figure 2-18 generically [27].

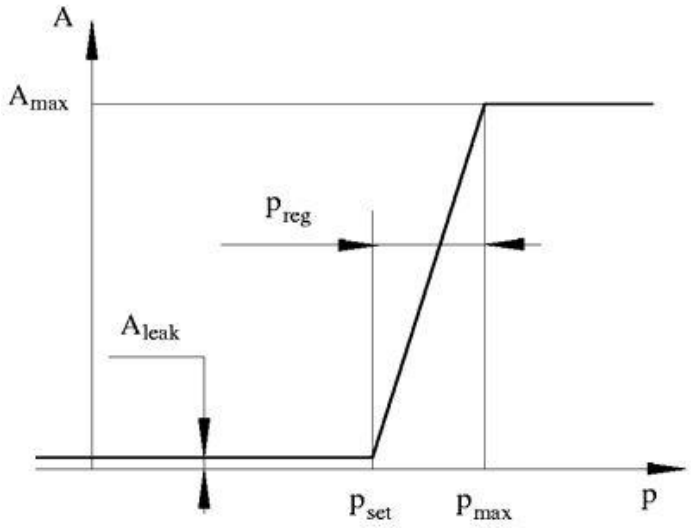

Figure 2-18 Opening Area vs. Upstream Pressure [27]

Although relief valves are normally closed valves, in the model it is required to define a leakage area (A_{leak}) in order to maintain numerical integrity of the circuit by preventing a portion of the system from getting isolated after the valve. Because isolated part could affect computational efficiency.

2.4.4 Orifice Modeling

"Fixed Orifice" block under SimHydraulics® library is used. Pressure differential across the orifice determines the flow rate. Fluid inertia is not taken into account in the model. In addition, transition between laminar and turbulent flow regimes is assumed to be sharp and taking place exactly at critical Reynolds number (Re). Flow discharge coefficient, critical Reynolds number and orifice area are the block parameters.

In all models where there is a flow over the component (relief valve, fixed orifice, variable area hydraulic orifice, directional control valve), laminar and turbulent flow regimes are taken into account by monitoring the Reynolds number and comparing its value with the

critical Reynolds number (Re_{cr}). According to comparison, flow rate is calculated according to following equations [27]:

$$Q = \begin{cases} C_d A \sqrt{\frac{2}{\rho}|\Delta P|} \cdot sign(\Delta P) & for\ \mathrm{Re} \geq \mathrm{Re}_{cr} \\ 2C_{dl} A \frac{D_h}{\nu\rho} \Delta P & for\ \mathrm{Re} < \mathrm{Re}_{cr} \end{cases} \tag{2.11}$$

where C_d and ΔP are the flow discharge coefficient and the pressure differential over valve, respectively. ρ and υ are the density and kinematic viscosity of the fluid. Terms related to turbulent flow regime C_{dl} and D_h are the flow discharge coefficient and the instantaneous orifice hydraulic diameter, respectively. Formulas for these terms are:

$$C_{dl} = \left(\frac{C_d}{\sqrt{\mathrm{Re}_{cr}}} \right)^2 \tag{2.12}$$

$$D_h = \sqrt{\frac{4A}{\pi}} \tag{2.13}$$

Detailed specifications, model block parameters and all related documents about compensator and sub-components can be found in APPENDIX B.

2.5 Hydromotor Modeling

Parker F12 Series Hydromotor with anti-cavitation check valve is used in the vehicle (see APPENDIX C for details). Standard "Hydromotor" and "Check Valve" models under SimHydraulics® library are used for modeling. The hydromotor model uses the following flow and torque equations [27];

$$\mathrm{Q} = d_m \omega + \mathrm{k}_{\mathrm{leak}} \Delta \mathrm{P} \tag{2.14}$$

$$\mathrm{T} = d_m\ \Delta \mathrm{P}\ \eta_{\mathrm{m,m}} \tag{2.15}$$

where Q is flow rate through the motor, d_m is the displacement of the motor, ω is the output shaft velocity, k_{leak} is the leakage coefficient which depends on the volumetric efficiency of the motor and finally ΔP is the pressure difference across the motor. Torque at the motor

output shaft, T, is the multiply of displacement, pressure difference and the mechanical efficiency of the motor. On the other hand, anti-cavitation check valve uses the Equation (2.11), (2.12), and (2.13).

Figure 2-19 illustrates SimHydraulics® model of hydromotor with anti-cavitation check valve.

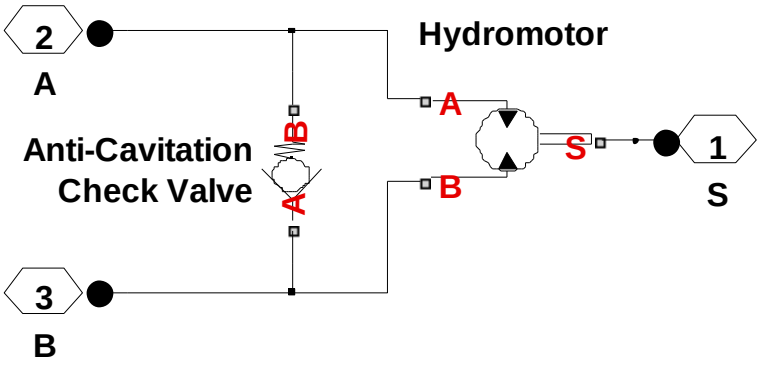

Figure 2-19 Hydromotor with Anti-Cavitation Check Valve

Note that anti-cavitation check valve is a standard check valve with low cracking pressure. It is used to prevent cavitation in the inlet to the hydromotor. Pump and hydromotor are directly connected, and if the flow coming out of the pump decreases at a rate faster than the flow being used by the hydromotor, cavitation will occur in the inlet of hydromotor. For example, when the engine stopped, there will be no flow out of the pump; however, inertia of the fan will try to rotate the hydromotor. In this case, hydromotor sucks the oil over the anti-cavitation valve that is drained by itself.

The model neglects the fluid compressibility inside the hydromotor. In addition, loadings on the motor shaft, such as inertia, friction are not considered in the model. Finally, leakage inside the motor (Q_{leak}) is assumed to be linearly proportional to its pressure differential. Leakage flow is computed by the Hagen-Poiseuille formula [27]:

$$Q_{leak} = \frac{\Delta P}{\mu} \frac{d_m \omega_{nom} (1 - \eta_{m,v}) \nu_{\text{nom}} \rho}{P_{nom}} \tag{2.16}$$

where ω_{nom}, υ_{nom}, and P_{nom} are the nominal values of angular velocity, kinematic viscosity and the pressure, respectively. Beside these, μ is the dynamic viscosity of the fluid.

2.6 Fan Modeling

Fan rotational speed and corresponding torque curve given by the supplier is shown in Figure 2-20 by the blue line.

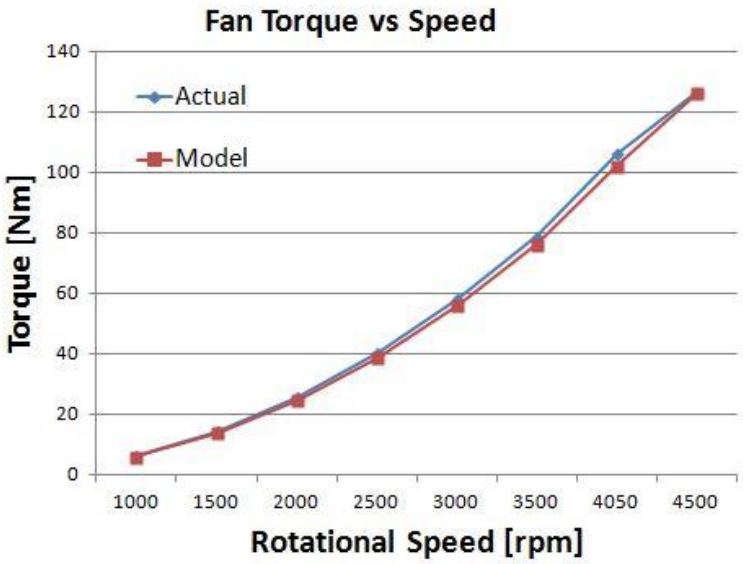

Figure 2-20 Fan Torque vs. Rotational Speed

By approximating that torque is proportional to the square of rotational speed; simplified torque equation is found and shown in Figure 2-20 by red line. Then total torque driven by the fan becomes:

$$T_{fan} = I_{fan}\,\dot{\omega} + D_{fan}\omega^2 \tag{2.17}$$

where T_{fan} is the torque driven by the fan and I_{fan} is the inertia of the fan. D_{fan} is the constant for the simplified fan torque equation.

Figure 2-21 illustrates the generated fan model in Simscape™ environment. The model is composed of inertia of the fan and an embedded Matlab function block to compute fan torque according to rotational speed. In addition, fan speed sensor is added into the model. Embedded Matlab function and specifications of the fan can be found in APPENDIX D

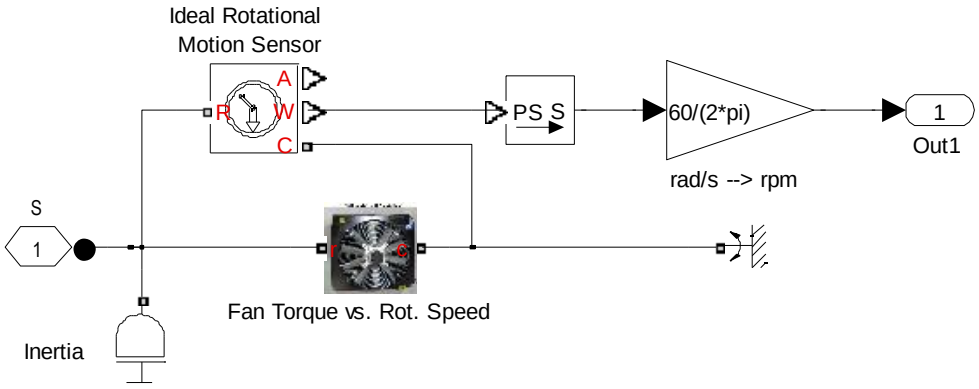

Figure 2-21 Fan Model

2.7 Pipeline Modeling

Standard "Hydraulic Pipeline" model under the SimHydraulics® library is used for modeling the flexible hoses which connect pump, hydromotor and tank. Figure 2-22 shows the SimHydraulics® model of the hydraulic pipeline. Two hydraulic resistive tubes calculate the frictional losses along the pipe length and fluid compressibility is evaluated under the constant volume hydraulic chamber block [27].

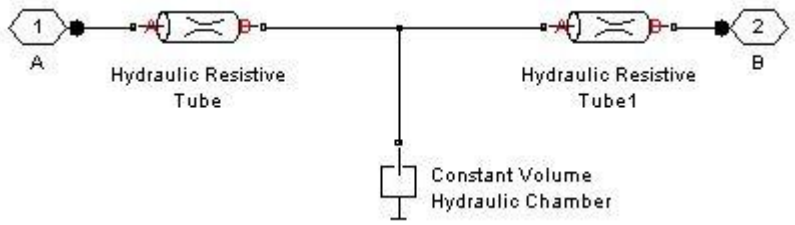

Figure 2-22 Pipeline Model [27]

Pipe cross section type, internal diameter, geometrical shape factor and pipe length of the pipe are taken into account in the model. Properties of hoses are tabulated in APPENDIX E.

2.8 Hydraulic Fluid Modeling

The oil used in the vehicle is not a standard oil. Thus, the most similar oil is selected from the hydraulic fluid list which is MIL-F-83282. Density of the oil is 825 kg/m^3 and viscosity is 17 cSt at 40°C working temperature. Additional specifications for the hydraulic fluid are tabulated in Table 2-1.

Table 2-1 Properties of Hydraulic Fluid

Properties	**MIL-F-83282**
Kinematic Viscosity	
@ 100°C	3.5 cSt
@ 40°C	17 cSt
@ -40°C	2000 cSt
Viscosity Index	128
Flash Point	230°C
Water Content	50 ppm

2.9 Summary

The Simulink® model containing all components described in this chapter is shown in Figure 2-24.

As mentioned before, one of the most important goals of fan drive systems is the regulation of fan speed independent of engine speed. In addition, electro-proportional fan speed control is invaluable property for fan drive systems.

For systems in which hydromotor and fan are directly connected, fan speed directly depends on hydromotor speed. Hence, fan speed is controlled by regulating the amount of fluid passing through hydromotor. For hydraulic fan drive applications, as the flow rate increases, fan speed increases and consequently, pressure level of the system increases. It can be concluded that, flow rate and pressure have strong relationship with each other. Therefore, by controlling the output pressure of the pump, fan speed can be regulated.

In the modeled system, electro-proportionally controlled compensator regulates the output pressure of the pump and fan speed is controlled indirectly. For constant current input to EPRV, compensator adjusts the swash plate angle (by adjusting the flow rate through bias and control pistons) in order to achieve constant output pressure by the pump. As a result, fan speed is controlled independent of engine speed.

Figure 2-23 is the generic illustration of the fan speed versus engine speed for 0% and 100% current input to EPRV. Red line indicates the maximum fan speed (no current to EPRV) with respect to engine speed. Note that for idle engine speed, for 0% current input to EPRV, swash plate angle is maximum however it is not sufficient to obtain the maximum fan speed since the flow delivered by the pump is low. Furthermore, as the engine speed increases, system pressure and fan speed increase until the relief valve on the compensator limits the pump outlet pressure. The engine speed at which the maximum fan speed obtained is called 'trim speed' and the pressure at this point is called 'cut-off' pressure. Note that for engine speeds higher than trim speed, fan speed is constant since the swash plate angle is decreased by the compensator and constant pump outlet pressure (cut-off pressure) is maintained. Green line indicates the minimum (idle) fan speed (100% current input to EPRV) with respect to engine speed. As it can be seen from the figure, idle fan speed is not zero. In order to stop the fan, swash plate angle should be reduced to zero. However, in order to reduce swash plate angle, control piston must be pressurized such that the force applied by the control piston is higher than the bias piston force plus the bias spring force. Besides that, in order to supply flow to control piston, left side pilot pressure acting on the spool should be increased such that it overcomes at least the spring force acting on the right side of the spool. Consequently, system has an idle pressure which corresponds to an idle fan speed.

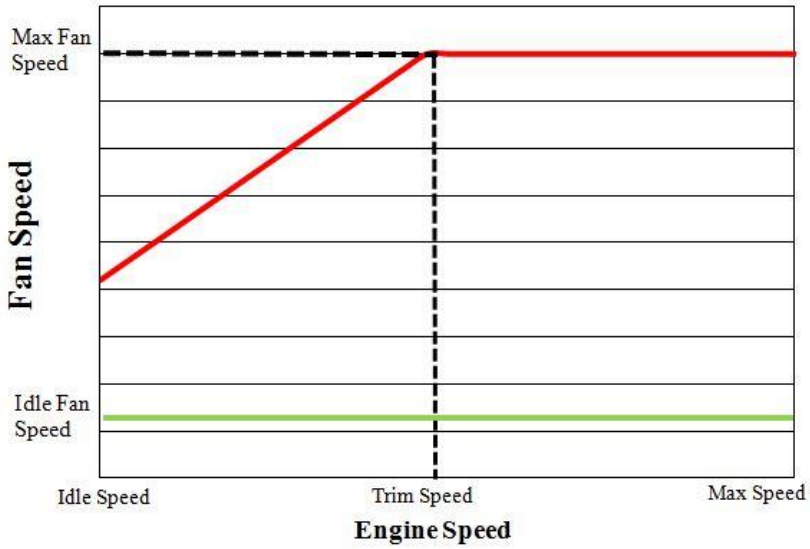

Figure 2-23 Fan Speed vs Engine Speed

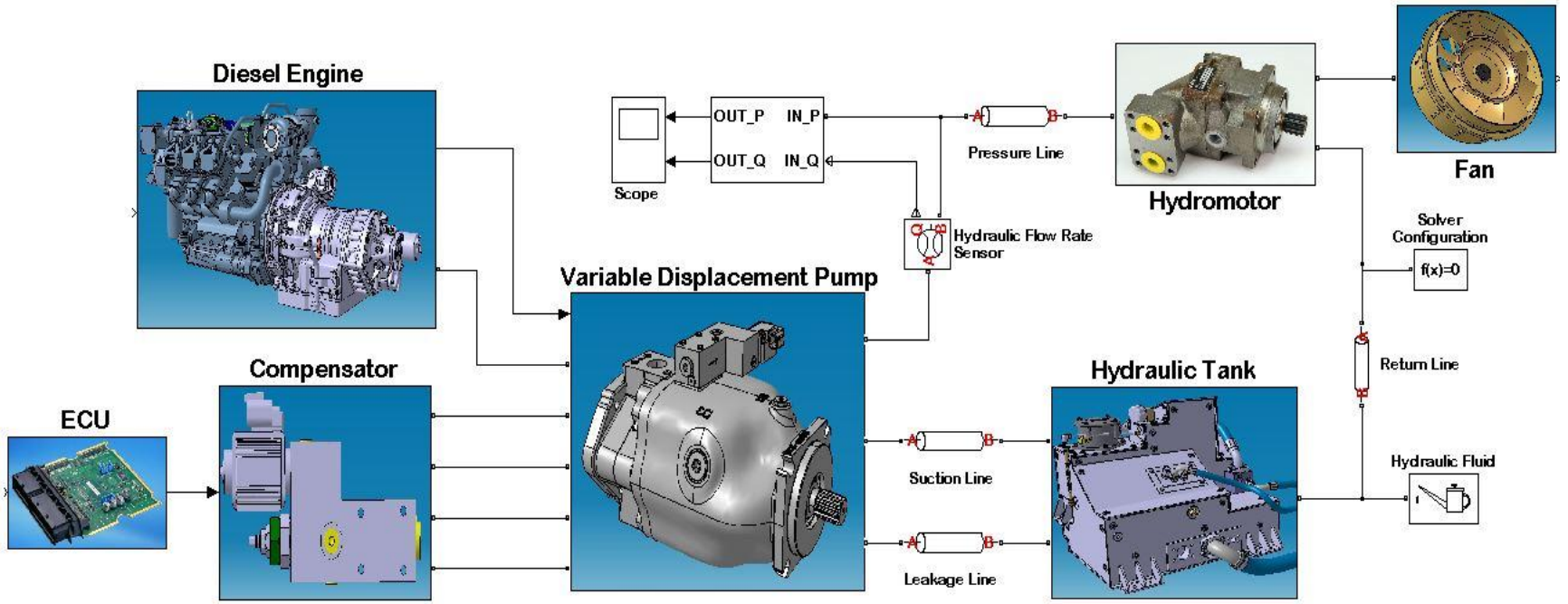

Figure 2-24 Hydraulic Fan Drive System Model

CHAPTER 3

SIMULATION AND EXPERIMENTAL VERIFICATION OF MODEL

3.1 Introduction

In Chapter 2, hydraulic fan drive system model is developed. The objective of this chapter is to verify the model experimentally. For verification, measured variables on the real system will be compared with simulation results.

In modeling and simulation environment, all system variables can be measured, even the leakage inside cylinders. However the situation is different for real world. On the real system, it is nearly impossible to measure some of the variables, which are available in the model, due to installation problems, space allocation, improper design, lack of proper measurement instruments and data acquisition system and so on.

In this study, measurements are done directly on the real system and measured variables are:

- Rotational speed of the diesel engine
- Pump discharge pressure
- Flow rate between pump and hydromotor
- Rotational speed of the fan

Other important variables such as swash plate angle, pressure inside control and bias pistons, position of the spool inside compensator and leakage rate due to compensator cannot be measured due to improper design of components.

In the start of this chapter, measurement instruments and the data acquisition system used in the test are clarified. Afterwards, experimental and simulation results are compared.

3.2 Measuring Instruments and Data Acquisition

There are embedded rotational speed sensors on the engine and the fan. Engine speed sensor is attached to the crankshaft of the vehicle engine. Speed sensor is the combination of a magnetic coil placed on the crankshaft and a metal disk. The speed data is send according to J1939 protocol with 20 ms sampling rate. Message content with hexadecimal numbering system is converted to decimal system and multiplied with the resolution of the sensor which is 0.125 rpm/byte.

Fan speed sensor is a proximity sensor providing an analog output and a switched output with 3.3 kHz frequency response. When the target (screws on the rotating part of the fan) is within the set point range of the sensor, the switched is normally open. When the target is out of view, switch is in a closed condition. The sensor sees screws and sends output voltage levels of between 0 and +5 V to ECU of the vehicle that tracks frequency of output voltage and calculates the fan speed. Turn on and turn off switching speeds of the sensor are 0.25 and 0.05 ms respectively [28].

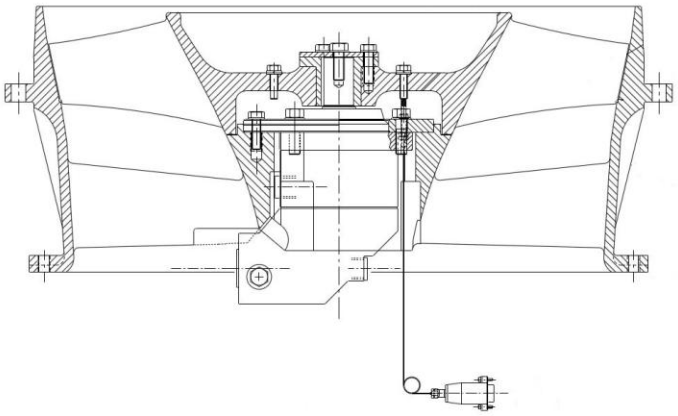

Figure 3-1 Fan with Embedded Speed Sensor

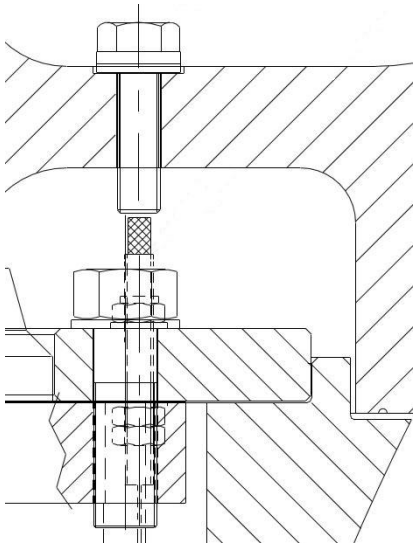

Figure 3-2 Fan Speed Sensor

PARKER SCPT-400 (400 bar) pressure transducer is used for measuring discharge pressure of the pump. The pressure transducer (Figure 3-3) has 1 ms response time and maximum ±0.5% error. In addition, embedded temperature sensor inside the pressure transducer has the capability of measuring fluid temperature between -25°C and 105°C with an accuracy of ±1.5%. Scanning rate of the transducer is 1 ms (1000 measured values/second).

Figure 3-3 PARKER SCPT-400 Pressure Transducer [30]

Flow rate between pump and hydromotor is measured with PARKER SCFT-150 (150 l/min) flow meter. It is a turbine type flow meter with ±1% accuracy and 50 ms response time. Figure 3-4 illustrates the flow meter.

PARKER Service Master Plus data acquisition instrument is used for collecting data from pressure transducer and flow meter. Up to 16 CAN-BUS sensor data can be collected simultaneously. Numerical, bar graph, pointer, and curve graphs can be displayed. In addition, measured data can be recorded and transferred to PC to analyze. Figure 3-5 illustrates the connection of pressure transducer and flow meter to Service Master Plus generically.

Figure 3-4 PARKER SCFM-150 Flow Meter [30]

Figure 3-5 PARKER Service Master Plus [30]

3.3 Experimental Verification

Model verification will be performed experimentally for two different scenarios. As mentioned before, there are two system inputs which are the engine speed and the current of the electro-proportional relief valve on the compensator.

At 700 rpm (nearly idle speed) and 2000 rpm (nearly maximum speed) engine speeds, by changing the input voltage of the electro-proportional valve, fan speed will be changed and simulation and experimental results will be compared. Note that resistance of the proportional valve is assumed to be constant, consequently, voltage and current is proportional. Thus, by changing the voltage input, it is assumed to change current input proportionally.

3.3.1 Scenario-1

Scenario-1 starts with 700 rpm engine speed and maximum voltage (24V) to EPRV. At t=10 s, ramp input with slope -1 V/s is given to EPRV until the input voltage is 0 V. At t=40 s, ramp input with slope 1 V/s is given until the input voltage is 24 V. Total simulation time is 70 seconds. Figure 3-6 illustrates the voltage input to EPRV versus time.

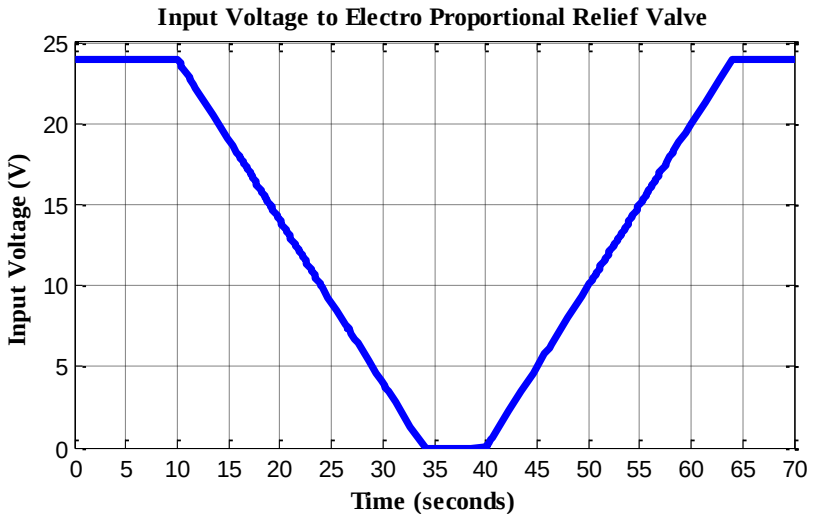

Figure 3-6 Input Voltage to Electro-Proportional Relief Valve

According to inputs, pump pressure, flow rate between variable displacement pump and hydromotor, engine speed and fan speed data are collected and transferred to MATLAB® environment.

Figure 3-7 shows the comparison between experimental and simulation results for the pump outlet pressure. According to Figure 3-7, despite some small discrepancies, results are in a good agreement. At 700 rpm engine speed and 24 V input voltage to proportional valve, pressure is approximately 28 bars. Although the input voltage is started to decrease at t=10 s, pressure of the pump starts decreasing at t=16 s due to characteristic of proportional valve (Figure 2-16). Pressure reaches ~65 bars at t=21 s. In this situation, although it is not measurable, according to hydraulic circuit diagram, swash plate angle and displacement of the pump are maximum and the pump behaves like a fixed displacement pump.

Simulation and experimental results for pump flow rates are shown in Figure 3-8. Similar to pump outlet pressure, results are consistent. The highest error occur at t=22 s which is less than 6%. In addition, during the increment and decrement of input voltage, there are small differences between the results in terms of slope of the curves and pressure levels.

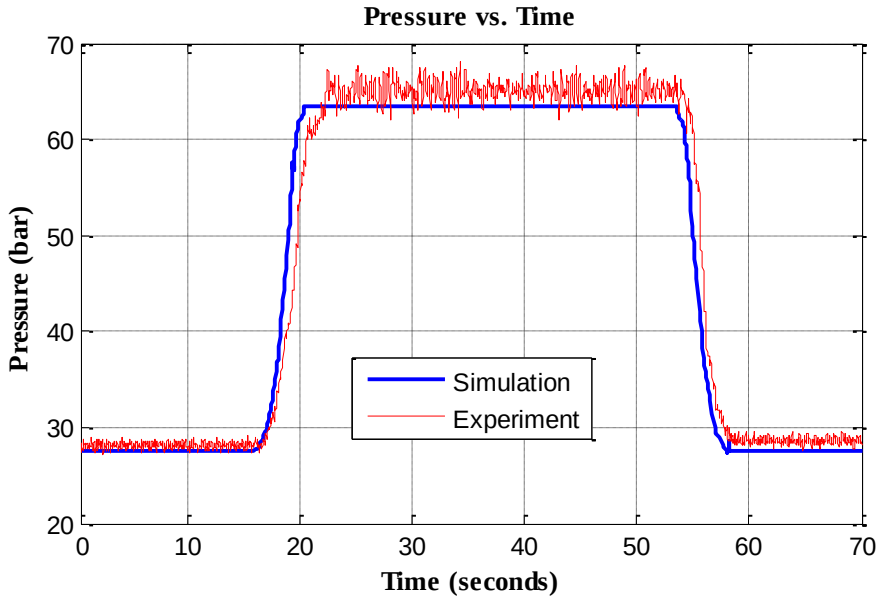

Figure 3-7 Pump Pressure vs. Time

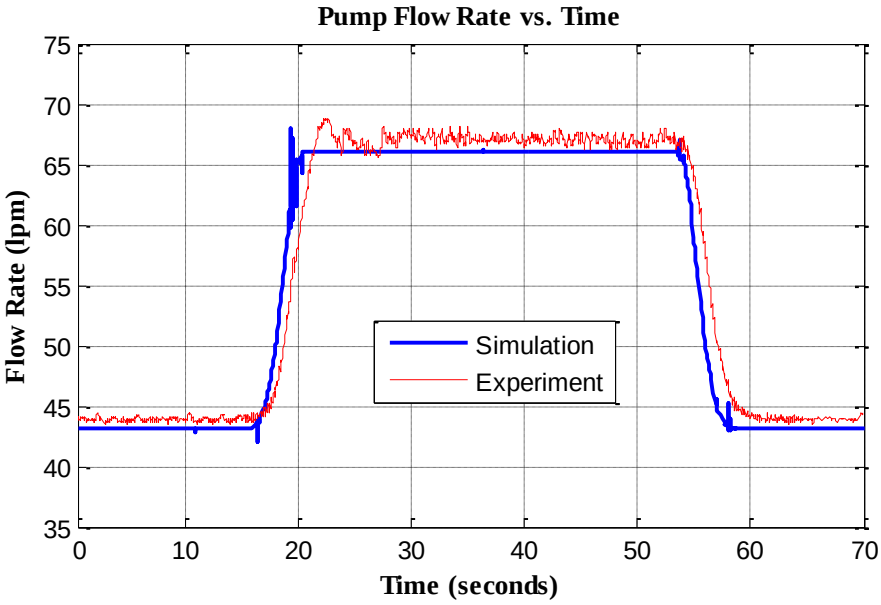

Figure 3-8 Pump Flow Rate vs. Time

In Figure 3-9 and Figure 3-10, fan speed and engine speed are plotted for simulation and experimental data. According to Figure 3-10, it can be concluded that modeling the engine as an angular velocity source is meaningful since the engine speed is nearly constant during the

measurements. From Figure 3-9, it can be interpreted that the fan model, which includes the fan inertia and the fan torque-speed curve, works well.

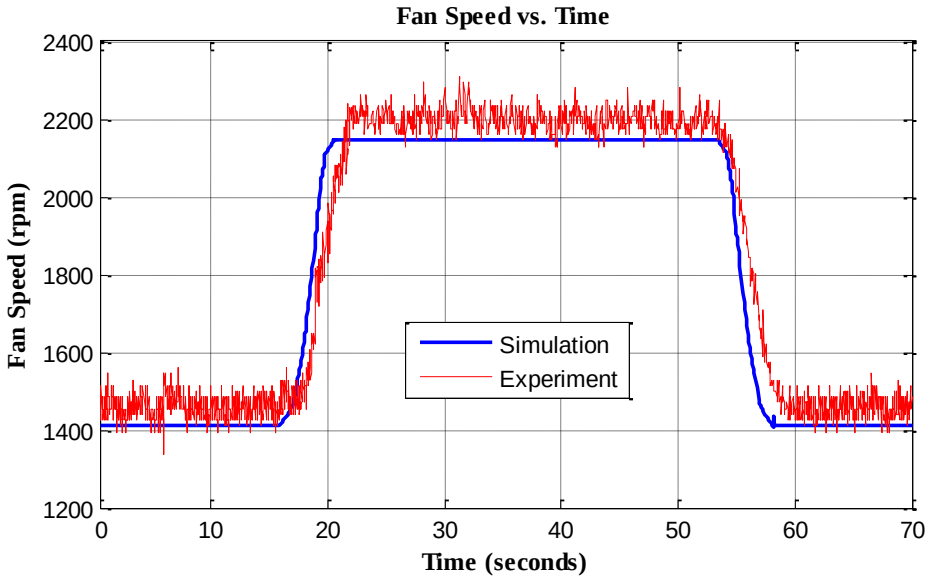

Figure 3-9 Fan Speed vs. Time

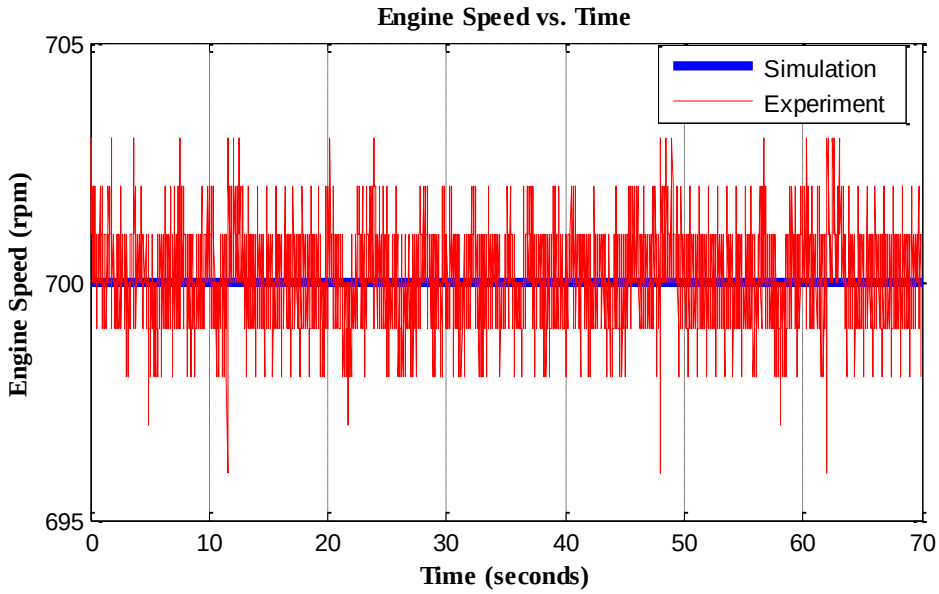

Figure 3-10 Engine Speed vs. Time

3.3.2 Scenario-2

Difference of Scenario-2 from Scenario-1 is the engine speed. During the simulation and experimentation of Scenario-2, engine speed is 2000 rpm. Same input voltage is applied to EPRV (Figure 3-6).

Simulation and experimental values for pump pressure are plotted in Figure 3-11. Similar to Scenerio-1, results are consistent.

During the first 15 seconds, although the engine speed is 2000 rpm, pump pressure is still ~28 bars (same as Scenario-1) until the voltage input to proportional valve is changed. This indicates that pump pressure is independent of the engine speed when the voltage input to proportional valve is maximum. In other words, idle fan speed is independent from engine speed. Similar to Figure 3-7, although the voltage input to proportional valve is started to decrease at t=10 s, pressure is started to increase at t=16 s due to characteristic of proportional valve (Figure 2-16).

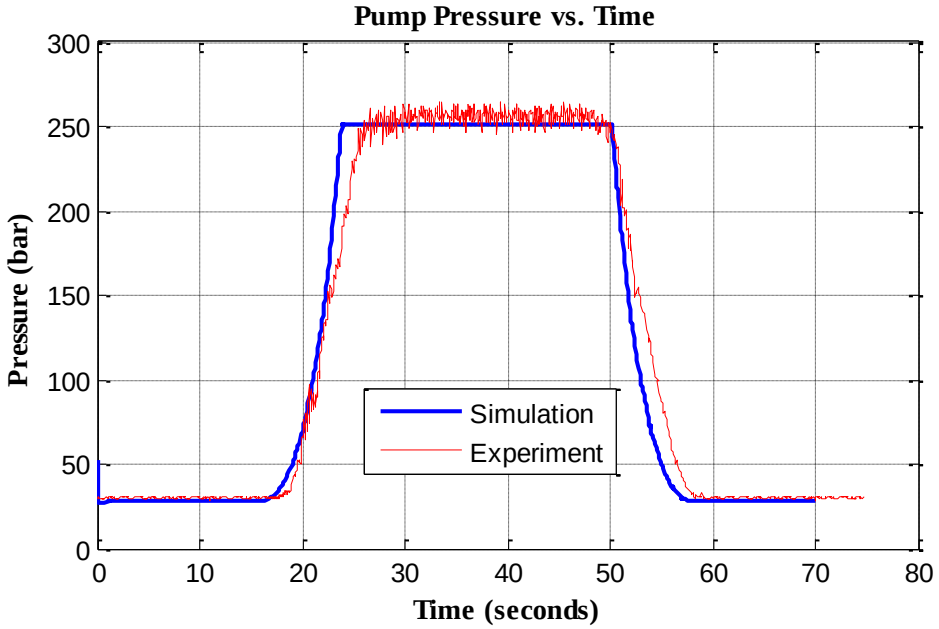

Figure 3-11 Pump Pressure vs. Time

The major difference between Scenerio-1 and Scenerio-2 is the maximum pressure of the system. For both scenarios, swash plate angle starts to increase as the voltage input of proportional valve decreases. For Scenerio-1, swash plate angle reaches its maximum value when the input voltage is zero. Pressure in this situation is determined by the torque on the

hydromotor shaft due to fan rotation (Figure 2-20). Although the pump has the maximum displacement, maximum flow provided by the pump is low because of low rotational speed of the engine. Consequently, due to low flow rate through hydromotor, rotational speed of the fan and the torque on the hydromotor are low. Finally, due to low torque on hydromotor, pressure in the system is low. On the other hand, for Scenario-2, since the rotational speed of the engine is necessarily high, pump can reach the relief valve setting on the compensator. As the voltage input of proportional valve is started to decrease, swash plate angle starts to increase. However, when the pump pressure reaches the cut-off pressure, relief valve opens and prevents the increment of swash plate angle.

Figure 3-12 illustrated the flow rate between pump and hydromotor. As the input voltage is decreased, pump flow rate increases up to 135 lpm. Similar to Figure 3-11, during the increment and decrement of input voltage, there are negligable differences between experimental and simulation results in terms of slope of the curves and pressure levels.

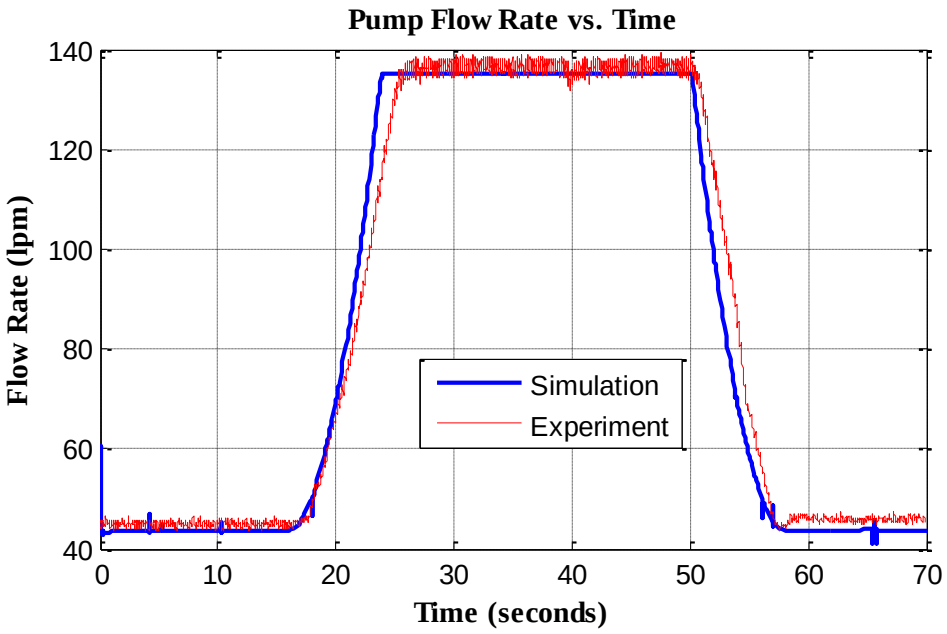

Figure 3-12 Pump Flow Rate vs. Time

Figure 3-13 and Figure 3-14 illustrate the fan speed and engine speeds for simulation and experimental results, respectively. Similar to Scenario-1, results show good agreement between simulation and experimental results.

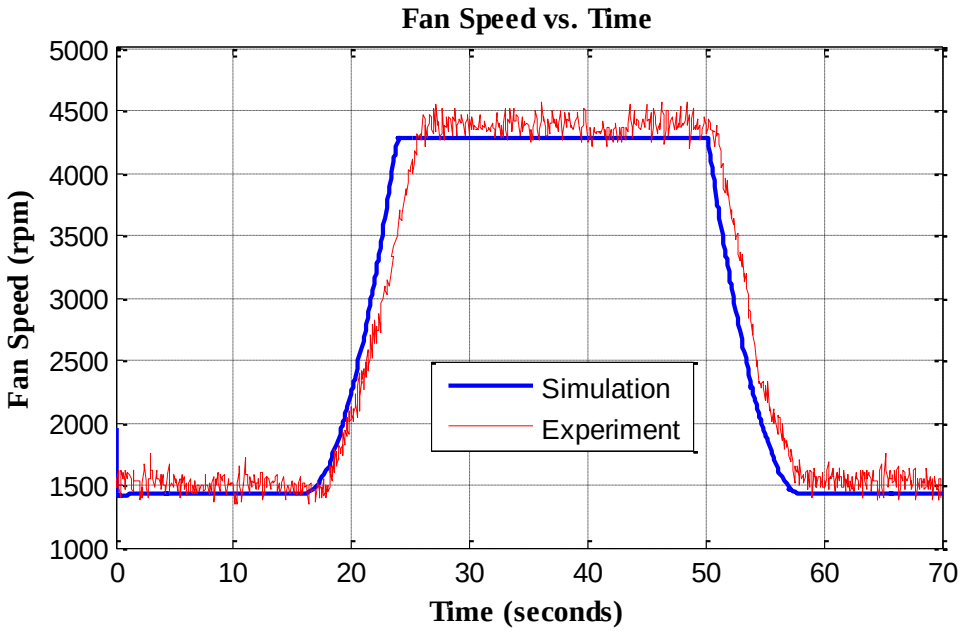

Figure 3-13 Fan Speed vs. Time

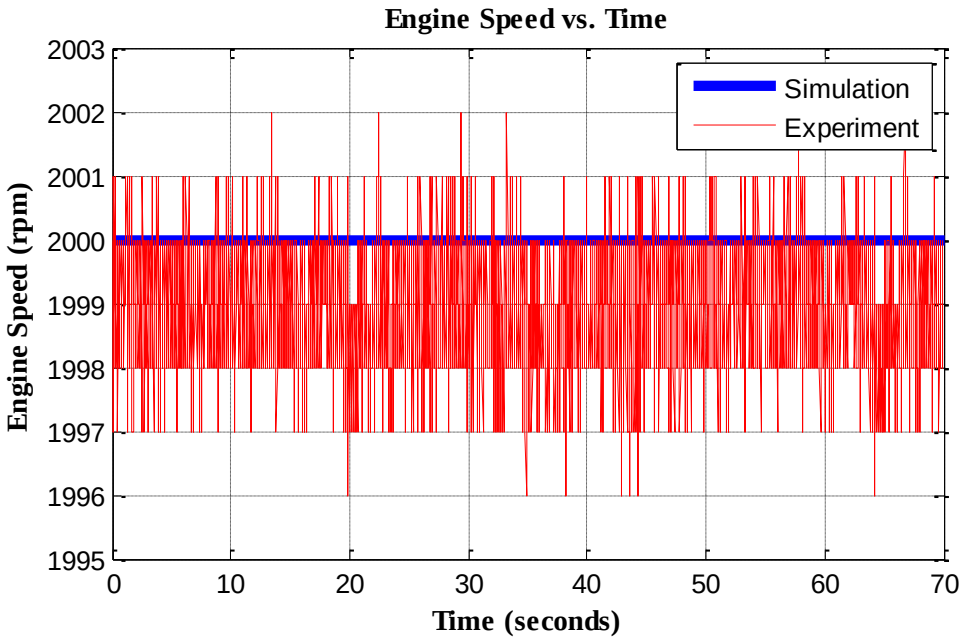

Figure 3-14 Engine Speed vs. Time

CHAPTER 4

INVESTIGATION OF THE COMPENSATOR AND SYSTEM DYNAMICS

4.1 Introduction

In Chapter 3, simulation results of the hydraulic fan drive system model are compared with the measurement values on the real system. It is concluded that simulation results show good agreement with the experimental results. In this chapter, prepared model is used to get deeper understanding of the system.

As mentioned before, main components of the hydraulic fan drive system are the engine, variable displacement pump with swash plate, compensator, hydromotor, fan, pipeline and the hydraulic fluid. All components have non-ignorable effect on the system performance. However, the compensator differs from other components since it is the main controller of the system. The swash plate angle which is one of the most important dynamic describer of the system is controlled by the compensator. In this chapter, sub-components and the working principle of the compensator are identified deeply and effect of orifice's sizes on the system is researched. Figure 2-12 is revisited here in order to examine the compensator.

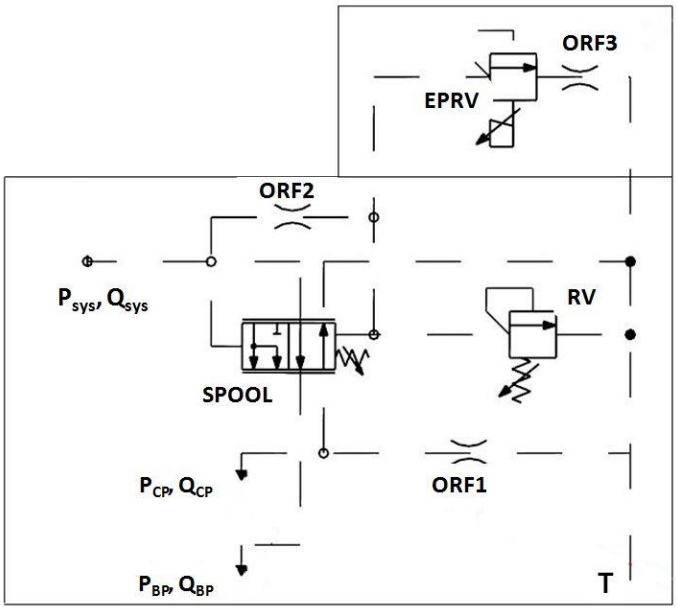

Figure 4-1 Hydraulic Circuit Diagram of the Compensator

4.2 Sub-Components and the Working Principle of the Compensator

As stated before, compensator is composed of a spool valve with a spring acting on it, an electro-proportional relief valve (EPRV), a relief valve (RV) and 3 orifices (ORF1, ORF2, ORF3). Inputs of the compensator are pressure and flow from the system and the current acting on the EPRV. Outputs of the compensator are the pressure and flow rate to bias and control pistons of the variable displacement pump and leakage. In Figure 4-2, Simulink® diagram of the compensator is shown.

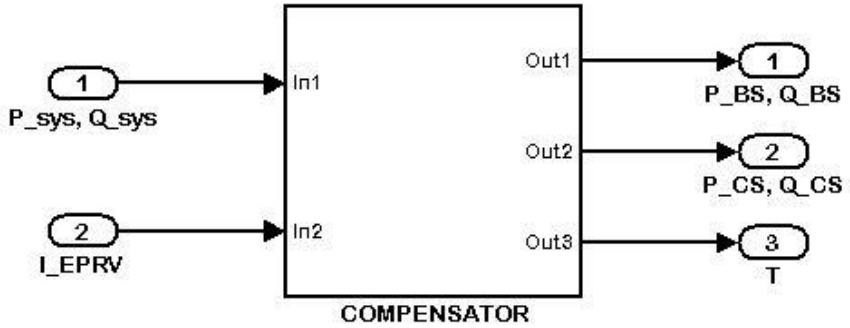

Figure 4-2 Compensator Block Diagram

Pilot pressures acting on the left and right sides of the spool and the spring force determine the spool position. According to spool position, flow supplied from the system is distributed to control and bias pistons on the pump. When the spool is in the position shown in Figure 4-1, flow supplied by the system is directed to the bias piston and control piston is open to the tank. In that case, swash plate angle and the displacement of the pump is maximum. As the spool position shifts, flow is divided between the bias and control pistons; as a result, the swash plate angle and displacement of the pump start to decrease. Areas that pilot pressures act on the spool, initial compression and the spring constant of the spring and, opening areas between ports with respect to spool position (Figure 2-14) are the most important parameters that define spool movement.

EPRV controls the pilot pressure acting on the right side of the spool. When EPRV is fully energized, it behaves like a relief valve with low pressure setting, in this case, 30 bars (Figure 2-16). In this situation, right side pilot pressure reduces and spool shifts to right side if the left side pilot pressure is higher than spring force plus the left side pilot pressure. It can be concluded that spring force acting on the spool affects the idle system pressure and the idle fan speed. When EPRV is de-energized, it behaves like a relief valve with high pressure setting, in this case, 330 bars. Since the system pressure cannot reach this pressure, it is fully closed (only leakage) if EPRV is de-energized. In that case, there is no flow through EPRV, consequently, there is no flow over ORF2 and pilot pressures acting on the spool become

equal. Due to spring force, spool comes to the position shown in Figure 4-1. As a consequence, swash plate angle becomes maximum. In summary, EPRV controls spool position via controlling the right side pilot pressure.

Relief valve (RV) limits the right side pilot pressure. When the right side pilot pressure exceeds the RV setting, it opens to tank, herewith; left side pilot pressure overcomes the forces on the right side and spool shifts to right side. Eventually, swash plate angle reduces and system pressure is limited. RV limits the maximum pressure of the system in an efficient way. A small amount of oil relieved over the RV. Instead of RV on the compensator, a high capacity relief valve can be used between the pump and hydromotor, but, in this case, system efficiency will be much lower since the relief valve will relieve much more oil in order to limit the maximum pressure of the system.

There are 3 fixed orifices inside the compensator. As mentioned before, ORF1 controls the oil flow to the control piston. ORF2 creates pressure drop between the left and right side of the spool and controls the spool movement and finally ORF3 creates a pressure in front of the electro-proportional relief valve in order to damp valve movement. Each of three has important effect on the system. In this chapter, effect of orifices on the system is investigated in terms of efficiency and response characteristic of the system. Effect of different orifice sizes is compared with the existing orifice sizes. It should be admitted that it is very time consuming to change an orifice on the real system and observe the effects. In addition, it can be dangerous since the orifices have effect on the system pressure level and changing an orifice carelessly can cause pressure to increase to undesirable levels which can damage the components.

4.3 Orifice-1

Some amount of oil passing through the spool to control piston is diverted to tank through the Orifice-1 (ORF1). As the size of the ORF1 increases, more amount of oil is diverted to tank and vice versa as the size of the ORF1 decreases, less amount of oil is diverted to tank. The amount of fluid diverted to tank affects the efficiency of the system. Apart from that, during the swash plate angle increment, oil inside the control piston is drained to tank through not only from the spool but also via ORF1. Size of the ORF1 affects the response of the system. In this part, by simulating the prepared model for different orifice sizes, effect of ORF1 on the system is investigated.

ORF1 size for the existing system is Ø1.2 mm. Simulation results for Ø1.0 and Ø1.4 mm orifice sizes are compared with the Ø1.2 mm. The simulations are performed at 700 rpm engine speed. In order to analyze the response of the system, step inputs are given to EPRV at t=10 s and t=10.5 s. Input voltage to the EPRV is shown in Figure 4-3. For clarity, only the time interval between t=9.5 to t=11 s is shown in the figure.

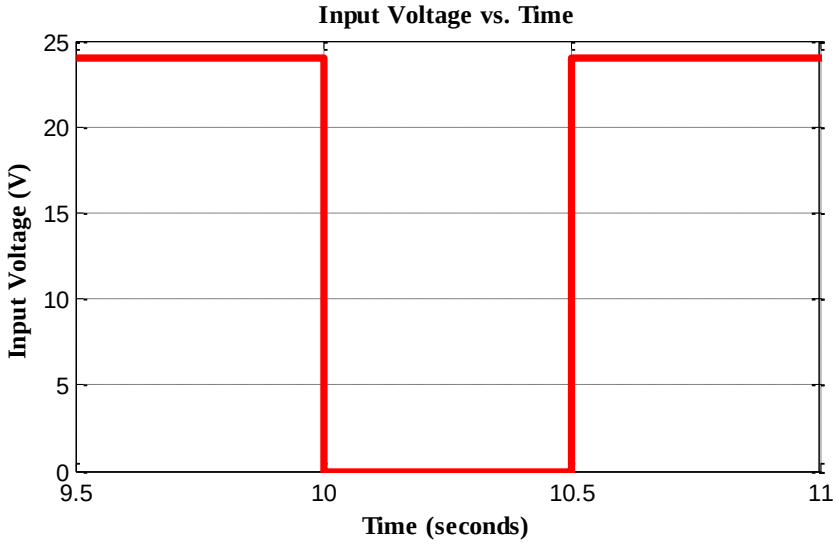

Figure 4-3 Input Voltage vs. Time

Figure 4-4 shows the pump discharge pressure versus time. According to figure on the left, as the orifice size increases, idle pressure (700 rpm engine speed and 24 V input voltage to EPRV) increases slightly. However, the main influence of ORF1 is on the response of system during rapid decrement of voltage, in other words, during the rapid increment of swash plate angle. For Ø1.0 mm orifice, it takes more than 0.1 seconds to system come to steady-state position. On the other hand, it is nearly 0.05 seconds for Ø1.4 mm orifice. ORF1 has no effect on the maximum pressure for this case.

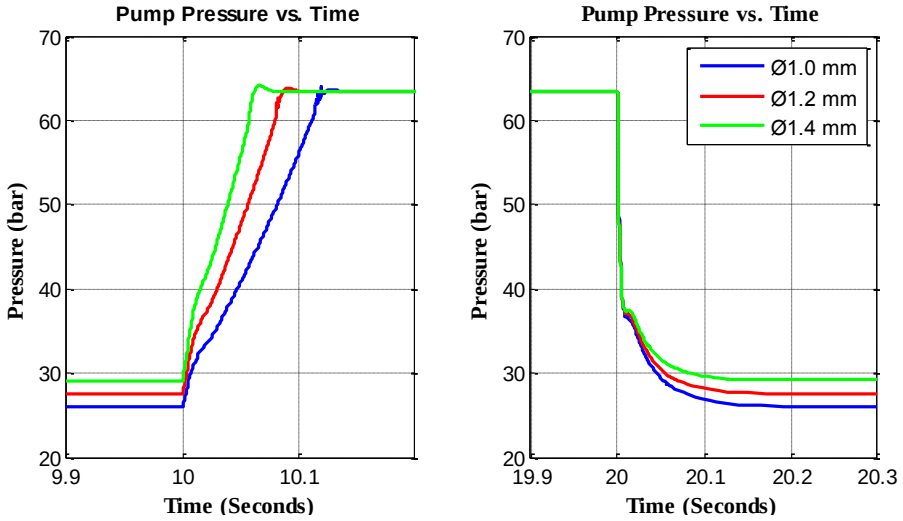

Figure 4-4 Pump Pressure vs. Time

This argument matches with the theoretical explanation. For 0 V input voltage at 700 rpm engine speed, spool position is same as shown in Figure 4-1 and swash plate angle is maximum. Since there is no flow over ORF1, maximum pressure of the system is not affected from ORF1 size. Figure on the right side illustrates the system response to step voltage input (24 V) to EPRV. In that case, swash plate angle reduces rapidly. System supplied oil is pumped to control piston via spool. According to figure, it can be concluded that ORF1 has ignorable effect during decrement of swash plate angle when compared to increment of angle.

Figure 4-5 shows the leakage on the compensator versus time. According to figure on the left, as the orifice size increases, leakage on the compensator increases at idle condition (700 rpm engine speed and 24 V input voltage to EPRV). Not only the orifice size rising cause more leakage, but also pressure rising affects the leakage. Similar to the case in Figure 4-4, ORF1 has no effect on leakage when the swash plate angle is maximum. In that case, although there is no flow over the ORF1, there is an approximately 1 l/m leakage on the compensator. This is due to the leakage area from pressure port to control piston port on the spool.

In order to see the effect of ORF1 when the system has cut-off pressure, simulations are repeated for 2000 rpm engine speed for the same input voltage to EPRV. Figure 4-6 and Figure 4-7 illustrate the effect of orifice size on the system pressure and the leakage rate, respectively. According to Figure 4-6, in contrast to Figure 4-4, ORF1 affects the maximum pressure of the system. The reason for this variation is, when the engine speed is 2000 rpm and input voltage is 0 V, system pressure exceeds the relief valve pressure settings. Thus, relief valve on the compensator steps in and prevents the further increment of swash plate angle. In this scenario, spool is in a mid position and flow over the ORF1 exists. The more flow over ORF1, the lower pressure on control piston and consequently the higher system pressure.

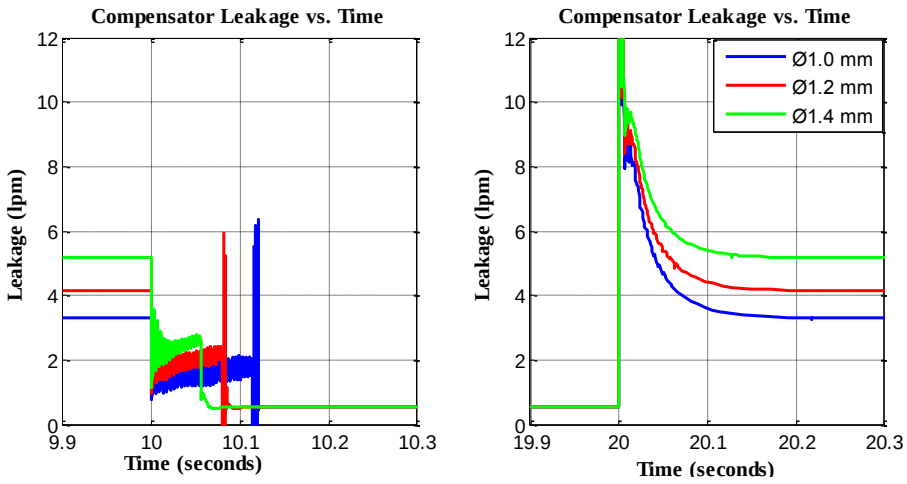

Figure 4-5 Compensator Leakage vs. Time

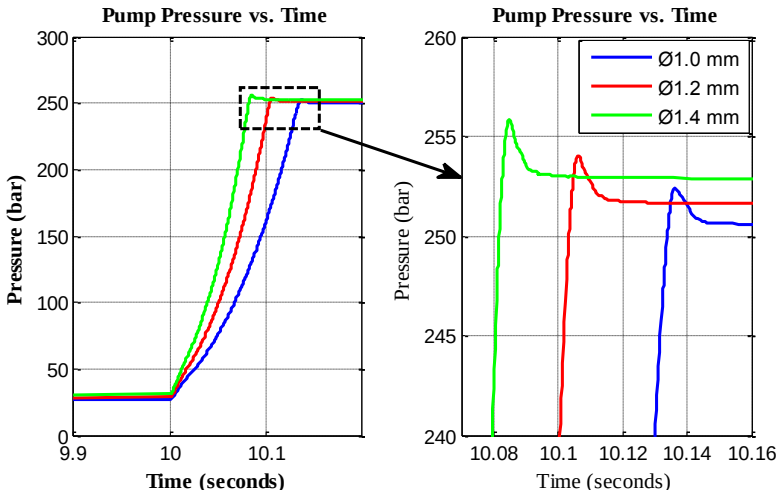

Figure 4-6 Pump Pressure vs. Time

When the first 10 seconds of Figure 4-5 and Figure 4-7 are compared, it can be concluded that leakage rates for each orifice size is same for 700 rpm and 2000 rpm engine speeds when the input voltage for EPRV is 24 V since the system pressures are the same for each case. However, when the step input is given to EPRV, situation is different for two scenarios. For 700 rpm engine speed, when system comes to steady-state position, swash plate angle is maximum and there is no flow over ORF1. On the other hand, for 2000 rpm engine speed, when system comes to steady-state position, swash plate angle is in a mid position and there is a remarkable oil flow over the ORF1.

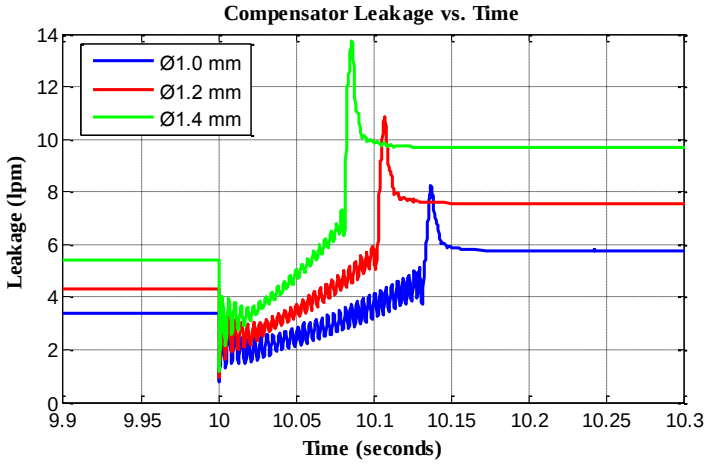

Figure 4-7 Compensator Leakage vs. Time

In summary, although ORF1 size affects the minimum and maximum pressure of the system slightly, the main effect of the ORF1 is the response time during increment of swash plate angle. Response time can be reduced by the increment of orifice size in spite of leakage rise.

4.4 Orifice-2

As indicated before, pressure drop between left and right side of the spool is created by ORF2. As the size of the ORF2 increases, pressure difference over ORF2 decreases and idle pressure of the system increases. On the contrary, as the size of ORF2 decreases, pressure difference over ORF2 increases and idle pressure decreases. In this part, by simulating the prepared model for different orifice sizes, effect of ORF2 on the system is investigated.

Simulations are performed in the same conditions as ORF1 (700 rpm engine speed and voltage input is shown in Figure 4-3). Pump discharge pressure versus time is illustrated in Figure 4-8. According to figure on the left, as the orifice size increases, idle pressure (700 rpm engine speed and 24 V input voltage to EPRV) increases as expected. However, although there is a slight increment on ORF2 size, idle pressure is increased remarkably. Note that slopes of pressure curves for each orifice are nearly equal. It can be concluded that effect of ORF2 on the response of the system can be ruled out.

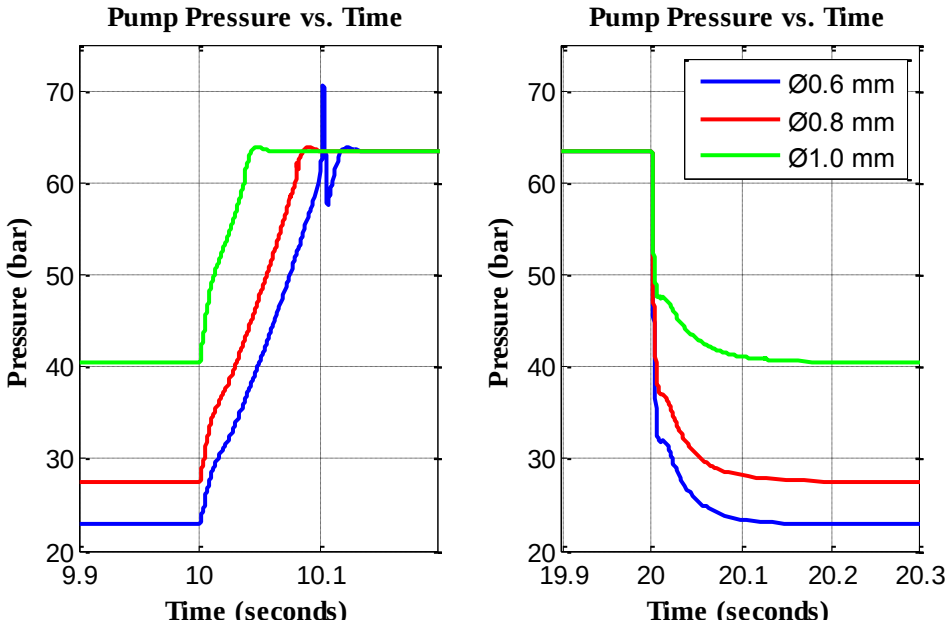

Figure 4-8 Pump Pressure vs. Time

If the first 10 seconds of Figure 4-8 and Figure 4-9 are compared, it can be figured out that the rate of pressure and leakage rise are proportional contrary to the case in ORF1 (Figure 4-4 and Figure 4-5). This can be explained on the circuit diagram of the system (Figure 4-1). As it can be seen from the figure, flow passing over ORF2 is not directly drained to tank.

EPRV and ORF3 are the other resistances in front of the flow. It can be interpreted that resistance of combination of EPRV and ORF3 is higher than the resistance of ORF2 and for this reason, although the size of ORF2 is increased, leakage increment is mainly due to pressure increment. Otherwise, leakage increment will be much higher than the pressure increment as in the case of ORF1.

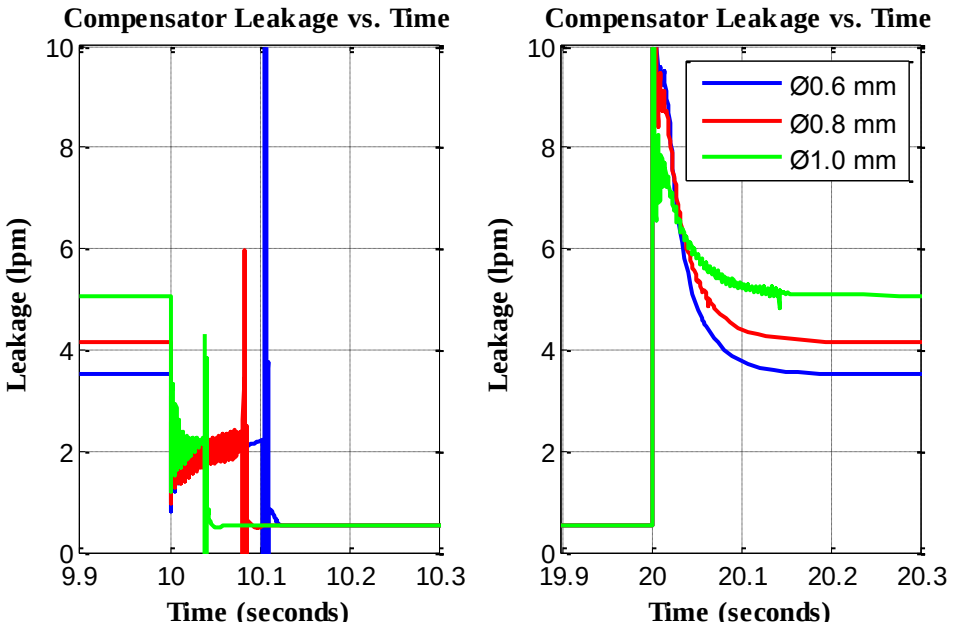

Figure 4-9 Compensator Leakage vs. Time

Simulations are repeated for 2000 rpm engine speed, similar to ORF1. Effect of orifice size on the system pressure and the leakage rate are presented in Figure 4-10 and Figure 4-11, respectively.

Similar to ORF1, as the size of ORF2 increases, maximum system pressure increases (Figure 4-10). As mentioned before, when the engine speed is 2000 rpm and the voltage input to EPRV is 0 V, system pressure exceeds the pressure setting of relief valve on the compensator. Consequently, relief valve steps in and flow passing over the ORF2 drained to tank through relief valve. Note that in that case EPRV is fully closed. It is required to mention that relief valve pressure setting is performed at a specific flow rate. If flow passes over the valve increases, then set pressure of the valve increases, like in this scenario. As the orifice size increases, more flow passes over the orifice and upstream pressure of relief valve increases which causes the system pressure to rise.

As in the case of ORF1 (Figure 4-7), leakage rate rises with an increase in orifice size. However, when Figure 4-7 and Figure 4-11 are compared, it is observed that, contrary to

ORF1, effect of ORF2 on leakage is much lower. It can be explained on the circuit diagram of the system. When the input voltage to EPRV is 0, it is fully closed. There are two different leakage paths. One of them is via ORF1 and the other one is via ORF2 and relief valve. Since the combination of ORF2 and relief valve creates higher resistance to flow, higher amount of oil drained to tank via ORF1.

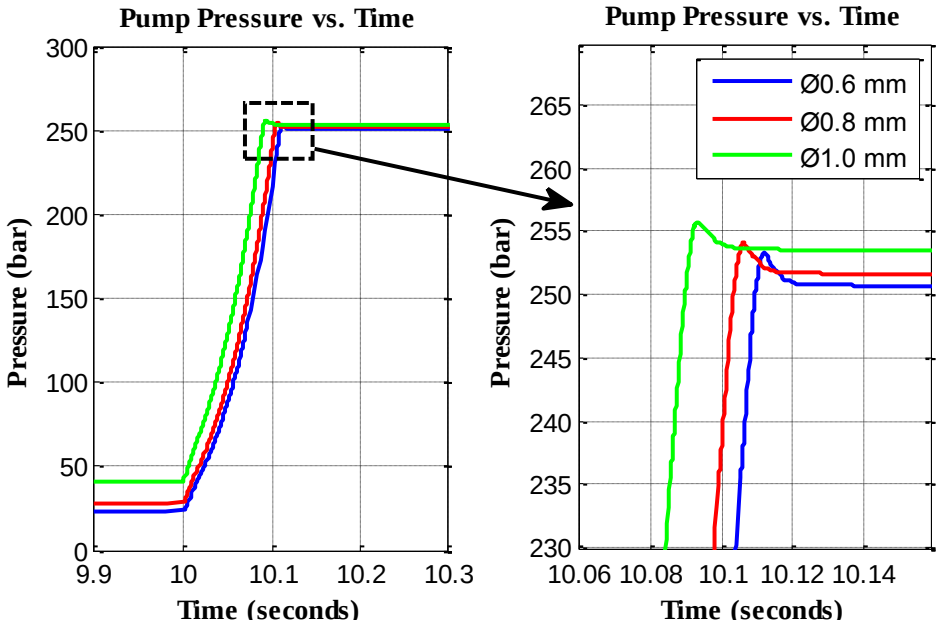

Figure 4-10 Pump Pressure vs. Time

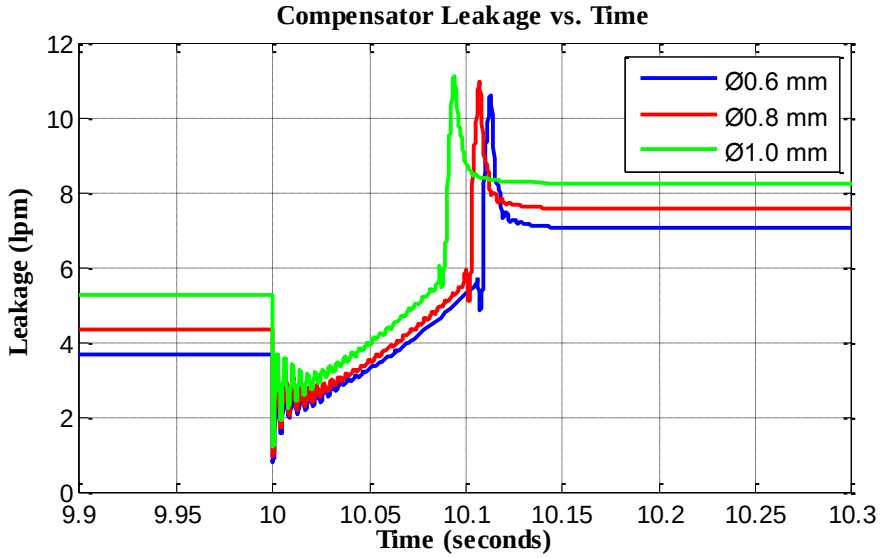

Figure 4-11 Compensator Leakage vs. Time

In conclusion, the most important effect of ORF2 on the system is the idle pressure, when the input voltage to EPRV is 24 V. The other effects (response to step input, maximum system pressure, leakage rate) on the system have less importance.

4.5 Orifice-3

Main duty of ORF3 is to create pressure in front of the EPRV in order to damp valve movement. However, since the valve dynamics (mass of the poppet valve, damping inside the valve and spring constant) is not modeled, effect of ORF3 on valve movement damping cannot be seen. In this part, effect of ORF3 on the minimum and maximum system pressures, and system efficiency are investigated.

For 700 rpm engine speed and step input voltage (Figure 4-3), simulations are performed for three different orifice size. According to Figure 4-12, contrary to ORF1 and ORF2, as the orifice size decreases, idle pressure of the system increases.

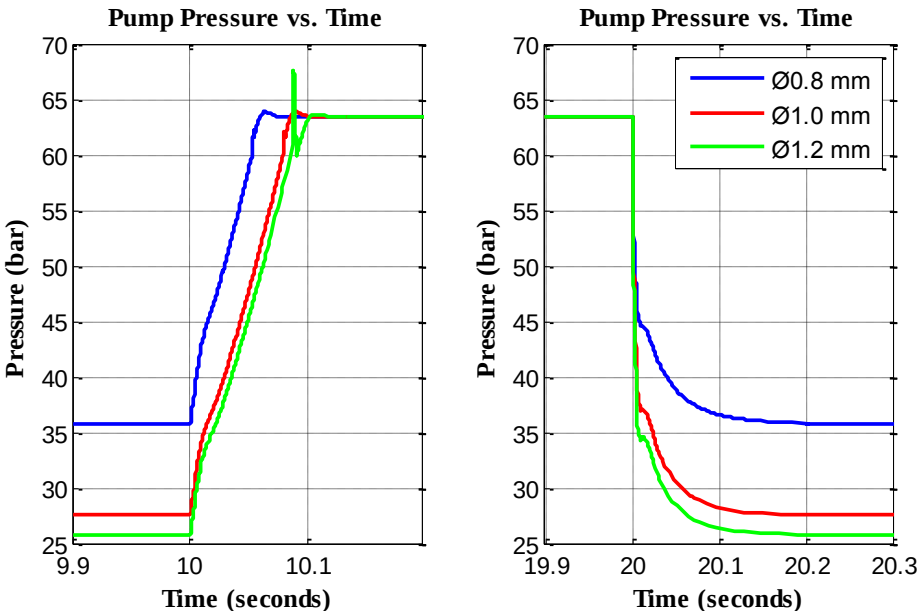

Figure 4-12 Pump Pressure vs. Time

The reason of this; as the orifice size decreases, pressure drop over ORF3 increases and since the downstream pressure of ORF3 is very low (tank side), upstream pressure increases. Therefore, left side pilot pressure of the spool increases which cause higher idle pressure. However, although there is a remarkable pressure drop between Ø0.8 and Ø1.0 mm orifices, difference between Ø1.0 and Ø1.2 mm orifices is lower. Theoretical explanation of this difference is that as the orifice size increases, it approaches the maximum opening of the

EPRV. In other words, ORF3 becomes ineffective after a point. It can be concluded that it is useless to install an orifice larger than Ø1.2 mm for ORF3. Similar to ORF1 and ORF2, when the input voltage of EPRV is 0 V and swash plate angle is maximum, ORF3 has no effect on the system pressure. In addition, similar to ORF2, slopes of pressure curves for each orifice are nearly equal; therefore, effect of ORF3 on the response of the system can be ignored.

An important outcome of the simulation is that ORF3 has negligible effect on the compensator leakage, as shown in Figure 4-13.

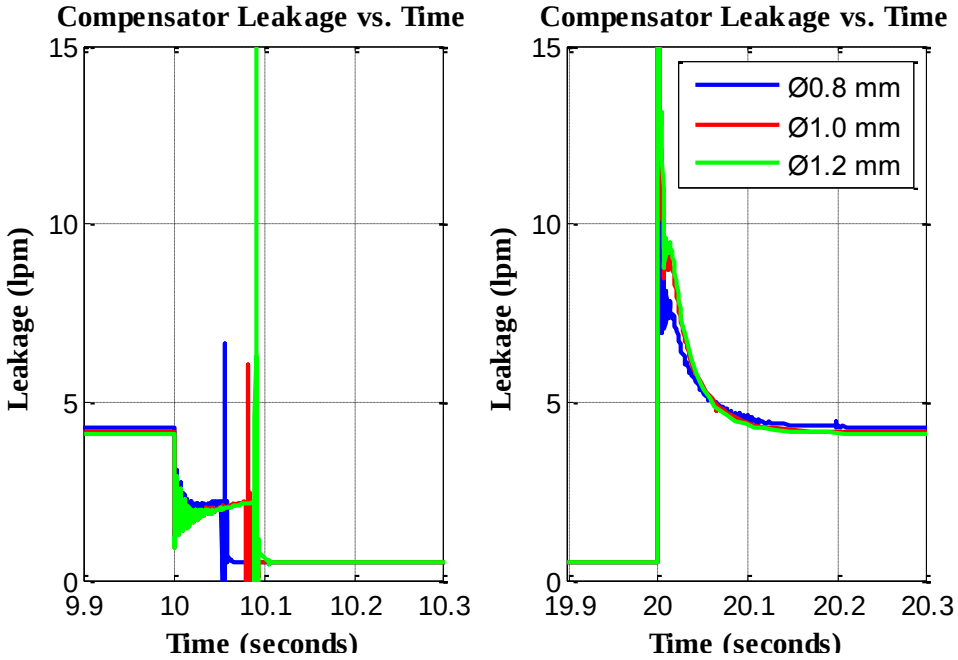

Figure 4-13 Compensator Leakage vs. Time

Simulations are repeated for 2000 rpm engine speed, similar to ORF1 and ORF2. Pressure and compensator leakage curves are shown in Figure 4-14 and Figure 4-15, respectively. According to Figure 4-14, ORF3 is the only orifice which does not affect the cut-off pressure of the system. And finally, leakage rate at cut-off pressure is not affected from the size of ORF3 (Figure 4-15).

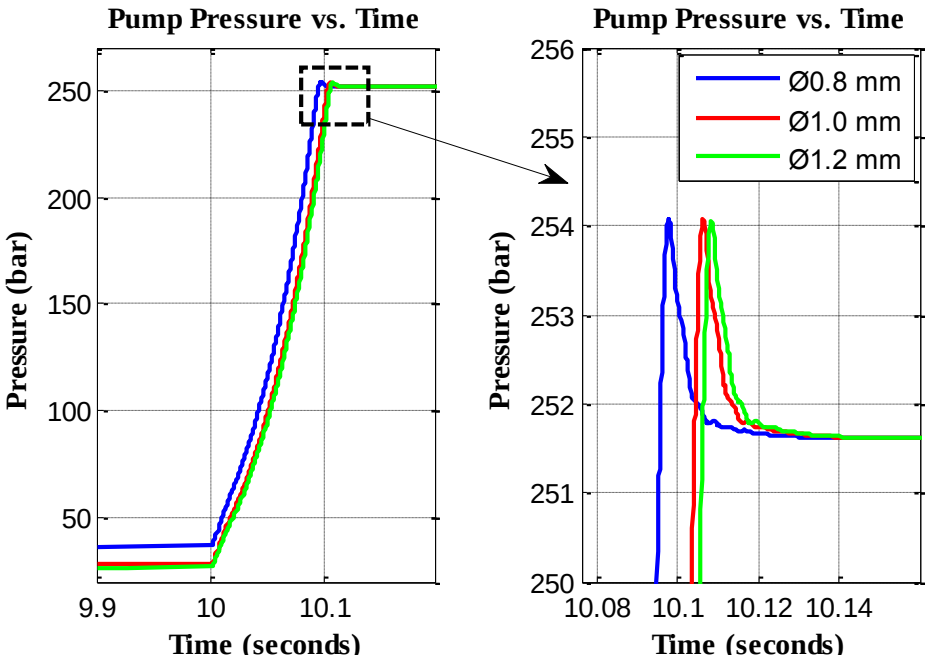

Figure 4-14 Pump Pressure vs. Time

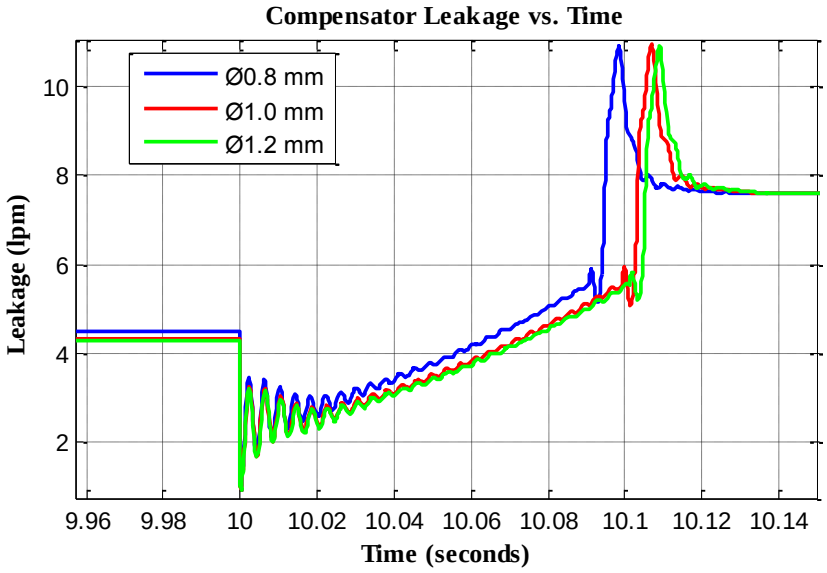

Figure 4-15 Compensator Leakage vs. Time

CHAPTER 5

DISCUSSION, CONCLUSION AND FUTURE RECOMMENDATIONS

5.1 Discussion and Conclusion

This thesis focuses on modeling of a hydraulic fan drive system. MATLAB/Simulink® software is used to develop the model. Since the system consists of different components i.e. engine, variable displacement pump, compensator, hydromotor, fan, and pipeline, it is an aggregation of each individual component model.

Variable displacement pump is one of the most important components in this work; therefore, a detailed literature research is conducted in order to understand previous works on this component. Previous researches on mathematical modeling of a variable displacement pump, assumptions and neglected terms on models, swash plate mechanism and control options are investigated and presented in Chapter-1.

Instead of deriving the equations of hydraulic and mechanical components, physical modeling toolboxes of MATLAB (SimHydraulics® and SimMechanics™) are used to model the system components. Standard blocks in SimHydraulics® library are used for modeling hydromotor, pipeline, hydraulic fluid, check and relief valves. On the other hand, diesel engine and fan models are adapted from the standard blocks.

Comprehensive models for variable displacement pump and compensator are generated. Swash plate mechanism of the pump including control and bias pistons is modeled by the help of SimMechanics™ toolbox. Inertial effects of swash plate and pistons are taken into account. On the other side, all sub-components of the compensator are modeled according to manufacturer's data.

Measurements are performed on the physical machine. Fan and engine speeds, pump pressure and flow rate between pump and hydromotor data are gathered in order to verify the prepared model. Comparing the simulation results with the experimental data reveals that the model is reasonably accurate.

In addition, the model is utilized in order to analyze the static and dynamic effect of varying orifice sizes. Response time change, leakage rate increment, minimum and maximum system pressure variation due to different orifice sizes are compared and effect of each orifice on the system is defined.

In conclusion, a comprehensive MATLAB/Simulink® model for hydraulic fan drive system is developed in this work. Prepared model is verified by comparison of simulation and experimental results. It should be admitted that although a dynamic model is prepared, system is not subjected to rapid changes (engine speed increment and EPRV current change). Developed model can be used for deeper understanding behind the hydraulic system and the components, as done in Chapter-4. System response to different input signals can be simulated and highly dynamic systems can be analyzed. Finally, points that are open to improvement can be determined over the model and potential alterations can be simulated before implementation on the real system.

5.2 Future Recommendations

In the present study, diesel engine is modeled as an ideal angular velocity source. In future investigations, a more comprehensive model including wide open throttle performance curve can be developed to see the effect of throttle input to the system.

Sub-components of the compensator (spool, relief valve and electro-proportional relief valve) are modeled as massless. In addition, coil of the electro-proportional valve is not modeled. Furthermore, "Double-Acting Valve Actuator" model under SimHydraulics® toolbox is used for computing the position of the spool according to left and right side pilot pressures and spring. This model neglects the flow consumption. These deficiencies can be filled in future study.

In addition, thermal effects are not taken into account. Heat generation due to hydraulic system, warming up of fluid and viscosity change due to temperature increment have important effect on the system.

Finally, flow forces (stable forces and unstable forces) on the spool are not taken into account. In future, these forces can be considered in order to see the effect on the system i.e. hydraulic locking, Quando effect, stationary and temporary flow uncertainty [31].

REFERENCES

[1] Regional Environmental Center. (2003, Jan 01). *Handbook on the Implementation of EC Environmental Legislation*. Retrieved from: http://ec.europa.eu/environment/ enlarg/handbook/noise.pdf, last visited on September 2013.

[2] European Parliament. (2009). Regulation No 595/2009 of the European Parliament and of the Council of 18 June 2009. *Official Journal of the European Union*, L(188), 1-13. Retrieved from http://eurlex.europa.eu/LexUriServ/LexUriServ.do?uri=OJ: L:2009 :188:0001:0013:EN:PDF, last visited on September 2013.

[3] *Cooling Systems*. Retrieved from http://www.worktrucksales.com/infocooling.htm, last visited on September 2013.

[4] National Automotive Radiator Service Association. Cooling system. Retrieved from http://www.automavericks.com/forum/threads/the-engine-cooling-system-of-a-car. 188/, last visited on September 2013.

[5] Ofria, C. (n.d.). *A short course on cooling systems*. Retrieved from http://www.carparts.com/classroom/coolingsystems.htm, last visited on September 2013.

[6] Kakaç, S., & Liu, H. (2002). *Heat Exchanger Selection, Rating, and Thermal Design*. (2nd ed., pp. 1-30). Florida: CRC Press.

[7] Viscous Fan Clutch. (n.d.) Retrieved from http://www.euro4x4parts.com/en/4x4_ mechanics_fan_clutch.htm, last visited on September 2013.

[8] Parker Hannifin. *Truck Hydraulics Fan Drive Systems Training*. Retrieved from http://www.dhauto.com/threads/3365-Truck-Hydraulics-Fan-Drive-Systems-Training_Basic-Overview, last visited on September 2013.

[9] Maria, A. (1997). Introduction to Modeling and Simulation. In Androttir, S., Healy, K. J., Withers, D. H., Nelson, B. H. (Eds.), Proceedings of the 1997 Winter Simulation Conference.

[10] Eaton Hydraulics. (2003) Fan Drive System Application Guide. Technical Focus E-SYFD-TM001-E.

[11] Parker Hannifin Pump and Motor Division. (2007). *Hydraulic Pump Series VP1-095 Catalog*. Retrieved from http://www.parker.com/literature/HY30-8220_VP1_095_SE.pdf.htm, last visited on September 2013.

[12] How does a Variable Displacement Pump Work? Retrieved from http://www.mekanizmalar.com/variable_displacement_piston_pump.html, lst visited on September 2013.

[13] Kaliafetis, P., & Costopoulos, T. (1995). Modelling and Simulation of an Axial Piston Variable Displacement Pump with Pressure Control. *Mech. Mach Theory,* 30(4), 599-612.

[14] Manring, N. D., & Johnson, R. E. (1994) Swivel Torque within a Variable Displacement Pump. *Technical Paper Series NFPA, 94* (1.3).

[15] Manring, N. D., & Johnson, R. E. (1996) Modeling and Designing a Variable-Displacement Open-Loop Pump. *Journal of Dynamic Systems, Measurement, and Control, 118,* 267-271.

[16] Zeiger, G., & Akers, A. (1986). Dynamic Analysis of an Axial Piston Pump Swashplate Control. *Proceedings of the Instution of Mechanical Engineers, 200,* 49-58.

[17] Prasetiawan, E. A. (2001). Modeling, Simulation and Control of an Earthmoving Vehicle Powertrain Simulator (Master's Thesis). University of Illinois, Urbana, Illinois.

[18] Kemmetmüller, W., Fucshumer, F., Kugi, A. (2009). Nonlinear Pressure Control of a Self-Supplied Variable Displacement Axial Piston Pumps. *Control Enginering Practive, 18,* 84-93.

[19] Casoli, P., & Alvin, A. (2013). Gray Box Modeling of an Excavator's Variable Displacement Hydraulic Pump For Fast Simulation of Excavation Cycles. *Control Engineering Practice, 21,* 493-494.

[20] Prabhu, S. M. (2007). Model-Based Design for Off-Highway Machine Systems Development. *The Mathworks Inc., 01* (4248). Retrieved from http://www.math works.com/tagteam/44719_Prabhu_2007-01-4248_Final.pdf, last visited on September 2013.

[21] Marius, P. (2010). Optimizing the Hydraulic Systems Using the SimHydraulics Programming Environment. *Journal of Engineering Studies and Research, 16*(4), 25-32.

[22] Lauvli, P. W., & Lund, B. V. (2010). Modeling, Simulation and Experimentation of a Hydrostatic Transmission (Master's Thesis). Faculty of Engineering and Science University of Agder, Grimstad.

[23] Hamzehlouia, S. (2012). Modeling and Control of Hydraulic Wind Energy Transfers (Master's Thesis). Purdue University, Indianapolis, Indiana.

[24] Kim, S. D., Cho, H. S., & Lee, C. O. (1987) A Parameter Sensivity Analysis for the Dynamic Model of a Variable Displacement Axial Piston Pump. *Proceedings of the Instution of Mechanical Engineers, 201(C4)*, 235-243.

[25] The MathWorks, Inc. (2013) SimMechanics™ Link User's Guide R2013b. Retrieved from http://www.mathworks.cn/help/pdf_doc/physmod/smlink_ug.pdf, last visited on September 2013.

[26] Parker Hannifin Corporation Hydraulic Cartridge Systems. (2010) *Threaded Cartridge Valves and Integrated Hydraulic Components. Catalogue HY15-3502/US.* Retrieved from http://www.hydraulkompanient.se/dokument/AP02B2YR35ANL. pdf, last visited on September 2013.

[27] The MathWorks, Inc. (2012) SimHydraulics® Referance R2012b.

[28] Kaman Sensors. (n.d.). *KD-2440 Sensor Data Sheet.* Retrieved from http://www.kamansensors.com/pdf_files/Kaman_KD-2440_data_sheet-web.pdf, last visited on September 2013.

[29] The MathWorks, Inc. (2013) SimScape™ Link User's Guide R2013b. Retrieved from http://www.mathworks.cn/help/pdf_doc/physmod/simscape/simscape_ug.pdf, last visited on September 2013.

[30] Parker Hannifin Corporation. (2010). *Senso Control. Catalogue 4054-2/UK*. Retrieved from http://www.parker.com, last visited on September 2013.

[31] Ercan Y. (1995). Akışkan Gücü Kontrolü Teorisi. (1. ed, pp. 97-119). Ankara: T.H.K.

[32] Parker Hannifin Corporation Hydraulics Group. (2011). *HP1/PD Series Medium Duty Axial Piston Pumps. Catalogue HY28-2665-01/P1/EN*. Retrieved from http://www.parker.com, last visited on September 2013.

[33] Parker Hannifin Corporation. (2009). *Hydraulic Motor/Pump. Catalogue HY30-8249/UK*. Retrieved from http://www.parker.com, last visited on September 2013.

[34] SCFM Corporation. (n.d.) Mixed Flow Fan P/N 91500. Retrieved from http://www.scfmfans.com/pdf/i-91500.pdf, last visited on September 2013.

[35] Parker Hannifin Corporation. (2010). *Hydraulic Hoses, Fittings and Equipment. Catalogue 4400/UK*. Retrieved from http://www.parker.com, last visited on September 2013.

APPENDIX A

PROPERTIES OF VARIABLE DISPLACEMENT PUMP

Table A-1 Pump Specifications [32]

Variable Displacement Pump		
Displacement		1000 cc/rev
		6.01 in^3/rev
Outlet Pressure	Continuous	280 bar
	Intermittent	320 bar
	Peak	350 bar
Maximum Speed	Boosted Inlet	2500 rpm
	1.0 bar abs Inlet	2100 rpm
	0.8 bar abs Inlet	1700 rpm
Minimum Speed		600 rpm
Case Pressure	Peak	4 bar abs
	Rated	2 bar abs
Fluid Temperature		-40/95°C
Fluid Viscosity	Rated	6 to 160 cSt
	Max Intermittent	5000 cSt (for cold starting)
	Min Intermittent	5 cSt
Fluid Contamination	Rated	20/18/14 (ISO)
	Maximum	21/19/16 (ISO)

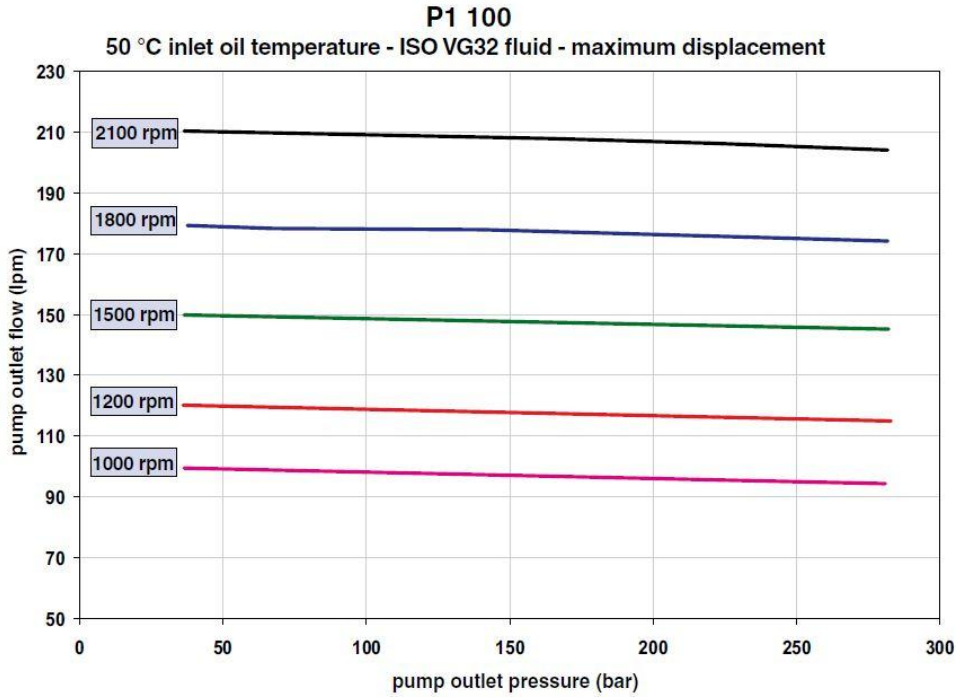

Figure A-1 Pump Flow Rate vs. Pressure [32]

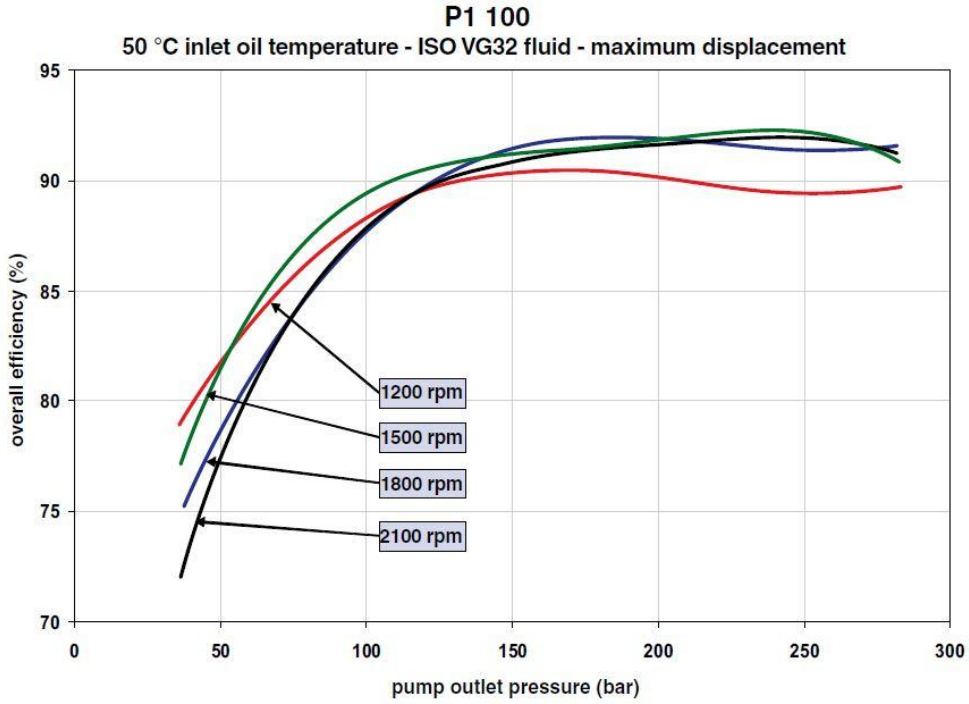

Figure A-2 Pump Overall Efficiency vs. Pressure [32]

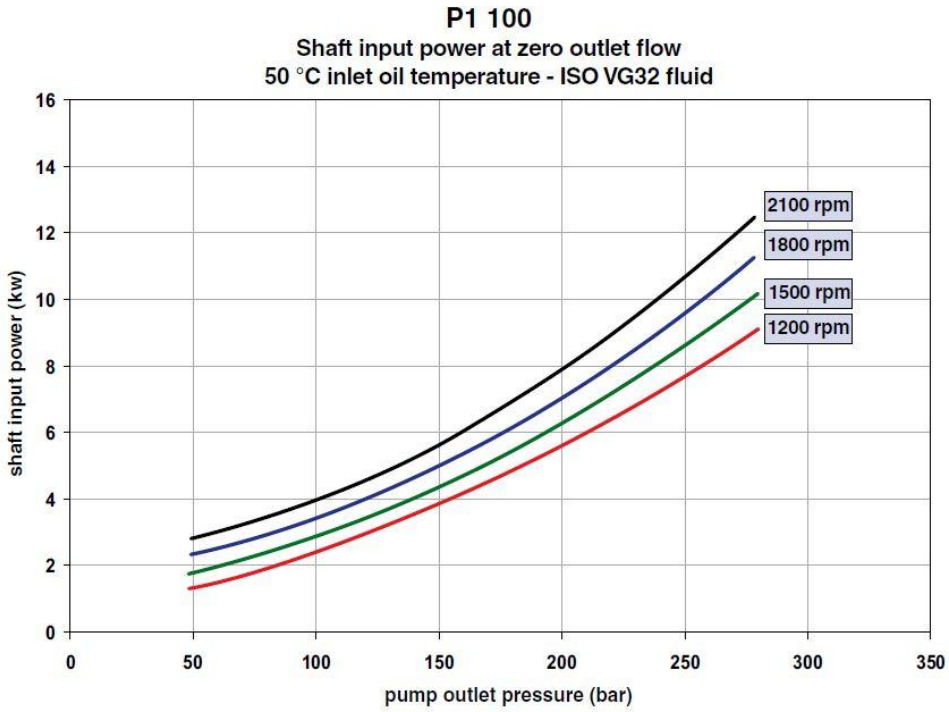

Figure A-3 Pump Input Power vs. Pressure [32]

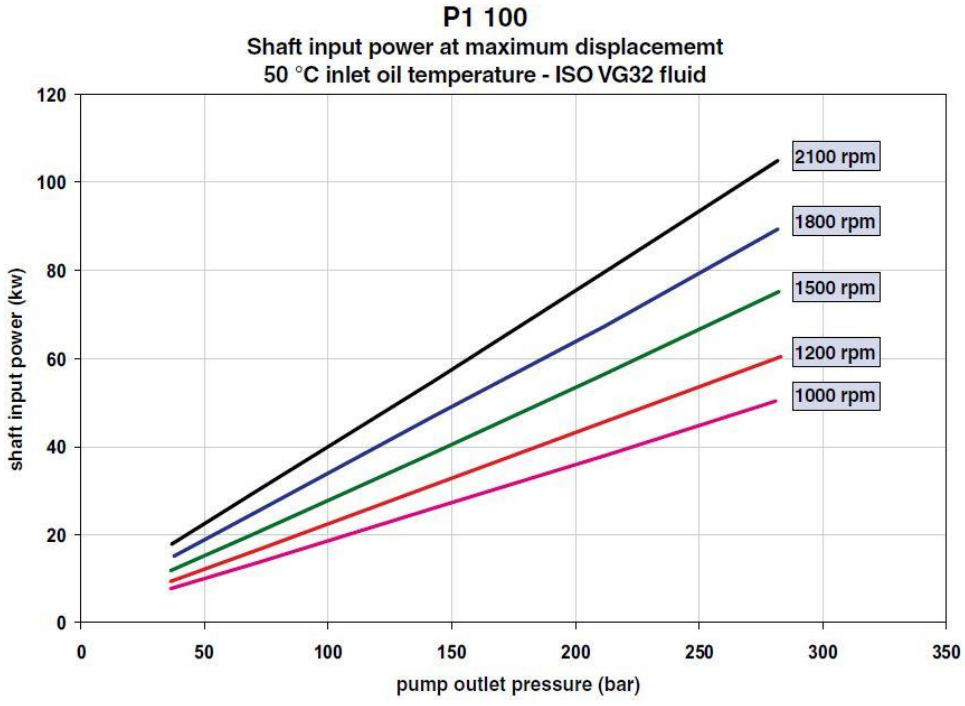

Figure A-4 Pump Input Power vs. Pressure [32]

Table A-2 Specifications for Swash Plate Mechanism

Swash Plate Mechanism		
Mass Moment of Inertia of Swash Plate	I	0.009 kgm^2
Mass of Control Piston	m_{cp}	0.6 kg
Mass of Bias Piston	m_{bp}	0.3 kg
Mass of Individual Piston	m_p	0.15 kg
Control Piston Diameter	d_{cp}	30 mm
Bias Piston Diameter	d_{bp}	20 mm
Individual Piston Diameter	d_p	25 mm
Control Piston Stroke	s_{cp}	25 mm
Bias Piston Stroke	s_{bp}	25 mm
Control Piston Moment Arm	L	85 mm
Bias Piston Moment Arm	L	85 mm
Individual Piston Moment Arm	r	45 mm
Bias Spring Constant	k	10000 N/m
Initial Compression of Bias Spring	l_0	60 mm
Number of Pistons	N	9
Pressure Carry-Over Angle	γ	35°

APPENDIX B

SPECIFICATIONS OF COMPENSATOR

Electro-Proportional Relief Valve (EPRV)

Table B-1 EPRV Specifications [26]

Electro-Proportional Relief Valve (EPRV)	
Rated Flow @ 70 PSI ΔP	1.9 lpm
Factory Set Relief Pressure When De-Energized	350 bar
Hysteresis @ 200 Hz PWM	<10%
Operating Temperature	-40 / +93°C
Filtration	SAE Class 4

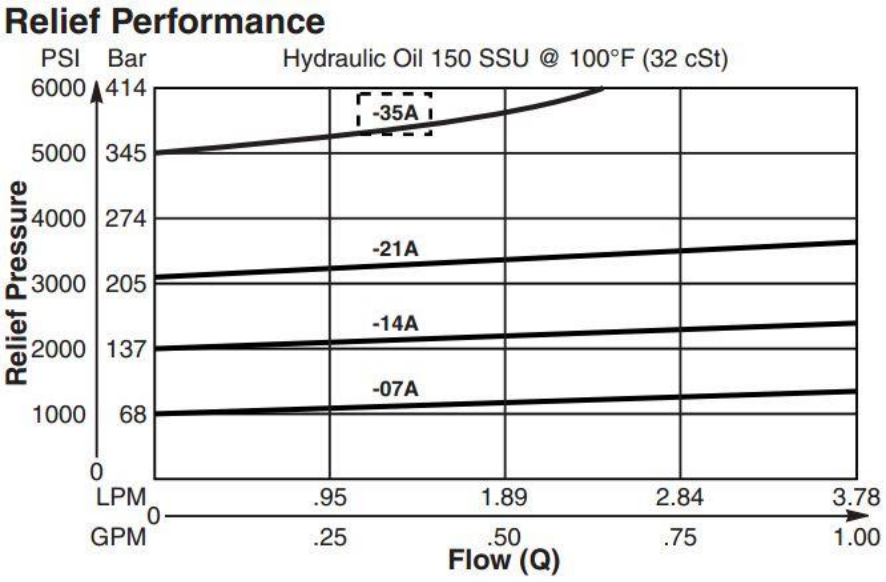

Figure B-1 Relief Pressure vs. Flow [26]

Relief Valve (RV)

Table B-2 Relief Valve Specifications

Relief Valve (RV)	
Preset Pressure	250 bar
Spring Rate	100 N/mm
Pilot Pressure Acting Area	8 mm^2
Valve Stroke	2 mm
Maximum Passage Area	0.3 mm^2
Flow Discharge Coefficient	0.7
Leakage Area	10^{-6} mm^2

Orifices

Table B-3 Specifications of Orifices

Orifices	
Diameter of ORF-1	Ø1.2 mm
Diameter of ORF-2	Ø0.8 mm
Diameter of ORF-3	Ø1.0 mm
Flow Discharge Coefficient	0.7

Spool and Spring

Table B-4 Specifications of Spool and Spring

Spool and Spring	
Spool Stroke	2.5 mm
Pilot Pressure Acting Areas	75 mm^2
Spring Constant	120 N/mm
Initial Compression of the Spring	0 mm

APPENDIX C

SPECIFICATIONS OF HYDROMOTOR

Table C-1 Specifications of Hydromotor [33]

Hydromotor		
Displacement		30 cc/rev
Operating Pressure	Continuous	420 bar
	Intermittent	480 bar
Operating Speed	Continuous	6700 rpm
	Intermittent	7300 rpm
	Min Continuous	50 rpm
Input Flow	Intermittent	219 lpm
	Continuous	201 lpm
Fluid Temperature		-40/80°C
Theoretical Torque @ 100 bar		47.6 Nm

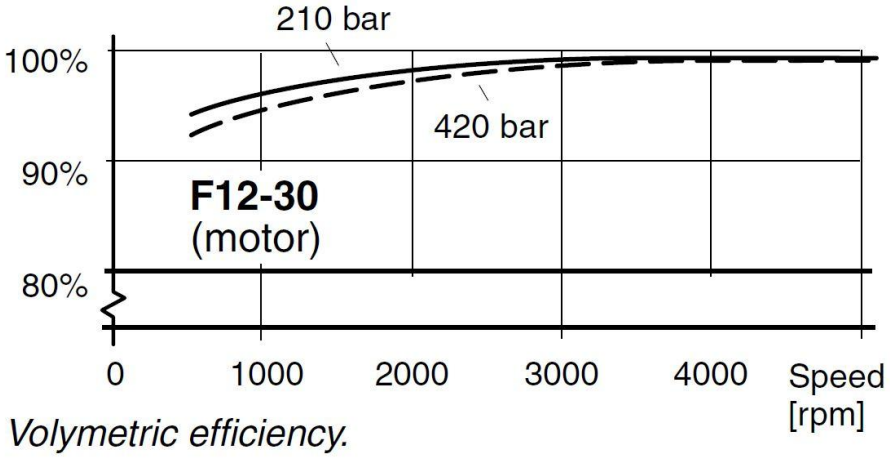

Figure C-1 Volumetric Efficiency of Hydromotor [33]

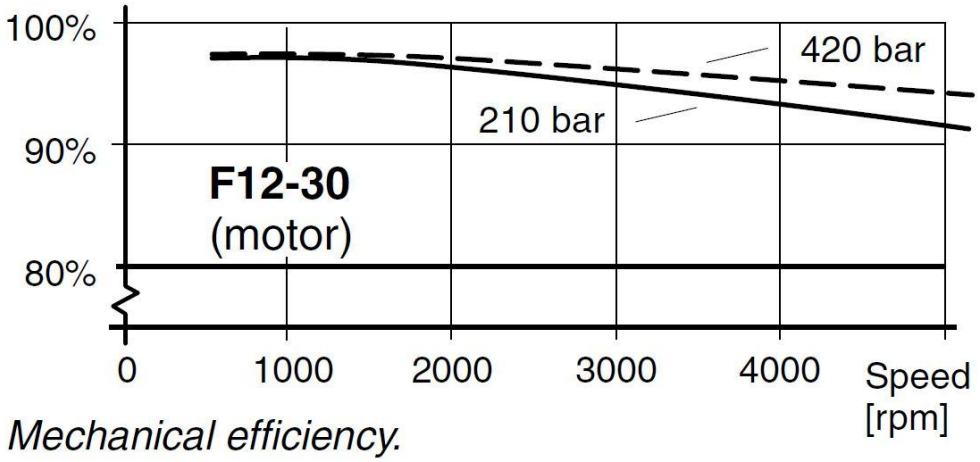

Figure C-2 Mechanical Efficiency of Hydromotor [33]

APPENDIX D

SPECIFICATIONS OF FAN

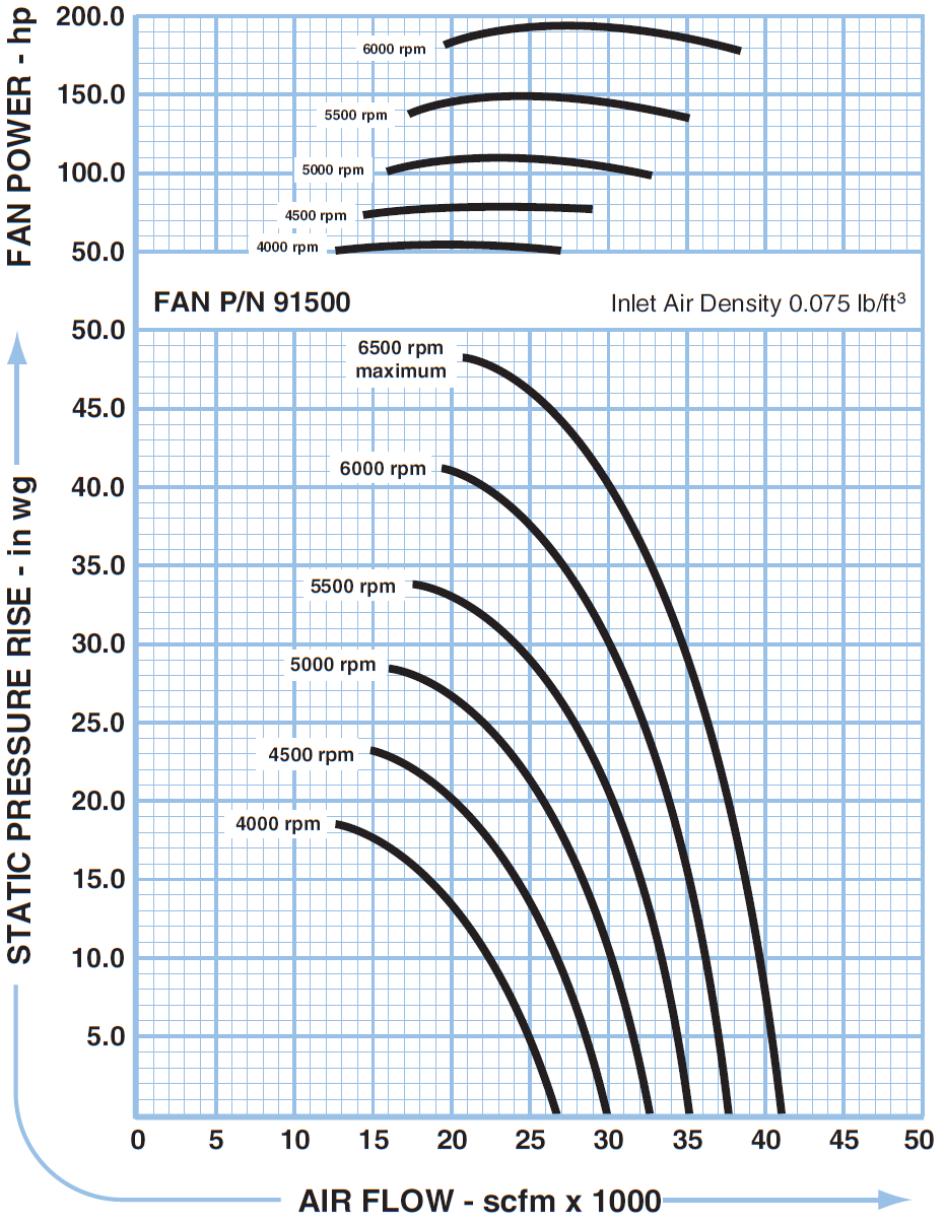

Figure D-1 Fan Performance Graph [34]

M-File and Block Parameters

```
component FanModel
% Fan Model
% This block implements a hydraulic driven fan.
% t=-D_fan*(theta.der)^2, where D_fan is the fan constant.
nodes
    r = foundation.mechanical.rotational.rotational; % r:left
    c = foundation.mechanical.rotational.rotational; % c:right
end

variables
    t = {0, 'N*m'}; % torque through
    w = {0, 'rad/s'}; % velocity across
    theta = {0, 'rad'};
end

parameters
    D_fan = { 10, 'N*m*s^2/rad^2'}; % Fan Constant
    theta0 ={0, 'rad'}; % Initial Deformation
end

function setup
if D_fan<0
    error('Spring rate must be greater than 0');
end
across(w, r.w, c.w); %velocity variable w from node r to node c
through( t, r.t, c.t); % torque variable t from node t to node c
theta = theta0
end

equations
    w == theta.der;
    t == D_fan*w*w*sign(w);

end
end
```

APPENDIX E

SPECIFICATIONS OF PIPELINE

There are four flexible hoses in the system. These are pressure line hose between pump and hydromotor, suction line hose between pump and reservoir, a leakage line between pump and reservoir and finally return line hose between hydromotor and tank.

Table E-1Specifications of Pipelines [35]

	Pressure Line	**Suction Line**	**Leakage Line**	**Return Line**
Supplier	PARKER	PARKER	PARKER	PARKER
Type	787TC-16	811-32	811-12	811-24
Hose Inner Dia.	Ø25 mm	Ø50.8 mm	Ø19 mm	Ø38.1 mm
Hose Outer Dia.	Ø35.7 mm	Ø63.6 mm	Ø30 mm	Ø52 mm
Working Pressure	350 bar	7 bar	21 bar	14 bar
Min. Bend Radius	150 mm	152 mm	64 mm	127 mm
Temperature	-40 to 125°C	-40 to 100°C	-40 to 100°C	-40 to 100°C
Hose Length	1000 mm	750 mm	750 mm	900 mm